Department of Physics and Astronomy

University of Heidelberg

UNIVERSITÄT
HEIDELBERG
ZUKUNFT
SEIT 1386

Master Thesis in Physics

submitted by

Adémọ́lá Theophilus-seun, Adéìféọ̀ba

Born in Lagos, Nigeria.

Towards the Structure of Black Holes in Asymptotically Safe Gravity

This Master Thesis has been carried out by

Adémọ́lá Theophilus-seun, Adéìféọ̀ba

at the

Institute for Theoretical Physics, University of Heidelberg

under the supervision of

Frau Dr. Astrid Eichhorn

For Atíńshọlá Àjíkẹ, my grandmother,

and to

a string of human who have been vital for my progress, including

Grace Olúyẹ́misí, Akinọ̀lá

Deborah Ọlayídé, Àjàyí

Adégbọ̀lá Peter, Akinọ̀lá

Adédèjì Zaccheus, Adélabú

"We are all different, but we share the same human spirit.
Perhaps it's human nature that we adapt and survive." – Stephen Hawking.

Statement of Authorship

I herewith declare that this thesis was solely composed by myself and that it constitutes my own work unless otherwise acknowledged in the text. I confirm that any quotes, arguments or concepts developed by another author and all sources of information are referenced throughout the thesis. This work has not been accepted in any previous application for a degree.

Universität Heidelberg

Abstract

Department of Physics and Astronomy

Towards the Structure of Black Holes in Asymptotically Safe Gravity

by Adémọ́lá Adéìfẹ́ọba

Asymptotically safe quantum gravity suggests a resolution to the classical spacetime singularity of Schwarzschild-(A)dS black holes. In particular, this is realizable only for a vanishing microscopic value of the dimensionless cosmological constant at the asymptotically safe fixed point. To accommodate a nonzero infrared value of the cosmological constant, we consider the linearized Renormalization Group flow away from the fixed point, which is characterized by two critical exponents in the Einstein-Hilbert truncation. In this study, we show that the realization of a regular de-Sitter core places a bound on the universal gravitational critical exponents. Accordingly, our study hints at the possibility of singularity resolution in black holes, as explicit estimates of the critical exponents in the literature point towards a realization of our bound.

Second Reviewer:

Prof. Dr. Luca Amendola
Institute for Theoretical Physics
Philosophenweg 16
D-69120 Heidelberg – Deutschland

Contents

Statement of Authorship i

Abstract i

Introduction iii

1 Black Holes 1
- 1.1 Classical Black Holes solutions within General Relativity . . . 2
- 1.2 Challenges of Classical Description of Black Holes . . . 5
  - 1.2.1 Black Hole Singularity . . . 5
  - 1.2.2 Singularity Theorem and Cosmic Censorship . . . 6
  - 1.2.3 The Thermodynamics of Black Holes . . . 7

2 Asymptotic Safety: The Pure Gravity Scenario 9
- 2.1 Overview of the Asymptotic Safety Paradigm . . . 10
  - 2.1.1 Asymptotic Safety Conjecture . . . 10
  - 2.1.2 Local behavior of the RG flow . . . 11
- 2.2 RG Machine . . . 14
- 2.3 Status of AS in Pure Gravity . . . 16
  - 2.3.1 Einstein-Hilbert Truncation . . . 16
  - 2.3.2 Beyond Einstein-Hilbert Truncation . . . 20

3 Black Holes in Asymptotic Safety 23
- 3.1 Physical RG-improvement schemes . . . 23
  - 3.1.1 Solution of the Improved Field Equation . . . 24
  - 3.1.2 RG-scheme at the Level of Classical Solution . . . 24
  - 3.1.3 Physical Scale Setting . . . 25
- 3.2 Renormalization Group Improved Black Holes . . . 27
  - 3.2.1 RG-improved Schwarzschild Solution . . . 28
  - 3.2.2 RG-improved Schwarzschild-AdS Solution . . . 31

4 Quantum Gravity Bound on the Critical Exponent 37
- 4.1 RG Scaling Relations for Gravity . . . 38
- 4.2 QG Bound on θ . . . 41
  - 4.2.1 Class I: Real Critical Exponent . . . 41
  - 4.2.2 Class II: Complex Critical Exponent . . . 46
- 4.3 Origin of the Singular-Free Improved Solution . . . 50

5 Summary and Outlook **54**

I On the Asymptotically Safe Flat Configurations **57**

Flat Configurations and Asymptotic Safety **58**
.1 The Non-trivial Flat Configuration of the Pure R^2 59
.1.1 Extremal RN Black Holes 61
.1.2 Non-trivial configurations 61
.2 Structural Aspect of AS Flat Configurations 65
.3 Hayward Type Black Holes 69

II Curvature Scalars and Invariants **72**

On the QG Bound on θ **73**
.1 The Real Critical Exponents 73
.2 Complex Critical Exponents 74
.2.1 Scalar Curvature 74
.2.2 Kretschmann Scalar 75

Bibliography **76**

Acknowledgement **84**

Introduction

To unravel the fundamental structure of quantum spacetime, the quest for a consistent quantum theory of gravity is under way[1] to unify two main ideas that have revolutionized the way we think about the universe – *General relativity (GR) and Quantum field theory (QFT).*

GR describes a classical law of gravity that embodies the nature of the gravitational interaction [2]. The emerging spacetime geometry is no more an ordinary background where classical physics only live, but a physical and dynamical entity which has its own degrees of freedom. Gravity is attractive. As such, galaxies and stars are formed and black holes emerge as a consequence of massive stars collapse. From the precession of the perihelion of Mercury to the most recent detection of gravitational waves at LIGO, GR remains one of the most tested theories of physics [3] and its confirmed validity is unchanged over a domain ranging from the very small length scale regime up to the very large length scales in the standard model of cosmology, making it very fundamental to the study of our universe as a whole.

Unlike Newtonian gravity, classical gravity in GR is not a force per se in a pre-existing spacetime, but rather the properties of spacetime structure. The formulation of GR is based on a set of physical and geometric principles such as spacetime structures, causality, general covariance and equivalence principles. Spacetime of physical events is modeled as a Lorentzian manifold $\mathcal{M}$ equiped with a pseudo-Riemannian metric $g_{\mu\nu}$. Based on these elements, GR is encoded in the following definition:

Definition 0.1. Let $(\mathcal{M}, g)$ be a spacetime, $T_{\mu\nu}$ be a symmetric covariant 2-tensor, and Λ be a real constant. We say $(\mathcal{M}, g)$ satisfies the Einstein Field Equation (EFE) with energy momentum tensor $T_{\mu\nu}$ and cosmological constant Λ if

$$G_{\mu\nu} \equiv R_{\mu\nu} - \frac{1}{2} g_{\mu\nu} R = 8\pi G T_{\mu\nu} - \Lambda g_{\mu\nu}, \tag{0.0.1}$$

where $G_{\mu\nu}$ is the Einstein tensor, $R_{\mu\nu}$ denotes the Ricci curvature and R the scalar curvature.

The conceptual idea here is that the matter and energy content in the universe determine the spacetime geometry, while the geometry in turn determines the geodesic path of freely moving particles. The key features of GR are that

- spacetime – geometry and matter – is dynamical;
- the energy-momentum tensor is covariantly conserved, $\nabla_\mu T^{\mu\nu} = 0$;
- the field equations are second order hyperbolic partial differential equations.

On the other hand, QFT provides a framework of modeling elementary particles [4]. The modern Feynman's path integral approach teaches us that a general QFT is defined by the path integral

$$Z = \int_{\mathcal{M}} \mathcal{D}\varphi_i \; e^{-\frac{1}{\hbar} S[\varphi_i; \alpha]}, \tag{0.0.2}$$

where φ_i represents various fields of interest, e.g metric $g_{\mu\nu}$ for spin-2 field (graviton), 1-form A_μ for spin-1, a Dirac field ψ for spin-$\frac{1}{2}$ and a scalar field ϕ for spin-0. $S[\varphi_i(x);\alpha]$ is the classical action and $\alpha = (\alpha_1, \alpha_2, \alpha_3, ...)$ represents the coupling space allowed by the underlie symmetry of the classical action. For example, the basic formalism of GR is captured by the Einstein-Hilbert action

$$S_{EH} = \frac{1}{16\pi G}\int_{\mathcal{M}} d^4x\sqrt{-g}\ (R - 2\Lambda) - \frac{1}{8\pi G}\int_{\partial\mathcal{M}} d^3x\sqrt{-h}\ \mathcal{K}, \tag{0.0.3}$$

where the second term on the r.h.s is the Gibbons-Hawking-York boundary term, which features an induced metric h_{ab} on the boundary $\partial\mathcal{M}$ and the trace of the extrinsic curvature $\mathcal{K}$. This term may become relevant for the consistency of solutions beyond asymptotically flat. The field equation, following the extremizing (0.0.3) in the presence of matter, gives the Einstein field equation (0.0.1).

In QFT, the world is quantum, classicality is just a limit $\hbar \to 0$ of it, and fields are nothing, but part of reality. The emergent particles are excitation of fields, e.g. the graviton emerges as excitation of gravitational field, and quantum operators $\hat{\mathcal{O}}_i(x)$ are built from $\varphi_i(x)$ at each spacetime points. Solving a QFT is then up to computing the n-points correlation functions

$$\langle\Omega|\,\hat{\mathcal{O}}_1(x_1)....\hat{\mathcal{O}}_n(x_n)\,|\Omega\rangle = \frac{1}{Z}\int \mathcal{D}\varphi_i\ e^{-\frac{1}{\hbar}S[\varphi_i;\alpha]}\mathcal{O}_1(x_1)....\mathcal{O}_n(x_n), \tag{0.0.4}$$

and perturbation theory is one of such solution formulation. The standard model of particle physics, modeled as a QFT, has lead to a high precision description of particles that make up the visible mass of the universe. So far, the SM has withstood many experimental test and its most recent landmark success is the verification of Higgs mechanism, which provides elementary particles with their respective mass. An historical account of this can be found in [5].

Einstein gravity features some intrinsic pathologies. In particular, the occurence of singularities is inevitable and consequently, there is a breakdown in future predictability [6]. Such singularities typically appear at the initial state of the universe and as generic end state solutions of continual gravitational collapse [7]. This lead to the Penrose-Hawking *singularity theorem* [8]. Ever since the proof of this theorem, many conceptual issues have emerged including several attempts to understand the final stages of black hole evaporation, where one can no more ignore the interplay between the singularity and *Hawking radiation*.

Among few attempts to avoid a conclusion of inevitability of the central singularity within classical GR is one which demands that the physical spacetime singularity be censored by an *event horizon*. The basic aim of Penrose's *cosmic censorship hypothesis* is to render the evolution of the whole spacetime as fully predictive by GR, so that physical singularities won't have any influence on observers outside the event horizon[9]. This attempt has been contested in various ways including an argument based on gravitational collapse models whose generic conclusions are in favour of formation of both black holes and naked singularities [10].

As nature is expected to be singularity-free, one may still wish to construct a regular black hole solution without any pronounced deviation away from standard classical physics. Models of this class seek a premise to implement the limiting curvature hypothesis, which strives to incorporate a fundamental limiting length, that would be realized in a fundamental gravity theory, into an effective field theory. Accordingly, they replace black hole singularity with a nonsingular de-Sitter core, and consequently, this induces the existence of an inner and outer horizon [11]-[16]. The curious part of this model is that it provide an effective description of black hole evaporation, allowing for trapped particles to finally make their way to external space after the evaporation is completed [17]. More recently, some issues about the stability of the

regular core were raised. In particular, it was shown that the inner horizon, and thus the core of any model of regular black hole is unstable against perturbation on a finite time scale and in addition, the evaporation time is infinite in contrast to finite evapration time suggested in earlier literature analysis [18]. As such it has been suggested that regular black hole models are not viable. If this claim holds, it would imply what is already expected, that to seek for a possible resolution to pathologies emanating from classical gravity theories, one would have to look beyond effective field description.

Obviously, the breakdown of all classical physics in the singularity regime shows that classical gravity has been pushed beyond the domain of its validity. As such, one is compelled to appeal to a more consistent quantum gravity theory to capture the fundamental quantum nature of spacetime. Although it is not guaranteed, however, the working assumption is that, such a fundamental theory would lead to a possible resolution to black hole singularity or at least weakens it.

There exist a strong argument supporting the idea that the spacetime gravitational field must be quantized. Starting with GR alone, the matter and energy contents in the universe determine the spacetime geometry. These energy contents in the universe are dynamical and as such, spacetime, which is the domain of these energy contents must be dynamical. Thus, spacetime, being dynamical, must be quantized according to the dictate of standard quantum field theory. Accordingly, one ask about the fundamental quantum nature of spacetime. The breakdown of classical description of gravity suggests that there must be a more fundamental description of gravity that capture the structure of quantum spacetime. As a consequence, classical geometry need a replacement since spacetime in small distance regime cannot be described by the same pseudo-Riemannian metric of the classical spacetime.

How does quantum spacetime emerge? Which conceptual and experimental paradigms underlie the formulation of viable model of quantum gravity? Minimally, one expect a fundamental theory to have a structure that all the low-energy phenomena and observables are recovered back in a very consistent way. For example, a reasonable quantum theory of gravity should recover back GR in the large distance limit and be consistent with observations of the infrared quantities, such as particle masses, coupling constants, and observations in astrophysics and cosmology. However, since there is no direct experimental hint for the moment, the questions about the fundamental structure of quantum spacetime remains at the heart of diverse approaches to quantum gravity. This means that there is currently no full discription of quantum behavior of gravity, and thus, questions about quantum spacetime remain open.

To confront this problem, diverse approaches have emerge. First, the perturbative quantum gravity treats graviton modes around a flat background. The incompleteness of GR as a standard perturbative QFT is evident in the appearance of the notorious ultraviolet (UV) loop divergencies [19]. These cannot be absorbed into the term already present in the action and therefore spoils perturbative renormalizability. At the level of quadratic curvature tensor correction to Einstein-Hilbert action, gravity is renormalizable at all loop orders [20]. However, the appearance of a massive ghost state which may spoil unitarity. As such, a task for perturbative gravity is in making renormalizability compatible with perturbative unitarity. However, renormalization attempts generally require infinitely many higher order curvature tensor as counter-term to absorb divergences. Thus, the traditional perturbative approach fails to capture the behaviour of gravity beyond the Planck scale where the singularity of classical gravity lives. This renders perturbative gravity usable at low energy, where quantum gravity effects can be captured within an effective field theorey formalism [21]-[24]. In turn, making sense of gravity at high energy scales would require either a new QFT machine or departure from standard QFT. Instances of such departures are found in various approaches to quantum gravity [25].

The failure of perturbative gravity at high energy opened the door to exploring quantum gravity based on the Wilsonian non-perturbative renormalization group (RG) philosophy. In particular, there exists a growing collection of evidence that a scale invariant regime of the RG flow could provide an adequate description of quantum gravity, and thus reveal the fundamental structure of quantum spacetime. This is Weinberg's *asymptotic safety paradigm* [26]. In this framework, the physics in the deep UV is ruled by the existence of a non-trivial fixed point, while the infrared limit of the renormalization group trajectory gives the analog classical description. As a consequence of the non-trivial fixed point, predictivity is highly enhanced, and quantum observables in this framework are free from possible pathologies at high energies, making it very interesting for phenomenology. This idea shall be the principal view point of our investigation of the black hole structure.

The structure of an asymptotically safe Schwarzschild solution has been investigated, with quantum gravity resolves the classical black hole singularity [80]. This investigation was extended to the Kerr solution in [83]. Unfortunately, the introduction of the cosmological constant spoils the earlier singularity resolution. Schwarzschild-(A)dS black holes are not asymptotically safe unless the microscopic cosmological constant at the fixed point vanishes [85]. Here, we will explore a setting where the fixed point value of the cosmological constant vanishes, but the flow to the infrared generates a non-zero cosmological constant in accordance with observation at the low energy. This requires to bare our study not just on the fixed-point properties of the asymptotically safe quantum gravity, but to extend the analysis into the (linearized) regime away from the fixed point. This regime is characterized by critical exponents, which encode how fast the flow to the fixed point is. These critical exponents defines a universality class, a concept familiar from statistical physics.

In the language of statistical physics, we can think of the gravitational fixed point as a critical phenomenon. As such, there exists a universal gravitational scaling law associated with a phase transition of gravitational field strength at the criticality. In $d = 4$, the gravitational critical exponent has been examined with several approaches ranging from 1-loop perturbative $2 + \epsilon$ expansion [67] to exact renormalisation group approach [58] and quantum gravity on lattice [111]. Asymptotically safe black holes provides a way to investigate the existence of a bound on the universal gravitational critical exponent and our study shall include the investigation of the possibility of this bound.

The structure of our study is as follows. In chapter 1, we introduce the relevant black hole concepts needed for our study and discuss why a classical description of gravity in some black hole regime needs to be replaced by a consistent quantum description of gravity. In chapter 2, we present the proposal of asymptotic safety of quantum gravity and use this proposal in chapter 3 to highlight implications in black hole physics. For a vanishing microscopic value of the cosmological constant, the quantum gravity bound for the universal critical exponents is studied in chapter 4. We conclude our discussion with some outlook in chapter 5. The realization of a regular core in the RG-improved Schwarzschild solution poses a question as to whether all asymptotically flat spacetime configurations are asymptotically safe in the sense that their classical singularity is resolved by RG-improvement. For future study, we studied some non-trivial flat configurations of the pure R^2 gravity. This can be found in the Appendix I. We have not checked whether the ansatzs constructed are just coordinate transformation of the Schwarzschild. If so, then it is reassuring that our conclusion, namely the absence of the singularity after RG improvement, persist under this changes.

Chapter 1

Black Holes

Black holes[1] are among the most interesting objects of physical importance. By now, most theoretical physicists and astronomers acknowledge that they play fundamental roles in our understanding of the universe and thus convinced that these objects exist, e.g. in our galaxy. The first object to be identified as a candidate black hole is the X-ray source Cygnus X-1 [28]. The observed behaviour of Cygnus X-1 is consistent with the general representation of a galactic black holes. This object is 33 times as massive as our sun. Ever since then, advanced technology has opened doors to progresses in the study of astrophysical black holes. For instance, observations suggest the existence of a very massive compact object in the center of our galaxy whose spatial extensions are too small to be composed of neutron stars or ordinary astrophysical objects [29]. The central mass of this object is about $4.3 \times 10^6 M_\odot$ and it is confined in a region of radius $4.4 \times 10^{10} m$ at the center of our Milky way. More recently, another strong indication of the existence of black holes surfaced at the Laser Interferometer Gravitational-wave Observatory (LIGO). In September 2015, the first-ever direct observation of gravitational waves was discovered. Since then, the LIGO Scientific Collaboration and Virgo Collaboration have confirmed the detection of three gravitational waves from energetic mergers of black hole pairs [30]. As shown in figure 1.1, the three detections – GW150914, GW151226, GW170104 – and one lower confidence candidate, LVT151012, suggest a population of binary black holes, whose merger masses are larger than $20M_\odot$ These observations provide new opportunities for exploring fundamental physics, as they offer insight into the strong-field gravity regime and create means to test gravity theories.

Black holes are, by the standard definition, regions of spacetime from which no causal signals can escape to an observer at infinity. This kind of object had been anticipated earlier by John Michell and Pierre-Simon Laplace within the framework of Newtonian gravity combined with the corpuscular theory of light [31]. In Newtonian gravity, the escape velocity from the surface of a compact body of mass M and radius R exceeds the speed of light c if $R < R_H$ with $R_H = \frac{2GM}{c^2}$. Following modern physics, special relativity imposes that c is the universal upper bound to all causal signal speeds in the physical world. This suggests that, at R_H, there exist a boundary of this compact body beyond which no causal signals can escape to infinity. This boundary is called *event horizon* and it is crucial in a formal definition of black hole. R_H can then be used as an estimate of the scale at which black holes form and thereby sets an elementary

[1] While it is unclear who invented the term "black hole", the first recorded use of the term can be found in a January 1964 report of AAAS meeting by journalist Ann Ewing. The term subsequently became accepted when it was later used by John Wheeler in a lecture at the NASA Goddard Institute of Space Studies in 1967 where he remarked that one just could not keep saying "gravitationally completely collapsed object". "How about black hole?" asked someone in the audience, and the term became favoured [27].

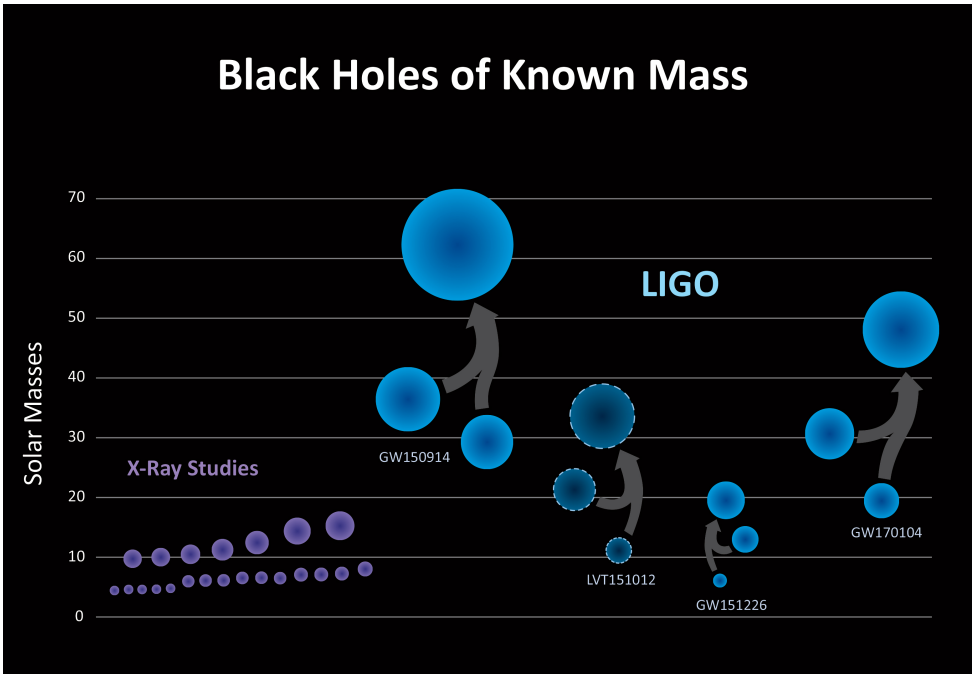

Figure 1.1: New Population of Binary Black Holes with masses larger than those observed with X-ray studies (purple). – **Source:** *LIGO/Caltech/Sonoma State (Aurore Simonnet) '17*

definition of black hole as a region of space-time in which the gravitational potential, GM/R_H, exceeds the square of the speed of light, c^2. Such a definition is congruent to hoops conjecture which demands that a black hole should form whenever the amount of energy M is crushed and compacted inside a region of spacetime whose circumference in all direction equals $2\pi R_H$ [32]. In this sense, black holes can in principle have any value of mass and the mass turns out to be the the typical quantity setting the size of its gravitational radius.

Our aim in this chapter is simple. We shall introduce some concepts of black holes relevant for our study and discuss why a classical description in some black hole regime need to be replaced by a consistent quantum description of gravity.

1.1 Classical Black Holes solutions within General Relativity

Black holes arise as a physical prediction of Einstein GR. In four dimensions, they are point-like and (in the absence of angular momentum) have SO(1,3) symmetry. The first encounter with black hole solution was by Karl Schwarzschild [33] who constructed a vacuum solution to EFE, i.e. a solution that satisfies $R_{\mu\nu} = 0$. In the presence of a cosmological constant, it satisfies $R_{\mu\nu} = \Lambda g_{\mu\nu}$. In four dimensions, the simplest stationary solutions of the EFE describing compact objects are spherically symmetric, having a metric of the form

$$ds^2 = -A(r)dt^2 + \frac{dr^2}{B(r)} + r^2 d\Omega_2^2 \tag{1.1.1}$$

where $d\Omega_2^2$ is the metric of the 2-sphere, and $A(r)$ and $B(r)$ are some lapse functions. Following Birkhoff's theorem, for $d \geq 4$, any d-dimensional spherically symmetric solution of the vacuum

EFE belongs to the family of Schwarzschild metric parametrized by mass M. The Schwarzschild-Tangherlini solution is given by [33, 34]

$$ds^2 = -\left(1 - \frac{\mu}{r^{d-3}}\right) dt^2 + \frac{dr^2}{1 - \frac{\mu}{r^{d-3}}} + r^2 d\Omega_{d-2}^2, \tag{1.1.2}$$

where

$$\mu \equiv \frac{16\pi G_d M}{(d-2)\Omega_{d-2}}, \tag{1.1.3}$$

and G_d is the Newton's coupling in d-dimensions.

One can establish the existence of a curvature singularity by showing that, along the timelike or null geodesic, curvature invariants becomes infinite. In our discussion, we shall mostly employ the Kretschmann invariant, $R_{\mu\nu\rho\sigma}R^{\mu\nu\rho\sigma}$, which is a coordinate independent quantity. This quantity measures gravitational field strength, and is expected to go to infinity as one approaches the singularity in, at least, classical description of gravity. This in turn signals a loss in future predictability. For Schwarzschild solution, the Kretschmann invariant is given by,

$$R_{\mu\nu\rho\sigma}R^{\mu\nu\rho\sigma} = \frac{48G^2M^2}{r^6}, \tag{1.1.4}$$

showing that solutions contain a spacetime singularity at $r = 0$. The singularity at $r = 0$ characterizes a region of spacetime where the density of matter as well as the spacetime curvature become infinite. The gravitational potential becomes arbitrarily strong and the law of physics, as we know them, break down. This true pathological feature of geometry near a singularity signals the failure of the theory and GR no more provides a good description of gravity in this regime.

Henceforth, we set $d = 4$ but similar result hold in an arbitrary dimension. One apparent feature of the Schwarzschild metric is that it is singular as $r \to 2GM$, however, this is not a true pathological features of Schwarzschild geometry as this singularity is a consequence of coordinate choice. In fact, one can indeed show that the Kretschmann invariant is regular as $r \to 2GM$. It is straightforward to see that, by replacing t with a new coordinate v defined as

$$v := t + g(r), \quad g'(r) = \frac{1}{f(r)}, \tag{1.1.5}$$

and consequently

$$v := t + r + 2GM \ln(r - 2GM) \tag{1.1.6}$$

the Schwarzschild metric can be brought to the form

$$ds^2 = -\left(1 - \frac{2GM}{r}\right) dv^2 + 2dvdr + r^2 d\Omega^2, \tag{1.1.7}$$

making the metric a well-defined Lorentzian metric on the set $v \in \mathbb{R}$, $r \in (0, \infty)$ and providing the analytic extention of the original metric. Classically, the characteristic feature of a black hole is its event horizon, which appears at $r = 2GM$ for a Schwarzschild black hole. The boundary covers the interior of the black hole, from where no light or any observer can send signals to a far away asymptotic external region.

Solution (2.2.7) is obtained in the absence of the cosmological constant Λ, thereby leading to an asymtotically flat Schwarzschild solution. Including Λ, the solution receive a modification leading to a lapse function

$$f(r) = 1 - \frac{2GM}{r} - \frac{1}{3}\Lambda r^2. \tag{1.1.8}$$

The spacetime solution is

$$\begin{cases} Schwarzschild - AdS & for \quad \Lambda < 0, \\ Schwarzschild & for \quad \Lambda = 0, \\ Schwarzschild - dS & for \quad \Lambda > 0. \end{cases} \tag{1.1.9}$$

In this case, the Kretschmann invariant for the Schwarzschild-(A)dS solution is

$$R_{\mu\nu\rho\sigma}R^{\mu\nu\rho\sigma} = \frac{48G^2M^2}{r^6} + \frac{8\Lambda^2}{3}, \tag{1.1.10}$$

indicating that the class of solutions posseses a real spacetime singularity at $r = 0$.

In four spacetime dimensions, the *no hair theorem* [35] postulates that all black-hole solutions to the Einstein-Maxwell equations are uniquely characterized by just three observable classical parameters: the mass (M), the electric charge (Q), and angular momentum (J), so that other black-hole solutions within GR are classifed in what follows.

- **Reissner-Nordström (RN) or Charged Black Hole:** is the solution to EFE equations for a spherically symmetric system with a radial electric field and zero 4-current density [36]. The metric takes the form

$$f(r) = ds^2 = -\frac{(r - r_+)(r - r_-)}{r^2}dt^2 + \frac{r^2}{(r - r_+)(r - r_-)} + r^2d\Omega^2, \tag{1.1.11}$$

  with event horizons located at the coordinate singularites

$$r_\pm = GM \pm \sqrt{G^2M^2 - GQ^2} \quad for \quad M < |Q| \ \ (Sub - Extremal). \tag{1.1.12}$$

  We note that for $M < |Q|$, the spacetime possesses a naked singularity at $r = 0$. This is the super-Extremal limit. At extremality, where $M = Q$, the event horizons coincide at the extremal radius $r_\pm = GM = |Q|$. In particular, the extremal black hole metric is given by

$$ds^2 = -\left(1 - \frac{GM}{r}\right)^2 dt^2 + \left(1 - \frac{GM}{r}\right)^{-2} dr^2 + r^2d\Omega^2. \tag{1.1.13}$$

- **Kerr Solution or rotating Black Hole:** represents the spinning generalization of the Schwarzschild solution and is relevant for astrophysical black holes [37]. The metric takes the the form

$$ds^2 = -\frac{\Delta}{\Xi}\left[dt - a\sin^2\theta d\varphi\right] + \frac{\Xi}{\Delta}dr^2 + \Xi d\theta^2 + \frac{\sin^2\theta}{\Xi}\left[(r^2 + a^2)d\varphi - adt\right]^2 \tag{1.1.14}$$

  where

$$\Delta := r^2 - 2GMr + a^2, \quad \Xi := r^2 + a^2\cos^2\theta. \tag{1.1.15}$$

  This solution describes a rotating black hole with angular momentum $J = aM$.

- **Kerr-Newman Solution:** represents spinning generalization of RN and the electrically charged Kerr solution [38]. The relevant metric is obtained by replacing Δ in the Kerr solution by

$$\Delta_Q := r^2 - 2GMr + a^2 + GQ^2. \tag{1.1.16}$$

1.2 Challenges of Classical Description of Black Holes

In this section, we shall discuss the breakdown in the classical description of black holes. The physical question following the failure of classical description lead to a motivation to seek for a more fundamental description of gravity. In the following are some pertinent issues that arise.

1.2.1 Black Hole Singularity

The idea of what a singularity should be seems to be intuitively very simple: *whenever any physical or geometrical quantity diverges, this signals a singularity.* Singularities naturally feature within the classical description gravity. In GR, such singularities typically appear at the initial state of the universe and at the final state of gravitational collapse leading to black hole formation. Attempts to define a spacetime singularity in GR are one of the most interesting problems of singularities [39]. Formally, one could ask if these singularities are artifacts of the high degree of symmetry of the black hole solutions and whether in an asymmetric collapse, no infinite density would develop such that realistic gravitational collapse would lead to singularity free solution. Two analyses, starting from Raychaudhuri [40] to the more general results due to Penrose and Hawking's [41] study of spacetime structures, lead to the *singularity theorem.* Basically, the singularity theorem requires that, if we assume the existence of a closed trapped surface[2], null energy condition and a non-compact cauchy surface, then a singularity is unavoidable within GR. In particular, timelike or null geodesic incompleteness is a good indication of the existence of spacetime singularities. Geodesic incompleteness refers to a situation in which there is a sudden disappearance of freely moving observers and consequently, a breakdown in future predictability. As such, black holes were shown by Hawking and Penrose to be generic final state solutions of gravitational collapses [7]. A Singularity in black hole solution is not a point per se in the spacetime manifold, but it is in the boundary of the spacetime. Figure 1.2 shows the Carter-Penrose diagram for a star collapasing into a black hole.

At a singularity, the spacetime curvature invariants diverge, the regularity of the spacetime metric is lost and the energy density of the collapsing matter blows up. In essence, classical physics can no more provide an adequate description of spacetime in the neigbourhood of the singularity. Obviously, this spells the breakdown of all classical physics as it has been pushed beyond the domain of its validity. One of the questions to then ask is: "What description of gravity should replace classical GR in the black hole regime where curvature grows unboundedly?" The answer to this question is obviously not simple, however, it is believed that quantum effects, ignored by the classical description of gravity, should intervene at the Plank scale, making quantum gravity effects relevant before the curvature reaches infinity. Indeed, while in GR the existence of spacetime singularity is inevitable, quantum gravity may provide a resolution to the singularity. As a consequence of abandoning the classical description of gravity at the Planck scale, the classical metric associated to the spacetime manifold should also be replaced by a quantum improved one, and a basic challenge for the relevant quantum gravity theory is how to encode the quantum effects into the metric that describe the spacetime at the Planckian regime. As we shall see later, it is possible to encode the relevant quantum effects by renormal-

[2]One can think of a close trapped surface as a 2-surface in the inner region of the event horizon where the gravitational influence is so strong that all light rays, ingoing and even outgoing, converge. An intuitive picture of this can be found in Penrose original proposal [[41],[42]]. Penrose noted that the original Oppenheimer-Snyder collapse model has a trapped surface and then used it to imply the existence of asingularity.

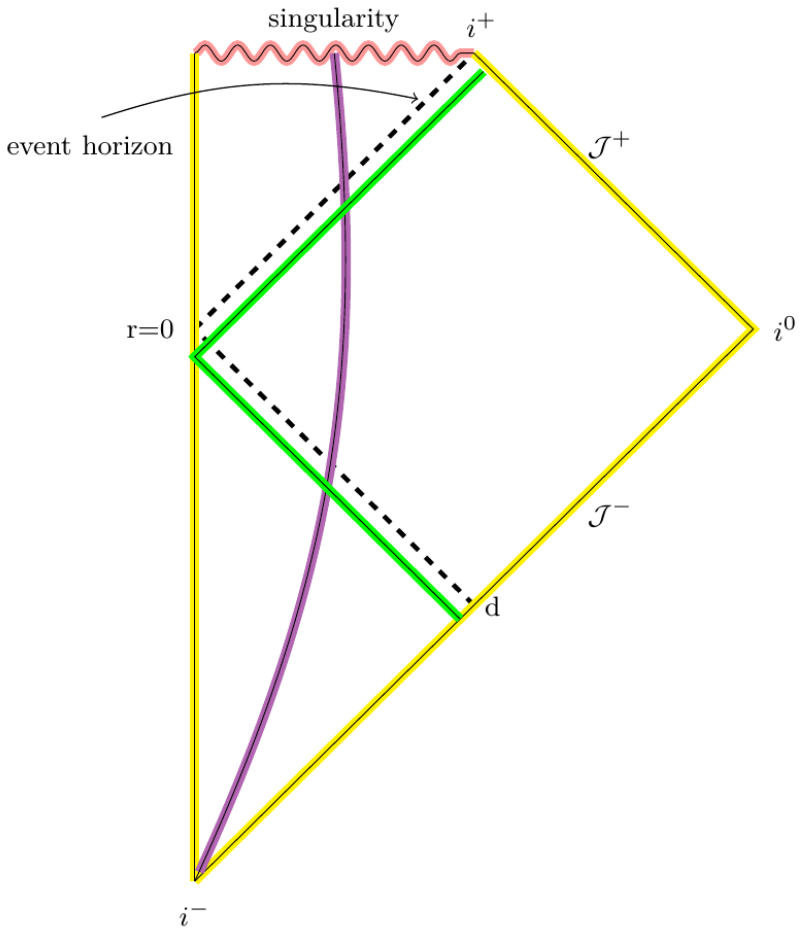

Figure 1.2: Carter-Penrose diagram for gravitational collapse of a star collapase into black hole. The collapsing star is represented by the violent curve. i^0 is the spatial null infinity ($r \to -\infty$). The past timelike infinity ($t \to -\infty$) is at i^- while future timelike infinity ($t \to \infty$) is at i^+ . $\mathcal{J}^-$ and $\mathcal{J}^+$ respectively represent the past and future null infinity. The black dotted line marked 'd' on $\mathcal{J}^-$ is he **event horizon**. Falling star collapse beyond event horizon is trapped. [43]

ization group improving the classical geometry. This approach has proved to have some useful phenomenological consequences and it shall be a cornerstone of our future analysis.

1.2.2 Singularity Theorem and Cosmic Censorship

As we have just seen, within GR, a singularity is inevitatble in the final state solution of continual gravitational collapse, leading to a breakdown in the future predictability. There were few attempts to avoid this conclusion within classical GR but the singularity theorem led to abandoning most of them. One not fully resolved attempt is due to the *Cosmic censorship hypothesis*. Penrose conjectured that one can have a future predictability within classical GR if nature avoids a naked[3] singularity. The conjecture is summarily captured in what follows.

- **The weak cosmic censorship conjecture** states that spacetime singularities that emerge in the final solution of gravitational collapse are always hidden inside of black holes. This means that if one evolves generic non-singular initial data on a suitable Cauchy

[3] A spacetime singularity is called naked if it is visible to a far away asymptotic observer in the universe.

hypersurface according to GR, no spacetime singularity visible to an observer at infinity will develop. This therefore suggests that a naked singularity within GR is unphysical and an event horizon must cover any physical singularity.

- **The strong cosmic censorship conjecture** postulates that a physically reasonable classical spacetime is globally hyperbolic. This basically enforces that GR can predict the evolution of the whole spacetime.

For years, these conjectures have attracted significant amount of debates [44]. Afterall, in its original form, Penrose-Hawking singularity theorem does not necessitate that the singularity developed in the process of gravitational collapse will turn out to become a black hole. The key question for gravitational collapse is therefore whether naked singularities may form with positive probability in the process of gravitational collapse.

Supposing the cosmic censorship conjecture is maintained, one might wish to argue further that there is no breakdown of future predictability since no physical singularities will lead to any effect on observers in the spacetime region outside the event horizon. Very little progress has been made toward a proof of the conjecture. Viewpoints on this are outlined by Wald [45] and studies consist primarily of the stability of black holes. For example, Wald performed a Gedanken experiment [46] to violate cosmic censorship. If one tries to over-charge an extremal Kerr-Newman black holes characterized by $M^2 = Q^2 + \frac{J^2}{M^2}$, by dropping into it a charged test particle whose charge is larger than the extremal black holes, then one might suppose that a naked singularity would appear as $M^2 < Q^2 + \frac{J^2}{M^2}$ is approached. However, he showed that this attempt to over-charge extremal Kerr-Newman black holes is not possible.

On the other hand, the cosmic censorship conjecture is contestable. Already, there are many examples of realistic gravitational collapse models within GR whose generic conclusion suggest that black holes and naked singularities do develop as the final state solution of spherical collapse. These include model with various forms of matter – dust, fluids and scalar fields [10]. Other arguments are centered on the hoop conjecture whose criterion is formulated such that gravitational collapse in all three spatial dimensions must occur for a black hole to form. While this criteria is crucial for formation of a horizon in non-spherical gravitational collapse, it is loosely formulated to allows such criteria to occur, and further, there is currently no experimental evidence for the conjecture.

It is fair to say that the conclusion about cosmic censorship is not resolved since most of the detailed models of spherical gravitational collase have been analyzed within the framework of Einstein gravity. If one maintain classical gravity, one way to resolve the problem is to test it observationally. In the absence of a reliable observational test, one may think about this problem within the framework of quantum gravity. The reason is that the conjecture has its root in the existence of singularity which is a common feature of classical gravity. As we saw earlier, allowing naked singularity within classical gravity will lead to a loss of future predictability. However, whether naked singularities within classical gravity are physical or unphysical, we expect that the relevant quantum theory of gravity should restore a suitable form of predictability.

1.2.3 The Thermodynamics of Black Holes

Although our study shall focus on the structural aspect of black hole spacetime. However, it is useful to introduce some basic elements of black hole thermodynamics due to the interplay between the central singularity and the mechanics of black holes.

Classical thermodynamics is well known to has its foundation in the non-gravitational physics but

its scope stretches relevance into black hole mechanics. According to Bekenstein [47], black holes carry an entropy S proportional to the event horizon area A, i.e. $S = A/4G$, and consequently, the relation

$$M^2 = \frac{1}{16\pi}A + \frac{4\pi}{A}\left(J^2 + \frac{1}{4}Q^4\right) + \frac{1}{2}Q^2 \tag{1.2.1}$$

was established to feature all information about the thermodynamical state of a non-extremal black hole, i.e. it relates the characteristic parameters describing a black hole. This led to the mass variation satisfying

$$\delta M = \frac{\kappa}{8\pi}\delta A + \Omega\delta J + \Phi\delta Q, \tag{1.2.2}$$

where κ is the surface gravity constant over the horizon, Ω is the angular velocity and Φ is the electrostatic potential. This is the first law of black hole mechanics. Analogously, a one-to-one correspondence was shown to exist between black hole thermodynamical laws and those of classical thermodynamics if there is an identification of black hole surface gravity κ with temperature, and the event horizon area with Bekenstein entropy [48]. On dimension ground, the proportionality, $S \propto A$ and $T \propto \kappa$, should involve a factor of the Planck constant $\hbar$. Since this similarity in thermodynamical laws was based on the classical GR, it was then considered to be just a mere analogy. However, by exploiting the quantum mechanical effect at the event horizon, Hawking showed [49] that a black hole emit radiation in a similar manner as a black body, at a temperature

$$T_H = \frac{\hbar\kappa}{2\pi} = \frac{1}{4\pi}\partial_r f(r)\Big|_{r=r_H}. \tag{1.2.3}$$

Following the analogy with the first law, black hole is then thought to carry Bekenstein-Hawking entropy given by

$$S_{BH} = \frac{A}{4\ell_p^2} = \frac{c^3 A}{4G\hbar}, \tag{1.2.4}$$

where ℓ_p^2 denotes the Planck length $G\hbar/c^3$. (1.2.3) and (1.2.4) feature the three of the fundamental constants of nature – $c, \hbar, G$. This suggest that black hole is at the very foundation of physics and offering hope that the study of black holes may lead towards a fundamental theory.

Hawking effect is also at the heart of the information paradox. Starting from the classical no-hair theorem, the large amount of data that describes a collapsing star within GR will reduce to a small number of quantities that describe a black hole, while the remaining information is not accessible once a black hole is formed. Now taking Hawking's semi-classical quantum mechanical effect into consideration, black holes evaporate on a time scale of $\tau \propto G^2M^3/(\hbar c^4)$ which is of the order of $10^{70}s$ for $M = M_\odot$. According to Hawking, the quantum evolution will take the initial pure state of the star to a mixed state, and consequently, Hawking radiation which is thermal, will carry no information contained in the initial wavefunction. Contrary to this, quantum mechanical principles dictate that evolution of wavefunction should be governed by a unitary operator, i.e information should be conserved by quantum evolution. The key questions is then whether the quantum mechanical evolution governed by unitary operator is compatible with black hole physics. This is the black hole information problem and it plays a role on the reason for quantum description of gravity.

Let us end this chapter by declaring that our study shall focus mainly on the structural aspect of quantum black hole within a specific paradigm of quantum gravity. In the next chapter, we shall highlight the principal viewpoint of our investigation of the black hole structure.

Chapter 2

Asymptotic Safety: The Pure Gravity Scenario

Quantizing gravity perturbatively around a classical background leads to perturbative non-renormalizability. In d dimensions, the canonical mass dimension of the Newton coupling is $[G] = 2 - d$, thus, its critical spacetime dimension is $d = 2$. Due to the negative mass dimension in $d > 2$, a power counting argument alone shows that traditional perturbative gravity can be applied only for low energies $E^2 \ll 1/G$, where the quantum gravitational corrections are captured by effective field theory (EFT). For instance, within the framework of EFT, quantum gravitational correction to the Newtonian potential between two point sources is given as[21]-[24]

$$V(r) = -\frac{Gm_1m_2}{r}\left(1 - \frac{G(m_1+m_2)}{rc^2} - \frac{167}{30\pi}\frac{G\hbar}{r^2c^3}\right) + \mathcal{O}\left(\left(\frac{G\hbar}{r^2c^3}\right)^2\right). \tag{2.0.1}$$

The quantum gravitatational correction is proportional to the Planck constant, while the term proportional to $\frac{G(m_1+m_2)}{r}$ is the post-Newtonian correction. This result is established despite the perturbative non-renormalizability complication at the very high energy. The higher-order counterterm introduced by renormalization can be negleted at leading order for energies $E \ll 1/M_{pl}$. So, gravity and quantum theory fit well in quantum gravity model below the Planck scale and the outstanding task boils down to resolving renormalizability at energies comparable with the Planck sclale, M_{pl}, where predictivity is lost. This is a consequence of the fact that all initially many counterterms, each with its own coupling, have to be taken into account in a perturbative treatment at the Planck scale. Indeed, the incompleteness of GR as a standard perturbative QFT is evident in the appearance of ultraviolet (UV) loop divergencies at each order in the expansion with respect to G, which cannot be contained by addition of few counterterm to the original gravity action[19]. Hence, one must look beyond the perturbative approach to provide a UV completion for gravity theories.

In this chapter, we shall introduce the idea of *asymptotic safety (AS)* [51, 52] in direct application to the pure gravity system. The AS paradigm is a non-perturbative approach whose philosophy stems from the Kadanoff-Wilson renormalization group [53],[54]. In a modern application to quantum gravity, funtional renormalization group (FRG), which amalgamates functional approach with the Wilsonian RG formalism of treating quantum fluctuations step-by-step, has been very successful in the construction of an exact renormalization group flow equation due to Wetterich[65]. The FRG is a powerful tool endowed with a resolution scale and capable of creating a connecting path from the macroscopic view of the world to a microscopic one.

2.1 Overview of the Asymptotic Safety Paradigm

According to Wilson[54], a QFT is just an effective description of physics, accurate up to a certain energy scale. Given any QFT with coupling parameters $\mathbf{g}$ associated with a reference scale k_0, a renormalization group (RG) is a transformation

$$\mathcal{G}_a : \mathbf{g} \longmapsto \mathbf{g}_{eff}, \tag{2.1.1}$$

such that $\mathbf{g}_{eff} := \mathcal{G}(a; \mathbf{g})$. The label $\frac{k}{k_0} := a \in \mathbb{R}$ is the rescaling parameter and $\mathbf{g}_{eff}$ are the effective coupling parameters associated with the scale k. An n-iteration would lead to

$$\mathbf{g}^n_{eff} := \mathcal{G}\left(a; \mathbf{g}^{n-1}_{eff}\right) = ... =: \mathcal{G}\left(a^n; \mathbf{g}\right) \tag{2.1.2}$$

In the limit $n \to \infty$, the rescaling factor $a^n \to 0$, suggesting that all degrees of freedom have been integrated out. As a consequence, $a = 1$ is associated with the full theory and $a = 0$ with the microscopic theory, so that $\mathcal{G}_a$ interpolate along the RG trajectory. It is trivial to show that $\mathcal{G}_a$ is, in fact, a *monoid*[1].

Thus, the basic idea of RG is simple: *renormalization group is a process of re-expressing the physical parameters* $\mathbf{g}$ *in terms of effective parameters* $\mathbf{g}_{eff}$*, while keeping unchanged the relevant physical aspects of the problem.*

In order to seek a UV completion of a given field theory, the QFT framework need not be abandoned, instead, we can explore its structure in the high energy regime with non-perturbative tools. In asymptotic safety paradigm, physics is structured on some basic propositions.

- First, the long and short distance physics are expected to be related through renormalization group flow. This is in consistent with the Kadanoff-Wilson RG.
- Second, the existence of a fixed point guarantees universality in the statistical physics sense[55]. In particular, scale-invariant theories define the universality classes of the RG flow.

2.1.1 Asymptotic Safety Conjecture

In the light of the behaviour of non-abelian gauge theories at high energy, where asymptotic freedom is realized[56], asymptotic safety seek to generalize asymptotic freedom. For example, an asymptotically free theory has its physical coupling appoach a high energy regime where it vanishes asymptotically. In this regime, the theory can be treated as non-interacting. On the other hand, the remarkable thing about asymptotically safe theories is that the dynamic in the deep UV contains residual interaction.

The domain in which this takes place is a submanifold of a *theory space* called the *critical surface*. The theory space is essentially the space of action functionals where RG acts on the theories' parameters – this is where all QFTs lives. Any action functional takes a general form

$$S(\phi) = \sum_j \bar{\lambda}_j(k)\mathcal{P}_j(\phi) \quad , \tag{2.1.3}$$

[1]Given that $a \in \mathbb{R}$, one can straightforwardly show that $\mathcal{G}_a$ inherit commutativity, associativity and identity associated to $a = 1$. Physically, $\mathcal{G}_a^{-1}$ may not exist since the elimination of field modes can change the number of effective coupling α_{eff}.

where $\{\bar{\lambda}_i(k)\}_{i=1,2,3,\dots}$ are scale k dependent parameters and $\mathcal{P}_i$ are the possible field monomials allowed by the underlying symmetry of the theory. For $i,j \in \mathbb{Z}$, let $\{\bar{\mathbf{g}}_i(k)\} \subseteq \{\bar{\lambda}_j(k)\}$ represent a subset of the full scale dependent parameters which cannot be removed by field redefinition. These parameters are refered to as the *essential parameters*. As a consequence, the field monomials in the dynamics also reduce to some operators $\mathcal{O}_i \subseteq \mathcal{P}_j$. For an essential coupling $\bar{\mathbf{g}}_i(k)$ with canonical mass dimension $d_{\bar{\mathbf{g}}}$, its dimensionless analog is $\mathbf{g}_i(k) = \bar{\mathbf{g}}_i(k)k^{-d_{\bar{\mathbf{g}}_i}}$. A theory for which all $\mathbf{g}_i$ approach a finite fixed point will feature observables that are free from possible divergences at high energies, and thus, such observables remain finite [26].

Proposition 2.1 (Weinberg, 1979 ([26])). *Let $\{\mathbf{g}_i(k)\}_{i=1,2,3,\dots}$ be the set of dimensionless essential coupling parameters of any QFT. A QFT is said to be* ***asymptotically safe*** *if*

$$\sup_{k\leq\infty} \mathbf{g}_i(k) < \infty, \qquad \lim_{k\to\infty} \mathbf{g}_i(k) = \mathbf{g}_i^* < \infty \quad \forall \quad i \in \mathbb{Z}. \tag{2.1.4}$$

The proposition 2.1 encodes the *asymtotic safety conjecture*. That the fixed point $\mathbf{g}^*$ encodes the quantum scale invariance of the theory is due to the fact that $\mathbf{g}^* = \mathcal{G}(a;\mathbf{g}^*)$. Thus, asymptotic freedom (with vanishing $\mathbf{g}^*$) or asymptotic safety (with non-trivial $\mathbf{g}^*$) straightforwardly imply scale invariance.

Indeed, such regimes can be reached in theories with dimensionful parameters. The reason is that, a dimensionful canonical scaling of the parameter, $-d_{\bar{\mathbf{g}}_i}\mathbf{g}_i$, can be balanced by quantum scaling $\eta_i(\mathbf{g})$ due to quantum fluctuation, so that the associated β-functions vanish:

$$0 := \beta_{\mathbf{g}_i^*} = k\frac{\partial \mathbf{g}_i^*}{\partial k} = -d_{\bar{\mathbf{g}}_i}\mathbf{g}_i^* + \eta_i(\mathbf{g}_i^*), \tag{2.1.5}$$

and as such, a fixed point emerge at

$$\mathbf{g}_i^* = \frac{\eta_i}{d_{\bar{\mathbf{g}}_i}}. \tag{2.1.6}$$

There are, in fact, some examples where theories which are asymptotically free in their critical dimension d_{crit}, where the coupling has zero canonical dimension, are asymptotically safe in $d = d_{crit} + \epsilon$ dimensions for $\epsilon > 0$ (cf. [57]). This is the case for Yang-Mill theory in $d = 4 + \epsilon$ dimensions where the structure of the 1-loop β-function of the gauge coupling parameter is

$$\beta_{gYM} = -\gamma g_{YM}^3 + \frac{\epsilon}{2} g_{YM} + \mathcal{O}\left(g_{YM}^5\right). \tag{2.1.7}$$

The triumph of asymptotic freedom is in the appearance of the negative 1-loop cooefficient of the β-function where $\gamma > 0$ is realized for vanishing ϵ. In $d = 4+\epsilon$, asymptotic safety is realized in a structure where the term $\frac{\epsilon}{2} g_{YM}$ in the β-function compete with the 1-loop term, so that fixed points appear at

$$g_{YM}^* = 0 \ \text{(Free)} \ \ \textit{and} \ \ g_{YM}^* = \sqrt{\frac{\epsilon}{2\gamma}} \ \text{(Safe for } \gamma > 0). \tag{2.1.8}$$

g_{YM}^* gaurantees scale invariance of the $d = 4+\epsilon$ Yang-Mill theory at very high energy, and thus, provide its UV-completion.

2.1.2 Local behavior of the RG flow

In order to determine the local behavior of the RG flow, we consider an infinitesimal change

$$\delta\mathbf{g}_i = \mathbf{g}_i - \mathbf{g}_i^* = \mathcal{G}(a;\mathbf{g}_i) - \mathcal{G}(a;\mathbf{g}_i^*), \tag{2.1.9}$$

which allows one to linearize the RG flow in the vicinity of the RG fixed point where β-functions vanish. Accordingly,

$$\beta_{\mathbf{g}_i} = \beta_{\mathbf{g}_i}\Big|_{\mathbf{g}_i=\mathbf{g}_i^*} + \sum_j \left(\frac{\partial \beta_{\mathbf{g}_i}}{\partial \mathbf{g}_j}\right)\Big|_{\mathbf{g}_i=\mathbf{g}_i^*} \delta\mathbf{g}_j + \mathcal{O}\left(\delta\mathbf{g}_i\right)^2, \tag{2.1.10}$$

$$= 0 + \sum_j \Theta_i^j \delta\mathbf{g}_j + \mathcal{O}\left(\delta\mathbf{g}_i\right)^2, \tag{2.1.11}$$

where

$$\Theta_i^j = \sum_j \left(\frac{\partial \beta_{\mathbf{g}_i}}{\partial \mathbf{g}_j}\right)\Big|_{\mathbf{g}_i=\mathbf{g}_i^*}. \tag{2.1.12}$$

is the stability matrix. The classification of the RG flow and thus, the relevance of the coupling in the fixed point regime is done by determining the eigenvalues of Θ_i^j. Since there is no reason to suggest that Θ_i^j is symmetric, Θ_i^j is not in general diagonalizable, so that one will have to distinguish between the left and right eigenvector. However, for our purpose, the right eigenvectors $\mathbf{v}_i^\alpha$ and the corresponding eigenvalue $-\theta_\alpha$ are sufficient, so that

$$\Theta_i^j \ \mathbf{v}_j = -\theta_\alpha \mathbf{v}_i^\alpha, \quad for \quad \alpha = 1, 2, 3 ... \sup[i, j]. \tag{2.1.13}$$

It is useful to project the $\delta\mathbf{g}_i$ onto the right eigenvectors $\mathbf{v}_i^\alpha$ of stability matrix Θ_i^j, so that one introduce coordinates $\hat{\mathbf{g}}_i$

$$\hat{\mathbf{g}}^\alpha = \sum_i \delta\mathbf{g}_i \ \mathbf{v}_i^\alpha. \tag{2.1.14}$$

in theory space that are centered around the fixed point. The linearized flow equation thus gives

$$k\frac{\partial \hat{\mathbf{g}}^\alpha}{\partial k} = -\theta_\alpha \hat{\mathbf{g}}^\alpha, \tag{2.1.15}$$

for which the solution of (2.1.10) is

$$\hat{\mathbf{g}}^\alpha(k) = c_\alpha \left(\frac{k}{k_0}\right)^{-\theta_\alpha}. \tag{2.1.16}$$

where c_α is a dimensionless constant of integration and θ_α is the critical exponent. From (2.1.14), it is straightforward to re-express (2.1.16) as

$$\mathbf{g}_i - \mathbf{g}_i^* = \delta\mathbf{g}_i = \sum_\alpha \mathbf{v}_i^\alpha \hat{\mathbf{g}}^\alpha(k), \tag{2.1.17}$$

so that

$$\mathbf{g}_i = \mathbf{g}_i^* + \sum_\alpha c_\alpha \ \mathbf{v}_i^\alpha \left(\frac{k}{k_0}\right)^{-\theta_\alpha}. \tag{2.1.18}$$

In the following, we analyse the local behaviour of the RG flow in the neigbourhood of the fixed point $\mathbf{g}_i^*$.

SUMMARY OF RG-FLOW IN $\mathbf{g}_i^*$ NEIGHBOURHOOD

- First, we note that θ_α is in general a $\mathbb{C}$-value, so that it assumes the form

$$\theta_\alpha = \mathbf{Re}\left(\theta_\alpha\right) \pm i \ \mathbf{Im}\left(\theta_\alpha\right). \tag{2.1.19}$$

- **Re** (θ_α) controls the local direction of the RG flow in the neigbourhood of $\mathbf{g}_i^*$. In particular, it describes the growth or decay of the dimensionless coupling. This is obvious from (2.1.18)
- **Im** (θ_α) controls the spiral nature of the RG flow in the fixed point regime.
- Table 2.1 highlights the local behavior of the RG flow in the neighbourhood of $\mathbf{g}_i^*$.

Local behavior of the RG flow in the neighbourhood of $\mathbf{g}_i^*$		
Critical Exponent	Direction of RG Flow	Comment on Parameter c_α
Re $(\theta_\alpha) > 0$	Relevant: **UV**-attractive direction	c_α are free parameter that must be fixed by experiment in the Infrared
Re $(\theta_\alpha) = 0$	Marginal: retain the first non-vanishing corrections to the coupling constants in order to determine whether the RG flow, towards the UV, approaches $\mathbf{g}_i^*$ or diverges away from it. If $\mathbf{g}_i^*$ is reached, coupling is marginally relevant, otherwise, it is marginally irrelevant	c_α assume relevant associated input after further analysis
Re $(\theta_\alpha) > 0$	Irrelevant: **UV**-repulsive direction	Reaching the fixed is up to setting the corresponding $c_\alpha = 0$, thus, no free parameter is associated to an irrelevant direction.

Table 2.1: Analysis of RG flow in the fixed point regime

- Starting from (2.1.13), we take the determinant of both side

$$\left| \sum_j \left(\frac{\partial \beta_{\mathbf{g}_i}}{\partial \mathbf{g}_j} \right) |_{\mathbf{g}_i = \mathbf{g}_i^*} \ \mathbf{v}_j \right| = \left| -\theta_\alpha \mathbf{v}_i^\alpha \right|. \tag{2.1.20}$$

  Recognising (2.1.5) and using the property that $\det(AB) = \det(A)\det(B)$ for square matrices A and B, one can straightforwardly show that

$$\theta_i \simeq d_{\bar{\mathbf{g}}_i} - \left. \frac{\partial \eta_i(\mathbf{g}_i)}{\partial \mathbf{g}_i} \right|_{\mathbf{g}_i = \mathbf{g}_i^*}. \tag{2.1.21}$$

  The contribution $\left. \frac{\partial \eta_i(\mathbf{g}_i)}{\partial \mathbf{g}_i} \right|_{\mathbf{g}_i = \mathbf{g}_i^*}$ is called the anomalous dimension around the UV fixed point. The running of the anomalous dimension stops at the fixed point and the realized critical exponent gaurantees universality. The critical exponent θ_i is related to the canonical mass dimension $d_{\bar{\mathbf{g}}_i}$ of the coupling. For asymptotic freedom where $\mathbf{g}_i^* = 0$, the contribution from the anomalous dimension vanishes, so that $\theta_i = d_{\bar{\mathbf{g}}_i}$. Critical exponent associated to the non-trivial fixed point of asymptotic safety receive an extra contribution from the anomalous dimension. (2.1.21) suggests that the canonical mass dimension will continue to dominate, unless quantum effect become very large.

- A viable fixed point features only a finite number of UV attractive directions exist in the neighbourhood of the non-trivial fixed point, and others are increasingly UV repulsive. The RG flow determines which interaction monomials are relevant in the neighbourhood of the FP and thus, defines the dynamics. As a consequence, interacting fixed points can be predictive since there are only a few relevant couplings with positive mass dimension, and others have increasingly negative canonical mass dimension that render them irrelevant.

2.2 RG Machine

To investigate the existence of the non-trivial fixed point and thus, asymptotic safety, qualitative analysis of RG flows is usually done through the β-functions. The functional Renormalization Group (FRG) provides a method/tool with which the extraction of β-functions is done efficiently. By introducing a UV cutoff Λ and an IR cutoff k, the basic input is the interpolating scale dependent effective average action

$$\Gamma_k\left(\varphi, \mathbf{g}_i(k)\right) = \sum_i \bar{\mathbf{g}}_i(k)\mathcal{O}_i\left(\varphi\right) = \sum_i \mathbf{g}_i(k)k^{d_{\bar{\mathbf{g}}_i}}\mathcal{O}_i\left(\varphi\right), \tag{2.2.1}$$

which contains physics at scale $k \in [0, \Lambda]$ such that

$$\Gamma_{k\to 0} = \Gamma_{\text{eff}}, \qquad \Gamma_{k\to\Lambda} \simeq S_{\text{bare}}. \tag{2.2.2}$$

$\mathcal{O}_i(\varphi)$ are field monomials allowed by the underlying symmetry of the classical action $S[\phi, \mathbf{g}_i]$ associated with essential dimensionless couplings $\mathbf{g}_i = \bar{\mathbf{g}}_i(k)k^{-d_{\bar{\mathbf{g}}_i}}$, where $\varphi = \langle\phi\rangle$. One can construct the interpolating action by means of a modified Legendre transform

$$\Gamma_k[\varphi] = \sup_j \left(\int j\varphi - \ln Z_k\right) - \Delta S_k[\varphi], \tag{2.2.3}$$

using a scale dependent generating functional

$$Z_k[j] := \int_\Lambda \mathcal{D}\phi \;\; \exp\left(S[\phi] - \Delta S_k[\phi] + \int dx \; j\phi\right), \tag{2.2.4}$$

where the infrared cutoff term

$$\Delta S_k[\phi] = \frac{1}{2}\int d^d x \phi \mathcal{R}_k(\Delta)\phi, \tag{2.2.5}$$

features the regulator $\mathcal{R}_k(\Delta)$ chosen such that it suppresses modes of momentum less than k^2 and only the high energy modes with momentum greater than k^2 contribute to (2.2.4). Δ is the cutoff operator with eigenvalue z. On a flat background, z is simply momentum squared p^2, and thus, $\mathcal{R}_k(z)$ has dimension of mass squared. The choice of $\mathcal{R}_k(z)$ is up to some certain requirements, namely,

- $\mathcal{R}_k(z)$ is a monotonically decreasing function of z for a fixed k;
- $\mathcal{R}_k(z) \to \infty$ for $k \to \infty$ such that $\Gamma_{k\to\infty} \to S_{\text{bare}}$;
- $\lim_{k\to 0}\mathcal{R}_k(z) = 0 \quad \forall \; z$, so that the limit $Z_{k\to 0}[j] = Z[j]$ and $\Gamma_{k\to 0} = \Gamma_{\text{eff}}$ are automatically realized.
- For $z > k^2$, $\mathcal{R}_k$ typically goes to zero. At $z = 0$, $\mathcal{R}_k(0) = k^2$.

Typical choices of $\mathcal{R}_k(z)$ in the literature have the following form

$$\mathcal{R}_k(z) = k^2 r(y) \quad \text{with} \quad y = z/k^2, \tag{2.2.6}$$

with dimensionless cutoff profile

$$r(y) = \begin{cases} \frac{y}{e^y - 1}, & \text{Exponential cutoff} \\ \lim_{\hat{R}\to\infty}\hat{R}\theta(1-y), & \text{Sharp cutoff[58];} \\ (1-y)\theta(1-y), & \text{Litim optimized cutoff[63].} \end{cases} \tag{2.2.7}$$

The change of (2.2.3) under a change of scale is given by an exact renormalization group equation

$$d_t\Gamma_k := k\frac{\partial\Gamma_k}{\partial k} = \frac{1}{2}\,\mathrm{Tr}\left[\left(\frac{\delta^2\Gamma_k}{\delta\varphi\delta\varphi}+\mathcal{R}_k\right)^{-1}\partial_t\mathcal{R}_k\right]. \tag{2.2.8}$$

This is the Wetterich flow equation [65]. With the Wetterich equation, we have a FRGE machine capable of zooming through different energy scales. Wetterich equation has a 1-loop structure and $\left(\frac{\delta^2\Gamma_k}{\delta\varphi\delta\varphi}+\mathcal{R}_k\right)^{-1}$ represents the exact propagator of the theory rather than the perturbative one. Taking $z = p^2$, figure 2.1 shows the influence of $\mathcal{R}_k$ on the flow equation for which the trace of the eigenmodes of the propagator is peaked for modes with eigenvalues close to k^2. By construction, $\mathcal{R}_k$ in the propagator guarantees the IR regularization while the $\partial_k\mathcal{R}_k$ implement the UV regularization since $\mathcal{R}_k$ typically goes to zero for $z > k^2$. Thus, the Wetterich equation is automatically UV and IR finite. Moreover, given an initial condition $\Gamma_{k_{ini}}$, the Wetterich equation induces a vector field in the theory space. Although generating this vector space is independent of knowing the full microscopic action, the Wetterich equation does allow us to seek for a subspace of $\{\Gamma_k\}_{k\in\mathbb{R}}$ where viable microscopic dynamics lives.

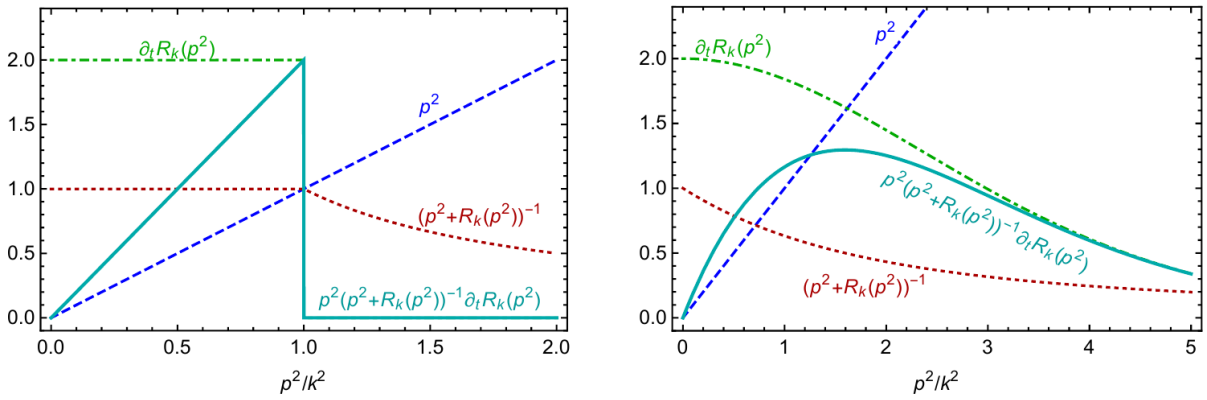

Figure 2.1: Behaviour of the full flow equation (turquoise continuous) for $z = p^2$. It features the influence of the UV regulator $\partial_t\mathcal{R}_k$ (green dot-dashed) and the inverse propagator $\frac{\delta^2\Gamma_k}{\delta\varphi\delta\varphi}+\mathcal{R}_k$ for $\frac{\delta^2\Gamma_k}{\delta\varphi\delta\varphi} = p^2$. Trace Tr becomes a momentum integral with measure p^2 in $d = 4$(blue dashed). Using the optimized cutoff (left panel) and the exponetial cutoff (right panel), the integrand in the flow equation is peaked at $\frac{z}{k^2}\approx 1$. [52]

The solution to the flow equation (2.2.8) is essentially the RG trajectory in theory space provided by the extracted β-function. We can see this directly by taking the scale derivative of the effective average action (2.2.1):

$$k\frac{\partial\Gamma_k}{\partial k} = k\frac{\partial}{\partial k}\sum_i \mathbf{g}_i(k)k^{d_{\mathbf{g}_i}}\mathcal{O}_i\,(\varphi) \tag{2.2.9}$$

$$= \sum_i \left(\beta_{\mathbf{g}_i}+\mathbf{g}_i d_{\mathbf{g}_i}\right)k^{d_{\mathbf{g}_i}}\mathcal{O}_i. \tag{2.2.10}$$

The extracted β-functions allow us to investigate asymptotic safety and thus, the existence of the non-trivial fixed point. We should emphasize that, in spite of the dependence of the RG trajectory on the regulator $\mathcal{R}_k$, the final end point, and thus, the fixed point is independent of $\mathcal{R}_k$.

2.3 Status of AS in Pure Gravity

There exists a growing collection of evidence that a scale invariant regime of the RG flow could provide an adequate description of quantum gravity, and thus could reveal the fundamental structure of quantum spacetime [58]-[62]. We shall briefly recall here those indication pertaining to the pure gravity system. More elaborated review on the status of asymtotic safety for gravity and matter is contained in [51, 52].

First, in $d = 2$ spacetime dimensions, Newton's coupling is dimensionless and thus, the Einstein-Hilbert action is power counting renormalizable in perturbation theory. However, the Einstein-Hilbert term is a topologically invariant term in two dimensions. In $d = 2 + \epsilon$ dimensions, the structure of the flow equation of the dimensionless Newton's coupling $g = k^{\epsilon}G$ is

$$\beta_g := k\frac{d}{dk}g = -\gamma g^2 + \epsilon g. \tag{2.3.1}$$

This structures remain the same for different kind of matter monomial added to the Einstein-Hilbert term. However, γ also depends on the choice of the matter added to the Einstein-Hilbert term[66, 67]. It has been shown that γ depend on parameterization of metric fluctuations in terms of a background metric $\bar{g}_{\mu\nu}$(cf [68],[69]). As a consequence, fixed points appear at

$$g^* = 0 \ \text{(Free)} \quad \text{and} \quad g^* = \frac{\epsilon}{\gamma} \ \text{(Safe for } \gamma > 0), \tag{2.3.2}$$

due to balance of the quantum fluctuations and canonical scaling term. The challenge is then whether a non-trivial fixed point can be realized for $\epsilon \geq 2$.

The theory space is very large, and spanned by many interaction monomials, ranging from the cosmological constant to infinitely many higher-order dervative terms. As such, an analysis of the full gravity action on the theory space is currently out of hand. Instead, one starts with a truncated gravity action as an initial condition, for which typically only a finite number of interaction monomial are retained.

2.3.1 Einstein-Hilbert Truncation

At the level of the Einstein-Hilbert truncation, the gauge fixed gravity action in d dimensions is given by

$$\Gamma_{EH}[g] = -\frac{1}{16\pi G}\int d^dx\ \sqrt{-g}\ (R - 2\Lambda) + S_{gf} + S_{gh}, \tag{2.3.3}$$

where the gauge-fixing term is typically chosen as

$$S_{gf} = \frac{1}{32\pi\alpha G}\int d^dx\sqrt{-\bar{g}}\ \bar{g}^{\mu\nu}F_\mu F_\nu, \quad F_\mu = \bar{D}^\kappa h_{\kappa\mu} - \frac{1+\beta}{d}\bar{D}_\mu h, \tag{2.3.4}$$

with the corresponding Faddeev-Popov ghost term

$$S_{gh} = -\sqrt{2}\int d^dx\sqrt{-\bar{g}}\ \bar{c}_\mu\left(\bar{g}^{\mu\rho}\left(\bar{D}^\kappa g_{\rho\nu}D_\kappa + \bar{D}^\kappa g_{\kappa\nu}D_\rho\right) - \frac{1+\beta}{2}\bar{D}^\mu D_\nu\right)c^\nu. \tag{2.3.5}$$

By promoting (G, Λ) to running couplings $(G(k), \Lambda(k))$, the analysis of the fixed point structure of the dimesnionless Newton's coupling $g(k) = k^{d-2}G(k)$ and that of the dimensionless cosmological constant $\lambda(k) = k^{-2}\Lambda(k)$ has been done for an arbitrary d dimensions through their

respective β-functions [58]. Using a sharp cutoff, the β-functions in $d = 4$ amount to

$$\begin{aligned} \beta_g &= (2+\eta)g, \\ \beta_\lambda &= -(2-\eta)\lambda - \frac{g}{\pi}\left[5\ln(1-2\lambda) - 2\zeta(3) + \frac{5}{2}\eta\right], \end{aligned} \tag{2.3.6}$$

with anomalous dimension

$$\eta = -\frac{2g}{6\pi + 5g}\left[\frac{18}{1-2\lambda} + 5\ln(1-2\lambda) - \zeta(2) + 6\right]. \tag{2.3.7}$$

Figure 2.2 describes the flow (2.3.6). The appearance of a pole at $\lambda = \frac{1}{2}$ means the flow is restricted to the plane

$$-\infty \leq g \leq \infty, \quad -\infty \leq \lambda \leq \frac{1}{2}. \tag{2.3.8}$$

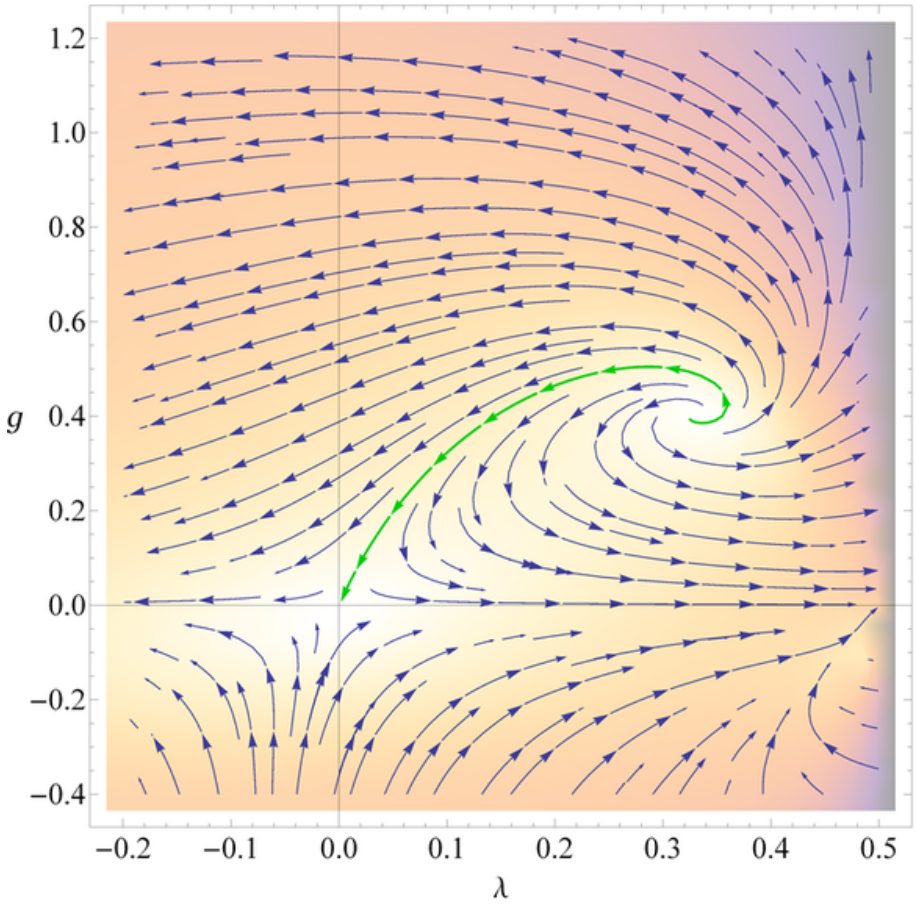

Figure 2.2: Flow diagram for the Einstein-Hilbert truncation in d = 4 for a sharp cutoff. The direction of arrow is towards the IR. The dark region beyond $\lambda = 1/2$ is the region where β_λ diverges. Phase diagram with optimized cutoff and other choices of cutoffs, parametrization and choices of gauge exists, with the qualitative picture of the UV fixed point the same [68].

The fixed points coordinate are:

$$\begin{aligned} &\textbf{Trivial Fixed Point:} && (g_*, \lambda_*) = (0,0) && \text{for} && \theta_1 = 2, \theta_2 = 2 - d = -2, \\ &\textbf{Non-Trivial Fixed Point:} && (g_*, \lambda_*) = (0.403, 0.330) && \text{for} && \theta_\pm = 1.941 \pm i3.147 \end{aligned} \tag{2.3.9}$$

- Fixed point at the origin governs the limit $k \to 0$. The corresponding critical exponent $\theta_{1,2}$ shows there there is one relevant direction and one irrelevant directions in the neighbourhood of (0,0).
- The non-trivial fixed point governs the UV-completion ($k \to \infty$) of gravity. Those trajectories that emerge from the non-trivial fixed point embody renormalized theories, one of which could be realized in nature [70]. These trajectories live in the upper half-space of figure 2.2, which signifies positive Newton's couplings. The spiral nature of the trajectories in the vicinity of the non-trivial fixed point is due to the non-vanishing imaginary part of the critical exponent which is a $\mathbb{C}$-value.
- As (g, λ) approaches the non-trivial (g_*, λ_*), scaling behavior of the dimensionful (G, Λ) at high energies is fixed as

$$\lim_{k\to\infty} G(k) = k^{-2} g_*, \qquad \lim_{k\to\infty} \Lambda(k) = k^2 \lambda_*. \tag{2.3.10}$$

- The figure also features a separatrix (green) indicating a trajectory running from the UV fixed point into an IR fixed point, reflecting the fact that the short and the long distance gravitational physics are related through renormalization group flow, i.e., we can realize the limits

$$\lim_{k\to 0} G(k) = G_0, \qquad \lim_{k\to 0} \Lambda(k) = \Lambda_0. \tag{2.3.11}$$

  They are the IR values of the Newton coupling and the cosmological constant. More cross over analysis of some classes of trajectories is contained in [58].
- While the details of the RG trajectory depend on the choice of regulator $\mathcal{R}_k$, we have emphasized that the fixed point structure is independent of the regulator choice. In fact, using other regulators, the crossover pattern is also independent of the choice of regulator (cf. [68]). As such, it is phenonmenological useful to analytically approximate the RG trajectories as a family of curves[71]

$$\begin{cases} g(k) = \frac{k^2 G_0}{1 + k^2/g_*}, \\ \\ \lambda(k) = \frac{g_* \lambda_*}{g} \left[(5+e) \left(1 - \frac{g}{g_*}\right)^{\frac{3}{2}} - 5 + 3g/(2g_*)(5 - g/g_*) \right], \end{cases} \tag{2.3.12}$$

  which captures the universal features of the RG flow.

Fixed points have been found for many choices of gauge fixing conditions. For instance, using Feynman gauge alongside with Litim's optimized cut-off, β-functions in an arbitrary d spacetime dimensions read[60]

$$\beta_g = \frac{(d-2) g P_2}{P_2 + 4(d+2)g}, \qquad \beta_\lambda = (d - 2 + \eta)g = \frac{P_1}{P_2 + 4(d+2)g}, \tag{2.3.13}$$

where

$$\begin{aligned} P_1 &= -16\lambda^3 + 4\lambda^2(4 - 10dg - 3d^2 g + d^3 g) + 4\lambda(10dg + d^2 g - d^3 g - 1) \\ &\quad + d(2+d)(d - 16g + 8dg - 3)g, \\ P_2 &= 8(\lambda^2 - \lambda - dg) + 2. \end{aligned} \tag{2.3.14}$$

The graviton anomalous dimension

$$\eta = \frac{(d-2)(d+2)g}{(d-2)g - 2(\lambda - \frac{1}{2})^2} \tag{2.3.15}$$

vanishes in $d = 2$ spacetime dimension, for diverging λ or vanishing g. Realization of a non-trivial gravitational fixed point imply $\eta_* = 2 - d$, which indicate that Newton's coupling is dimensionless in $d = 2$.

In the limit of vanishing λ, the flow of the dimensionless Newton's coupling become

$$\beta_g = \frac{(1 - 4dg)(d - 2)g}{1 + 2(2 - d)g}, \tag{2.3.16}$$

for which two fixed points are realized:

$$\begin{aligned} g^*_{free} &= 0 \qquad \text{for} \quad \theta_{free} = 2 - d, \\ g^*_{safe} &= \frac{1}{4d} \qquad \text{for} \quad \theta_{safe} = 2d\frac{d-2}{d+2}. \end{aligned} \tag{2.3.17}$$

For non-vanishing λ, we can seek for non-trivial fixed point for which β_g and β_λ in (2.3.13) vanish simultaneously. For $d \geq \frac{1}{2}\left(1 + \sqrt{17}\right)$, a non-vanishing fixed point is realized at

$$\lambda^*_{safe} = \frac{d^2 - d - 4 - \sqrt{2d(d^2 - d - 4)}}{2(d - 4)(d + 1)}, \qquad g^*_{safe} = \frac{2\Gamma\left(\frac{d}{2} + 2\right)(4\pi)^{d/2-1}}{d^2 - d - 4}\lambda^{*2}_{safe}. \tag{2.3.18}$$

In $d = 4$, the two critical exponents are complex, but with positive real parts, with similar values to (2.3.9)

$$\theta_\pm = \frac{5}{3} \pm i\frac{1}{3}\sqrt{167} = 1.667 \pm 4.308. \tag{2.3.19}$$

Separatrix for flow 2.3.13 is shown in figure 2.3. That one can realize the low low energy physics from the high energy analog makes the UV fixed point also suitable for the asymptotic safety requirement.

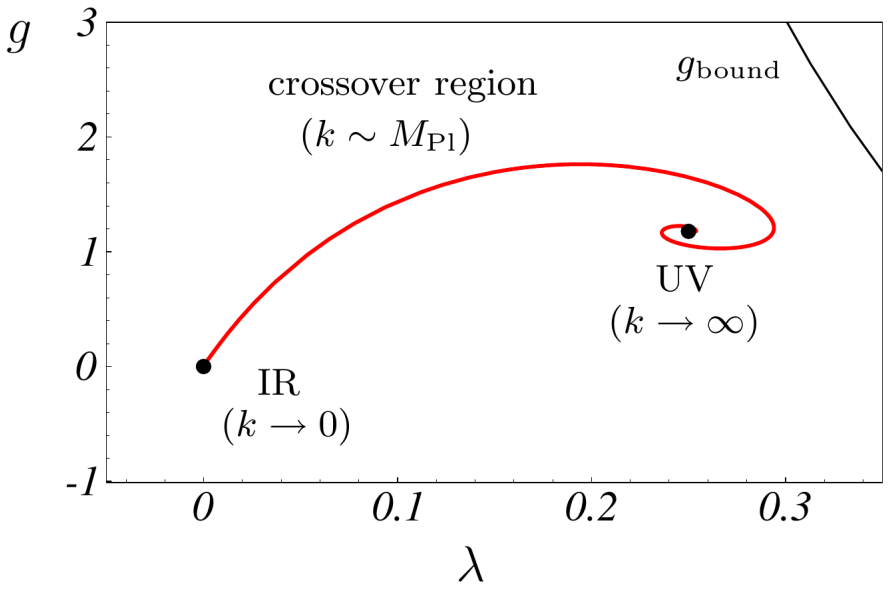

Figure 2.3: The separatrix in four dimensions. Some trajectories terminate at the boundary g_{bound}. [60].

To make a comparism with the evidence from the $2 + \epsilon$ expansion, let us take for instance the flow equation arising from using de Donder gauge fixing parameters $\alpha = 1, \beta = \frac{d}{2} - 1 = 1$ in

$d = 4$. The structure of the β-functions for type **Ia** regulator takes the form [61]

$$\begin{aligned}\beta_g &= 2g - \frac{g^2}{3\pi}\frac{11 - 18\lambda + 28\lambda^2}{(1-2\lambda)^2 - \frac{1+10\lambda}{12\pi}g},\\ \beta_\lambda &= -2\lambda + \frac{g}{6\pi}\frac{3 - 4\lambda - 12\lambda^2 - 56\lambda^3 + \frac{107-20\lambda}{12\pi}g}{(1-2\lambda)^2 - \frac{1+10\lambda}{12\pi}g}.\end{aligned} \tag{2.3.20}$$

In the absence of cosmological constant, the analysis of the flow of the Newton's coupling is straightforward. The β-functions at the leading order takes the form

$$\beta_g = -\frac{11g^2}{3\pi} + 2g. \tag{2.3.21}$$

This structure is the same to that we saw from the $2 + \epsilon$ expansion (cf. (2.3.1)) with the value of γ now $\frac{11}{3\pi}$ due to our analysis at $d = 4$ spacetime dimensions which corresponds to $\epsilon = 2$. Figure 2.4 provides a clear picture of the realized fixed point of the flow and scale dependence of the Newton coupling.

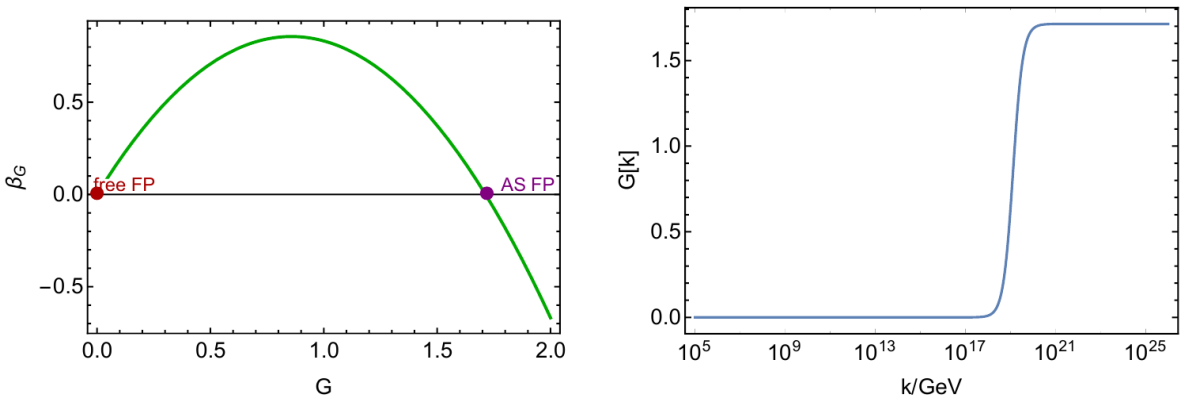

Figure 2.4: On the left is the flow of the β-function of dimensionless Newton's coupling. A UV repulsive free (red dot) and safe (purple) UV attractive fixed point are realized. On the right, the scale dependence of the Newton coupling according. Scale invariance of the AS coupling become obvious at energy of the order of 10^{19}GeV and beyond [52].

2.3.2 Beyond Einstein-Hilbert Truncation

Improving the truncation of the gravity action is necessary in order to show reliability of the existence of asymptotically safe fixed point. In [62], the truncation subspace (2.3.3) was enhanced to

$$\Gamma^{grav}[g] = \int d^4\sqrt{-g}\left(\frac{1}{16\pi G}(-R + 2\Lambda) - \frac{\omega}{3\sigma}R^2 + \frac{1}{2\sigma}C_{\mu\nu\rho\sigma}C^{\mu\nu\rho\sigma} + \frac{\theta}{\sigma}E\right) \tag{2.3.22}$$

where $E = R^2 - 4R_{\mu\nu}R^{\mu\nu} + R_{\mu\nu\rho\sigma}R^{\mu\nu\rho\sigma}$ is the Gauss-Bonnet term, which is essentially a topological invariant term in $d = 4$ and thus, has no influence on the overall dynamics since its variation with respect to the metric vanishes. As such, one can rearrange the action, so that one just has to account for four essential couplings. In particular, a non-trivial fixed point requires that none of ω and θ must be infinite and a combination of σ with any of ω or θ must be non-zero.

For this kind of theory, perturbative renormalizability is already a feature that makes quadratic gravity very attractive at the expense of the appearance of a spin-2 massive ghost which may spoil unitarity [20]. In the analysis, perturbative fixed points were recovered. In addition to this, analysis shows that the inclusion of tensor structures such as R^2, $R_{\mu\nu}R^{\mu\nu}$, $C_{\mu\nu\rho\sigma}C^{\mu\nu\rho\sigma}$ is campatible with the existence of a non-trivial fixed point. In fact, it increases the number of UV-attractive direction to three.

The appearance of the massive ghost is not peculiar to adding higher order of the curvature term to the Einstein-Hilbert term. In fact, this scenario also occur if one considere gravity-matter system to circumvent the situation. In particular, while the non-Gaussian fixed points in the matter sector may even provide a higher predictive power[72], the non-vanishing gravitational interactions may induce potentially dangerous higher-derivative terms, that are associated to the Ostrogradski ghost and thus the violation of perturbative unitarity[73], into the fixed point action. Thus, what remains is to verify the compatibility of asymptotic safety with perturbative unitarity.

There are few attempts to catch this ghost. For example, more recently, a gravity-scalar system was studied, where the truncation subspace (2.3.3) was enhanced by N_s scalar fields action

$$\Gamma^{\varphi}[\varphi, g] = \frac{1}{2} Z \sum_{i=1}^{N_s} \int d^4x\sqrt{-g}\ \varphi^i \left[\Delta + \kappa\Delta^2\right] \varphi_i. \tag{2.3.23}$$

$\Delta = -g^{\mu\nu}D_\mu D_\nu$, Z is the wavefunction renormalization and κ is a scale dependent coupling of the higher-derivative contribution to the scalar propagator. In a Fourier basis, the associated scalar propagator has the structure

$$G(p) = \frac{1}{Z}\left(\frac{1}{p^2} - \frac{1}{p^2 + \kappa^{-1}}\right), \tag{2.3.24}$$

which features a massless state, and a Ostrogradski ghost state of mass $m = \kappa^{-1}$ leading to instability of the theory. Obviously, (2.3.25) suggests that pushing the mass of the Ostrogradski ghost to infinity would lead to decoupling of the ghost from the theory. The study in [74] shows that there exist a fixed point solution for which $\kappa_* = 0$ is realized for all N_s, thereby implying such a decoupling of the ghost since its mass is ultimately pushed to infinity at the fixed point. This suggests that a non-trivial fixed point would render the gravity-matter system asymptotically safe and free of ghosts for now, it is not yet known if this analysis holds for a more general type of gravity-matter system.

There are other studies involving truncations beyond Einstein-Hilbert whose interest is in checking the relevance of the higher terms. For example, the effect of adding the Goroff-Sagnotti two-loop counterterm[75]

$$\Gamma^{GS} \sim \int d^4x\sqrt{-g}\ C_{\mu\nu}{}^{\kappa\lambda} C_{\kappa\lambda}{}^{\rho\sigma} C_{\rho\sigma}{}^{\mu\nu}, \tag{2.3.25}$$

to the Einstein-Hilbert truncation has been studied. The study in [76] shows that the C^3 operator approaches a non-trivial fixed point in the UV and becomes irrelevant at the UV fixed point, although in perturbation theory, it appears as a counterterm with a new free parameter.

Physical Application

The Asymptotic safety paradigm has found various application in gravity. The structure of quantum spacetime has been investigated([77],[78]), and departure from a smooth spacetime manifold, that characterizes the formulation of classical gravity, is expected at short distance scales. In particular, the scale k is identified with the scale of the geometry, so that the metric is a scale dependent object. An interpretation of this is that, as we zoom into the spacetime geometry associated with resolution k by δk, new spacetime geometry with the metric $g_{\mu\nu}(k+\delta k)$ appears. Asymptotic safety therefore suggests that there ought to exist an invariant system of the world at some extremely high resolution scale where spacetime may be characterized by a fractal-like structure, with spectral properties of spacetime changing on various typical length scales[79].

That there should exist a scale invariant geometry of spacetime allows one to re-investigate the structure of black hole([80]-[87]) and also gain insight about the final stage of black hole evaporation([88]-[89]). Further application have been found in cosmology([90]–[97]).

Chapter 3

Black Holes in Asymptotic Safety

General relativity breaks down in physically relevant settings, but this breakdown is a natural feature of all classical gravity theories. For black hole solutions of $d = 4$ gravity theories, the unavoidable classical singularity led to breakdown in future predictability and furthermore conceptual issues in attempts to understand the final stages of black hole evaporation, where the interplay between the singularity and Hawking radiation cannot be ignored. Regular black hole solutions in $d = 4$ gravity theories have been proposed, with a basic aim of replacing the black hole singularity with a nonsingular de-Sitter core, thereby inducing an inner horizon in addition to the outer horizon [11]. However, it is not clear if such black holes are viable as the inner horizon may be unstable against perturbation [18]. This suggests that we must look beyond the effective field description of gravity in order to seek for a possible resolution of the classical singularity – a fundamental theory of gravity to the rescue. Although it is not guaranteed, such a fundamental theory would lead to a possible resolution to various pathologies within the classical description of gravity.

Within the asymptotic safety paradigm, the exploration of quantum spacetime becomes possible through the RG-improvement scheme. In this scheme, asymptotic safety encodes the quantum effect in the gravitational effective average action Γ_k which satisfies the exact Wetterich equation (2.2.8). This feature allows to investigate the quantum corrections to classical physics by implementing the effect of scale-dependent parameters either at the level of the classical Lagrangian, classical field equations, or the classical solutions to the field equation. As a consequence, this procedure has been exploited in the study of the structure and mechanics of quantum improved black holes ([80]-[89])

In this chapter, we shall detail the practical RG-improvement schemes and use it to discuss the developments and status of black holes within asymptotic safety paradigm.

3.1 Physical RG-improvement schemes

Starting from the Einstein-Hilbert truncation of the dynamics, there are two different approaches to implementing the effects of scale-dependent parameters on black holes physics. One approach is to renormalization group (RG) improve the classical black hole solution by promoting the classical coupling into scale-dependent couplings and then physically motivate a cutoff identification that allows for meaningful extraction of the quantum gravitational effect. Another approach is

to first obtain an improved gravitational theory that features scale dependent couplings and then seek for black hole solution of the improved field equation[98]. While we shall briefly outline the procedure of the second approach, our study will be based on the first framework. The first approach was advocated in the first study of RG-improved black holes[80], and it has been embraced in various other studies in gravity models, for example in cosmology (cf. [96]).

3.1.1 Solution of the Improved Field Equation

The procedure adopted here basically carries out the scale-setting of the system at the level of the classical Einstein-Hilbert action. By promoting (G, Λ) to scale dependent couplings $(G(k), \Lambda(k))$, the running action is

$$\Gamma_k[g] = \int_{\mathcal{M}} d^4x\sqrt{-g}\,\left(\frac{R-2\Lambda_k}{16\pi G_k} + \mathcal{L}_m\right) - \frac{1}{8\pi}\int_{\partial\mathcal{M}} d^3x\sqrt{-h}\,\frac{\mathcal{K}}{G_k}. \tag{3.1.1}$$

The corresponding quantum improved field equation is

$$G_{\mu\nu} = -g_{\mu\nu}\Lambda_k + 8\pi G_k T_{\mu\nu} - \Delta t_{\mu\nu}, \tag{3.1.2}$$

for which the coordinate dependence of the G_k may induce further contribution

$$\Delta t_{\mu\nu} = G_k\left(g_{\mu\nu}\Box - \nabla_\mu\nabla_\nu\right)\frac{1}{G_k} \tag{3.1.3}$$

to the energy momentum tensor $T_{\mu\nu}$. (3.1.3) assumes that a scale identification of k with a function of coordinate has been performed, such that $\nabla_\mu G_k \neq 0$. By insisting on conservation of the energy momentum tensor, $\nabla^\mu T_{\mu\nu} = 0$, one obtain the relation

$$R\,\nabla_\mu\left(\frac{1}{G_k}\right) - 2\nabla_\mu\left(\frac{\Lambda_k}{G_k}\right) = 0. \tag{3.1.4}$$

Equation (3.1.4) can in fact be used to derive a physical scale identification. Replacing the k-dependence of the couplings by a r-dependence, we can demand for a spherically symmetric metric (1.1.1) of (3.1.2), with the form

$$f(r) = 1 - 2\frac{\Sigma G(r)}{r} - \frac{l(r)}{3}r^2 \tag{3.1.5}$$

where Σ is assocated with the effective black hole mass, and $l(r)$ is associated with effective cosmological constant. One is then left with the task of solving independent differential equations assocated with the ansatz (3.1.5) of (3.1.2). This procedure was explored in [99]. In particular, a non-trivial solution of the improved field equations exist and it is dominated by the non-trivial fixed point of the induced flow of the scale dependent field equation.

3.1.2 RG-scheme at the Level of Classical Solution

The RG-improvement in this scheme is based on renormalization group improves the classical geometry at the level of the classical solution by using the beta functions obtained from asymptotically safe gravity to fix the scale-dependence of the parameters in the lapse function. The basic steps entail the following:

- The lapse function is a function depending on the coordinates and the coupling $\bar{\mathbf{g}}_i$, i.e. $f(r, \bar{\mathbf{g}}_i)$. Promote the coupling parameters to scale dependent quantities $f(r, \bar{\mathbf{g}}_i(k))$. For example, the geometry with lapse function (1.1.8) is of the form $f(r, G, \Lambda)$. This procedure results in a replacement $G \to G_k$ and $\Lambda \to \Lambda_k$.
- The coupling parameters are in general dimensionful. We focus on their dimensionless counterparts $\mathbf{g}_i(k) = \bar{\mathbf{g}}_i(k) k^{-d_{\bar{\mathbf{g}}_i}}$, e.g. $g_k = k^2\, G_k$, $\lambda_k = k^{-2}\, \Lambda_k$, through which their corresponding β-functions are expressed. In the fixed-point regime, the dimensionless coupling parameters are computed. The linearized flow away from the fixed point takes the form (cf. (2.1.18))
$$\mathbf{g}_i = \mathbf{g}_i^* + \sum_\alpha c_\alpha\, \mathbf{v}_i^\alpha \left(\frac{k}{k_0}\right)^{-\theta_\alpha}.$$
- The proceeding steps introduce a running RG-scale k into the lapse function, i.e. $f^*(r, \mathbf{g}_i^*, k, \theta_\alpha)$. We want the lapse function at the fixed point be scale invariant, and thus, independent of the scale k.
- The RG-improvement procedure then associates the scale k with a physical cutoff scale of the system. The relevant scale identification must be physically motivated. Once motivated and adopted, the fixed point lapse function of the quantum improved geometry is a pure function of r. With the exception of the coupling parameters which assume non-trivial values at the fixed point, the remaining parameters are free. Some of them are determined in the Infrared regime.

Our next aim is to physically motivate the relevant scale identification.

3.1.3 Physical Scale Setting

To physically motivate the cutoff identification, one needs to recognise the relevant degrees of freedom that encodes the scale dependence in the system. Earlier, we encountered the Newton's coupling G as a function of k, rather than r. We then introduce a function $\mathcal{R}_k$ as the regulator. While the regulator is a priori not physical, in many systems, external physical scales serve as an effective infrared regulator. For instance, the curvature scale can act as an effective cutoff scale, such that higher curvature means effectively larger momentum scale. We will assume that quantum effect become relevant near the singularity, such that one should associate k with a function of r. Note that the high degree of symmetry of the Schwarzschild black holes explicitly singles this out as a unique scale identification since all physical scales are function of r.

It is obvious that the coupling parameters are related to the scale k through their promotion to scale-dependent quantities, but the scale itself should be related to a physical cutoff scale. We will work here with $k(r)$. It has been advocated that this identification must be a diffeomorphism invariant one [80], so that it preserves the symmetry of the classical configurations arising from the classical field equations.We should thus construct $k(r)$ in a way that it embodies the requirements of coordinate invariance.

Let us emphasize here that asymptotic safety put a restriction on the form of any consistent scale identification. This consistency condition can be seen directly from (3.1.4), which is tantamount to (cf. [100])
$$R \left(\frac{1}{G_k}\right)' - 2\left(\frac{\Lambda_k}{G_k}\right)' = 0, \tag{3.1.6}$$

where the primes denote derivatives with respect to k. At the non-trivial fixed point, the Newton coupling and the cosmological constant scale as $g_k = k^2\, G_k$, $\lambda_k = k^{-2}\, \Lambda_k$, so that (3.1.6) yields an identification

$$R = 4\lambda_*\, k^2, \tag{3.1.7}$$

at the fixed point regime. This kind of identification is similar to the ansatz, $R = \xi\, k^2$ proposed in [101]–[104] and it is expected that this identification continues to dominate at the UV fixed point. This could in fact set a consistency requirement for any well motivated scale identification.

In [80], a scale identification of the form

$$k(r) = \frac{\xi}{d(r)}, \tag{3.1.8}$$

was motivated from the RG based computation of the Uehling correction to the classical Coulomb potential, $V_{cl}(r) = \frac{e^2}{4\pi r}$, where the charge e^2 was replaced by its scale-dependent analog,

$$e^2(k) = \frac{e^2(k_0)}{1 - \frac{e^2(k_0)}{6\pi}\, \ln\left(\frac{k}{k_0}\right)}, \tag{3.1.9}$$

and the IR renormalization scale identification $k \sim r^{-1}$ was adopted, leading to the quantum improved Coulomb potential

$$V(r) = -\frac{e^2(r_0^{-1})\left[1 + \frac{e^2(k_0)}{6\pi}\, \ln\left(\frac{k}{k_0}\right) + \mathcal{O}(e^4)\right]}{4\pi r}. \tag{3.1.10}$$

ξ is a constant parameter to be fixed by physics argument. Obviously, in the case of a black hole, $d(r)$ must be a coordinate invariant quantity for the scale identification (3.1.8) to satisfy the requirement that it must preserves the symmetry of the classical configurations. In the following, we list scale matchings motivated in the literature.

- In [80], k was matched with the inverse of the diffeomorphism invariant proper distance $d(r)$, measured from a coordinate r to the center of the black hole along a radial curve $\mathcal{C}$. Obviously, there are infinitely many such curve $\mathcal{C}$. In this case, $dt = d\theta = d\phi = 0$. As such, $d(r)$ is defined as

$$d(r) = \int_{\mathcal{C}} \sqrt{|ds^2|} \tag{3.1.11}$$

$$= \int_0^r dr'\, |f_{\rm cl}(r')|^{-1/2} \tag{3.1.12}$$

  An alternative to this identifies the cutoff with the proper time measured by a freely falling observer. This identification lead to a similar result.

  A conceptual issue with this is that $d(r)$ is not well defined at the event horizon where $f(r) = 0$. Furthermore, the radial curve $\mathcal{C}$ cannot be well tracked in the high curvature regime since there is geodesic incompleteness in such region of spacetime.

- In [84], some distance functions $d(r)$ were introduced. In particular, dimensional analysis was used as a guide. First notice that the identification (3.1.8) assumes that, for dimensional reason, the RG scale k should vary inversely with the physical distance scale $d(r)$. Therefore, by dimensional analysis, one could write down a more general matching between k and $d(r)$, with $d(r)$ defined as

$$d(r) = c_\gamma\, r_0^{-\gamma+1}\, r^\gamma, \tag{3.1.13}$$

where r_0 is the classical horizon radius, so that

$$d(r) \propto \begin{cases} r_0^{-\gamma+1}\, r^{\gamma}, & \text{for} \quad r < r_0, \\ r & \text{for} \quad r \geq r_0. \end{cases} \tag{3.1.14}$$

c_γ is a positive constant and γ controls the scaling power law. The requrement (3.1.8) takes into consideration the asymptotic limit $r \to \infty$ as well as the scaling in the singularity regime. A similar ansatz of this form has been proposed in [105] where an identification

$$\frac{k(r)}{k_0} = \left(\frac{\Phi_{\text{Newt}}}{\Phi_0}\right)^{\gamma}, \tag{3.1.15}$$

was physically motivated to study galaxy rotation curves from RG correction. It was in fact shown in [106] that this identification is what one should expect for spherically symmetric astrophysical objects. Using the leading order term in the Newton's potential Φ_{Newt}, one will arrive at similar scaling (3.1.14).

- Notice that r_0 will in general feature the infrared Newton coupling G_0. One can in fact put the whole scale identification procedure in a more general form, still by using dimensional analysis as a guide. For instance, one could write down an identification of the form

$$d(r) = c_\gamma\, G(r)^{-\gamma+\delta+1}\, \Lambda(r)^{-\delta}\, r^{\gamma}, \tag{3.1.16}$$

which includes the effective Newton coupling $G(r)$ and the cosmological constant $\Lambda(r)$. For any scaling of this form, it is sufficient to demand its self-consistency by requiring that the corresponding RG-improved spacetime geometry satisfies the scaling $R \sim k^2$ in the fixed point regime (cf. (3.1.7)). The scaling $R \sim k^2$ should, at least, be expected for any well motivated scale identification.

3.2 Renormalization Group Improved Black Holes

RG-improvement of asymptotically flat black hole solutions have been investigated to some detail. In [80], the structure of an asymptotically safe Schwarzschild solution was investigated. This investigation was extended to the Kerr solution in [83]. Away from asymptotically flat solutions, the cosmological constant was introduced into the classical solution, so that the structure of the corresponding Schwarzschild-(A)dS black hole was investigated[85]. Here, we shall present the basic findings of the investigation of the RG-improved Schwarzschild-(A)dS black holes. This is expected to fully capture our motivation towards our study.

The classical Schwarzschild-(A)dS black holes was presented in (1.1.8). As a reminder, it features the lapse function

$$f(r) = 1 - \frac{2G_0 M}{r} - \frac{1}{3}\Lambda_0 r^2 \tag{3.2.1}$$

so that the spacetime solution is

$$\begin{cases} \text{Schwarzschild-AdS} & for \quad \Lambda_0 < 0, \\ \text{Schwarzschild} & for \quad \Lambda_0 = 0, \\ \text{Schwarzschild-dS} & for \quad \Lambda_0 > 0. \end{cases} \tag{3.2.2}$$

Notice that G_0 and Λ_0 are the infrared values of the Newton's coupling and the cosmological constant, i.e. they are associated with $k \to 0$. The corresponding Kretschmann invariant of this solution is

$$\mathcal{K}_{Schw-(A)dS}(r) = R_{\mu\nu\rho\sigma}R^{\mu\nu\rho\sigma} = \frac{48G_0^2M^2}{r^6} + \frac{8\Lambda_0^2}{3}, \tag{3.2.3}$$

which indicates that the class of solution has a curvature singularity at $r = 0$.

3.2.1 RG-improved Schwarzschild Solution

The classical Schwarzschild solution is simply characterized by it mass M. Its lapse function is $f(r) = 1 - \frac{2G_0M}{r}$. We shall now follow the step-by-step RG-scheme at the level of calssical solution. First, we promote the coupling G_0 into a scale-dependent quantity. The effective lapse function becomes

$$f_k(r) = 1 - \frac{2G_kM}{r}. \tag{3.2.4}$$

The effective lapse function features the running of dimensionful Newton constant, which according to (2.3.12), is captured by

$$G_k := k^{-2}\, g_k = \frac{G_0}{1 + \omega\, G_0\, k^2}, \tag{3.2.5}$$

whose asymptotic behaviour in the IR and UV regime is given by

$$G_k \approx \begin{cases} G_0 - \omega\, G_0 k^2 & for \quad k \to 0, \\ 1/(\omega\, k^2) & for \quad k \to \infty \end{cases} \tag{3.2.6}$$

The RG-scale k is then identified with the proper distance $d(r)$, which according to (3.1.11), lead to an asymptotic behavour

$$d(r) = \begin{cases} r + \mathcal{O}(r^0) & for \quad r \gg 2GM, \\ \frac{2}{3}\frac{1}{\sqrt{2G_0M}} r^{3/2} + \mathcal{O}(r^{5/2}) & for \quad r \ll 2GM \end{cases} \tag{3.2.7}$$

The full asymptotic behaviour (3.2.13) can be captured by an interpolating function

$$d(r) = \left(\frac{r^3}{r + \varrho\, G_0\, M} \right)^{1/2}, \tag{3.2.8}$$

where ϱ is a free parameter. This doesn't change the qualitative properties of the RG improved black hole for $\varrho \geq 0$. For $\varrho = 0$, one returns back to $d(r) = r$. For large r, one recovers $d(r) = r^{3/2}/\sqrt{\varrho G_0 M} + \mathcal{O}(r^{5/2})$, setting $\varrho = 9/2$.

Inserting the identification (3.1.8) into (3.2.5), one obtain,

$$G(r) = \frac{G_0 r^3}{r^3 + \tilde{\omega}\, G_0 (r + \varrho\, G_0\, M)}, \tag{3.2.9}$$

where $\tilde{\omega} = \omega\xi^2$. The asymptotic limit of (3.2.9) is given as

$$G(r) = \begin{cases} G_0 - \tilde{\omega}\frac{G_0^2}{r^2} + \mathcal{O}(r^{-3}) & for \quad r \to \infty, \\ \frac{r^3}{\varrho\ \tilde{\omega} G_0\ M} + \mathcal{O}(r^4) & for \quad r \to 0 \end{cases} \tag{3.2.10}$$

The asymptotic behaviour $r \to \infty$ has, in fact, been used to obtain the leading quantum correction to Newton's potential $\Phi_{\rm cl}(r) = -\frac{G_0 m_1 m_2}{r}$ of two point sources m_1 and m_2, by promoting the infrared Newtong coupling G_0 to $G(r)$. Reinstating $\hbar$, the RG-improved gravitational potential reads

$$\Phi_{\rm imp}(r) = -\frac{G_0 m_1 m_2}{r}\left(1 - \tilde{\omega}\frac{G_0\hbar}{r^2 c^3} + \mathcal{O}\left(\frac{G_0\hbar}{r^2}\right)^2\right) \tag{3.2.11}$$

This fixes $\tilde{\omega} = \frac{167}{30\pi}$(cf. (2.0.1)).

Returning back to improving the classcial Schwarzschild solution, G_k in (3.2.5) has been identified with $G(r)$ in (3.2.9). The resulting improved lapse function is

$$f_{\rm imp}(r) = 1 - \frac{2G_0 M r^2}{r^3 + \tilde{\omega}\, G_0(r + \varrho\, G_0\, M)}, \tag{3.2.12}$$

whose asymptotic behaviour is given by

$$f(r) \simeq \begin{cases} 1 - \frac{2G_0 M}{r}\left(1 - \tilde{\omega}\frac{G_0}{r^2}\right) + \mathcal{O}(r^{-4}), & \text{Large distance regime,} \\ 1 - \frac{2r^2}{G_0 \varrho \tilde{\omega}} + \mathcal{O}(r^3) & \text{Short distance regime.} \end{cases} \tag{3.2.13}$$

In the following, we summarize the essential geometric features of the RG-improved Schwarzschild black hole.

- In the large distance regime $r \to \infty$, the leading quantum correction to the classical solution appears at order r^{-3}. The effective classical lapse function correctly recovers the leading correction to Newton's potential (compare (3.2.11)):

$$\Phi_{\rm imp}(r) = \frac{f(r) - 1}{2}. \tag{3.2.14}$$

- The improved black hole solution has similar properties to the Hayward black holes[11]. In the small distance regime $r \to 0$, it features a regular *de Sitter core* with effective cosmological constant $\Lambda_{\rm eff} = 6/(G_0 \varrho \tilde{\omega}) > 0$. The regularity is made obvious from the finite value of the invariant Kretschmann scalar

$$\mathcal{K}^*_{Schw}(r) = R_{\mu\nu\rho\sigma} R^{\mu\nu\rho\sigma} = \frac{96}{G_0^2 \varrho^2 \tilde{\omega}^2}. \tag{3.2.15}$$

- As one can observe from figure 3.1, the position of the horizon depends on how the mass of the improved solution compares to the critical mass $M_{\rm cr} = \sqrt{\tilde{\omega}/G_0} = \sqrt{\tilde{\omega}} M_{\rm pl}$. Hence, for $M > M_{\rm cr}$, the horizon radius is at

$$r_\pm = G_0 M \left(1 \pm \sqrt{1 - \Omega}\right), \tag{3.2.16}$$

  with $\Omega = (M_{\rm cr}/M)^2$, so that the improved solution features,

$$\begin{cases} \text{two horizons at } r_+ > r_- & for \quad M > M_{\rm cr}, \\ \text{one horizon at } r_+ = r_- = \sqrt{\tilde{\omega} G_0} & for \quad M = M_{\rm cr}, \\ \text{no horizon} & for \quad M < M_{\rm cr}. \end{cases} \tag{3.2.17}$$

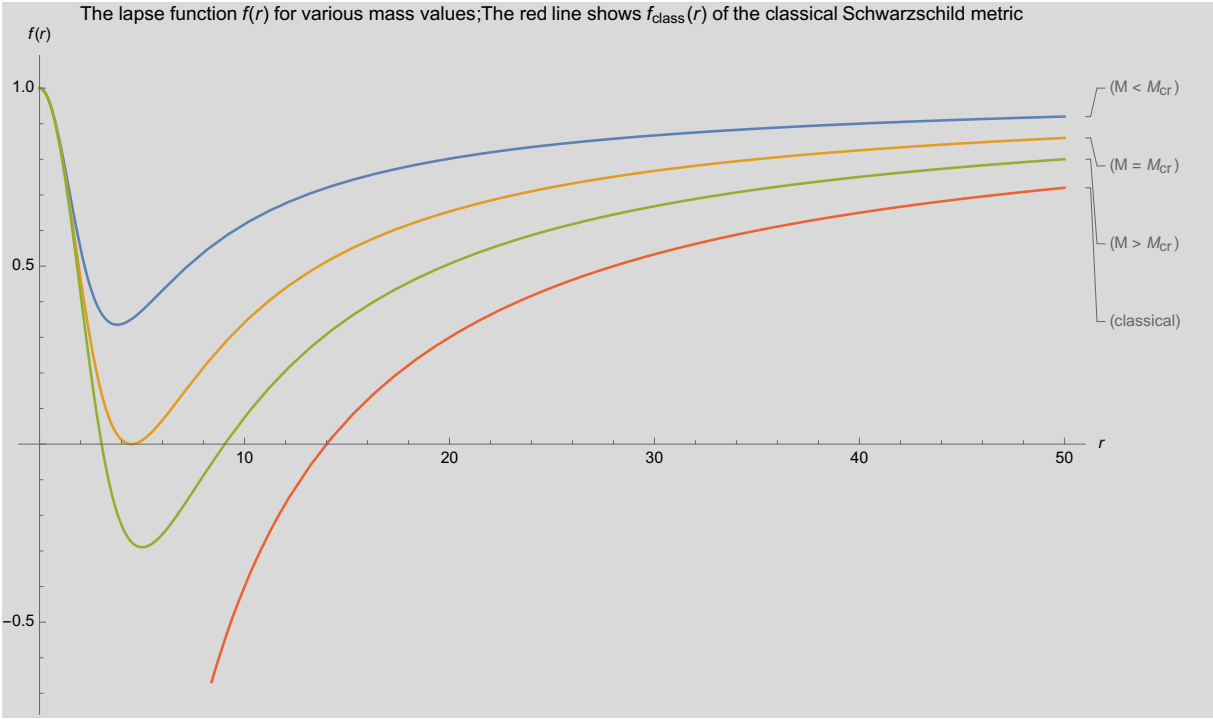

Figure 3.1: The RG improved lapse function $f(r)$ for various mass values.

- One can investigate the final state solution of evaporation by studing the Bekenstein-Hawking temperature (1.2.3). The temperature is given by

$$T_{BH} = \frac{\hbar\kappa}{2\pi} = \frac{1}{4\pi}\partial_r f_{\rm imp}(r)\Big|_{r=r_+} \tag{3.2.18}$$

$$= \frac{\sqrt{\Omega(1-\Omega)}}{1+\sqrt{1-\Omega}}\frac{M_{\rm cr}}{4\pi\tilde{\omega}} \tag{3.2.19}$$

  with large mass expansion

$$T_{BH} = \frac{1}{8\pi G_0 M}\left[1 - \frac{1}{4}\left(\frac{M_{cr}}{M}\right)^2 - \frac{1}{8}\left(\frac{M_{cr}}{M}\right)^4 + \mathcal{O}(M^{-6})\right]. \tag{3.2.20}$$

  As $\Omega \to 1$, i.e $M \to M_{\rm cr}$, the temperature vanishes. This is depicted clearly in figure 3.2. This suggest that the extremal solution $M = M_{\rm cr}$ leave a cold remnant of the evaporation, and Hawking radiation stops when the mass of the improved black hole solution is critical.

- Further investigations on the spacetime structure of evaporating black hole within the RG-scheme are detailed in ([88],[89]).

Having detailed the essential features of the improved Schwarzschild black hole which feature a de sitter core, one asks if this conclusion holds when cosmological constant is introduced into the system. Indeed, even if cosmological constant is set at zero in the microscopic regime, one expects that a non-trivial cosmological constant should be generated along the RG trajectory. The generalization to a cosmological constant, that is present at all scales, underlies the investigation in [85]. We shall present the construction of this corresponding improved solution and discuss the essential points we learn from it.

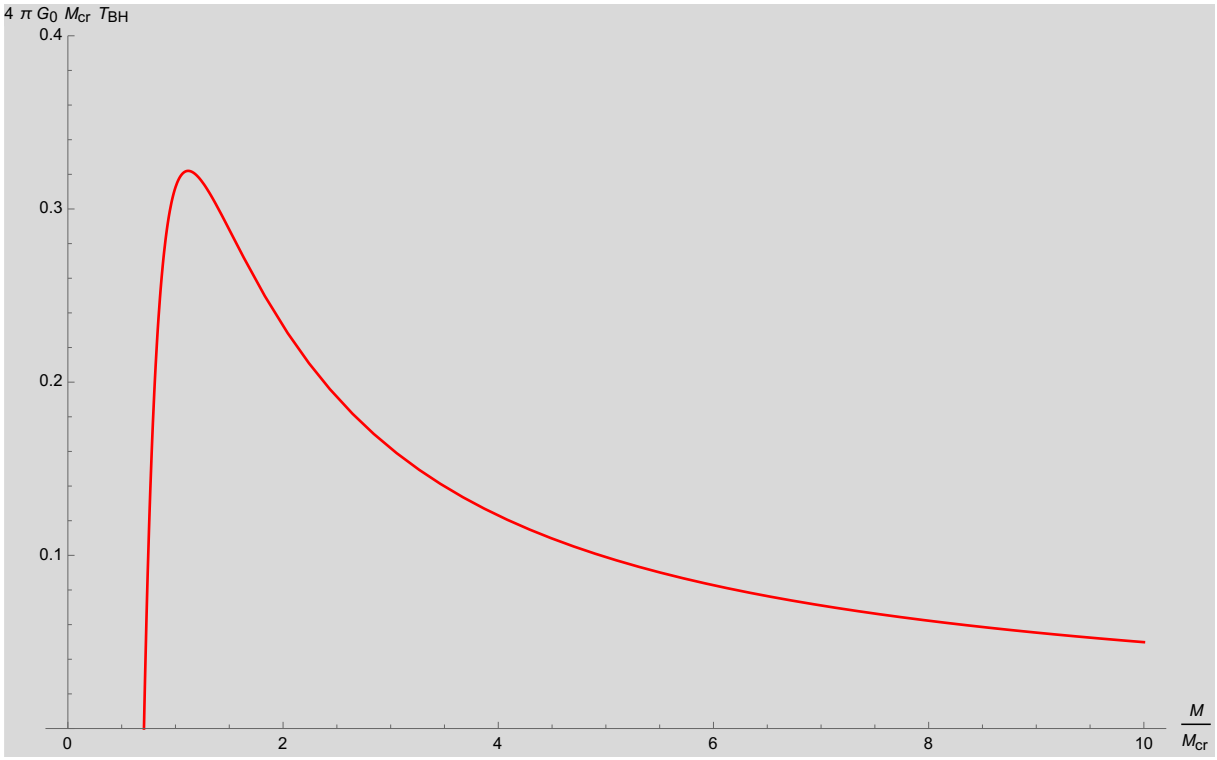

Figure 3.2: The Bekenstein-Hawking temperature of the quantum improved black hole. Evaporation stops, leaving behind a finite cold remnant.

3.2.2 RG-improved Schwarzschild-AdS Solution

For non-vanishing cosmological constant, the Schwarzschild-(A)dS black hole has been shown to be stable against linearized gravitational perturbations[107]. It features a spacetime singularity at $r = 0$ (cf. (3.2.3)) and its event horizons are located at the zeros of (3.2.1). The zeros are

$$r_0 = -\mathcal{R}^{-/3} - \frac{1}{\Lambda}\mathcal{R}^{1/3} \,, \tag{3.2.21}$$

and

$$r_\pm = -\frac{1}{2}\left(1 \pm i\sqrt{3}\right)\mathcal{R}^{-/3} - \frac{1 \pm i\sqrt{3}}{2\Lambda_0}\mathcal{R}^{1/3} \,, \tag{3.2.22}$$

where

$$\mathcal{R} = 3G_0 M\Lambda_0^2 + \sqrt{9G^2M^2\Lambda_0^4 - \Lambda_0^3}. \tag{3.2.23}$$

Thus, the event horizons are located at

$$\begin{cases} \mathrm{r}_0 & for \quad \text{Schwarzschild-AS}, \\ \mathrm{r}_\pm & for \quad M < \frac{1}{3G_0\sqrt{\Lambda_0}}, \text{Schwarzschild-dS} \\ \text{no horizon} & for \quad M < M_{\mathrm{cr}} = \frac{1}{3G_0\sqrt{\Lambda_0}}. \end{cases} \tag{3.2.24}$$

RG-improvement proceeds in a similar fashion as the Schwarzschild case and the investigation of the structure of the improved black hole at the UV fixed point follows straighforwardly. Starting from (3.2.1), we promote the Newton's coupling and the cosmological constant to their scale-dependent analog, so that the effective lapse function is

$$f_k(r) = 1 - \frac{2G_k M}{r} - \frac{1}{3}\Lambda_k r^2. \tag{3.2.25}$$

The RG already provides us the scaling behavior of (G_k, Λ_k) at high energies. The behaviour at the non-trivial fixed point is

$$\lim_{k\to\infty} G_k = k^{-2} g_*, \qquad \lim_{k\to\infty} \Lambda_k = k^2 \lambda_*.$$

This will change the classical black hole geometry into

$$f_*(r, k(r)) = 1 - \frac{2g_* M}{k(r)^2 r} - \frac{1}{3} k(r)^2 \lambda_* r^2. \tag{3.2.26}$$

The dependence on $k(r)$ has now appeared, while g_* and λ_* are both dimensionless. The completion of the improvement now follow from the scale identification. The investigation here still follows from the identification (3.1.8) with $d(r)$ taken as the proper distance.

The infrared part of the analytic behaviour of $d(r)$ is completely fixed by the cosmological constant Λ_0. Depending on whether the solution is anti-de Sitter or de Sitter, the leading order term of the analystic $d(r)$ is given as

$$d_{\mathrm{IR}}(r) \simeq \begin{cases} \sqrt{\frac{3}{\Lambda_0}}\ \sin^{-1}\left(\sqrt{\frac{\Lambda_0}{3}}\ r\right) & for \quad \Lambda_0 > 0, \\ r & for \quad \Lambda_0 = 0, \\ \sqrt{\frac{3}{\Lambda_0}}\ \sinh^{-1}\left(\sqrt{-\frac{\Lambda_0}{3}}\ r\right) & for \quad \Lambda_0 > 0. \end{cases} \tag{3.2.27}$$

However, the UV behaviour of $d(r)$ is independent of the cosmological constant Λ_0, rather, it is completely fixed by the mass M and the infrared Newton's coupling G_0. This is given as

$$d_{\mathrm{UV}}(r) \simeq \frac{2}{3} \frac{1}{\sqrt{2G_0 M}} r^{3/2} \left(1 + \frac{3}{10} \frac{r}{2G_0 M}\right) + \mathcal{O}(r^2). \tag{3.2.28}$$

Inserting the leading order term of (3.2.28) into (4.2.16), the improved spacetime geometry is associated with the lapse function

$$f_*(r) = 1 - \frac{2G_0 M}{r} \left(\frac{3}{4}\lambda_* \xi^2\right) - \frac{1}{3}\left(\frac{4g_*}{3G_0 \xi^2}\right) r^2. \tag{3.2.29}$$

The structure of the improved lapse function is the same as that of the its classical analog. In particular, the scale identification basically switches the r^{-1} term which features the classical Newton's coupling for the r^2 term that features the cosmological constant, and vice versa.

In summary, the quantum improved Schwarzschild-AdS black holes feature the following characteristics:

- there exists a critical mass

$$\Delta_{\mathrm{cr}} = M_{\mathrm{cr}} \xi_{\mathrm{cr}} = \frac{2}{3\lambda_*} \frac{1}{\sqrt{3G_0 g_*}}, \tag{3.2.30}$$

  such that, the improved Schwarzschild-AdS solution features

$$\begin{cases} \text{two horizons at} & for \quad M\xi < \Delta_{\mathrm{cr}}, \\ \text{one horizon at} & for \quad M\xi = \Delta_{\mathrm{cr}}, \\ \text{no horizon} & for \quad M\xi > \Delta_{\mathrm{cr}}. \end{cases} \tag{3.2.31}$$

  This shows that for a sufficiently light Schwarzschild-AdS black holes, a new horizon emerges in the improved solution. To see this clearly, we provide a plot in figure 3.3,

showing the improved lapse function of the classical Schwarzschild-AdS black holes for different mass values. The relationship of the mass to the parameter ξ is further shown in figure 3.4.

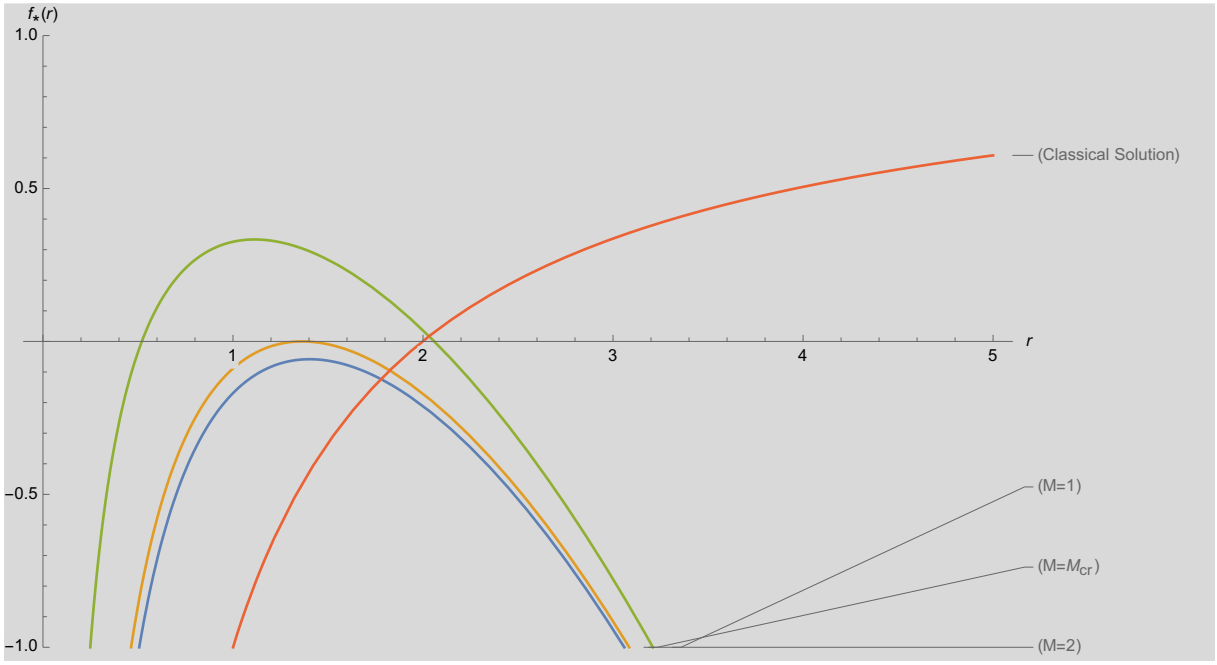

Figure 3.3: The RG improved lapse function of the classical Schwarzschild-AdS black holes for different mass values. The curves are obtained for UV fixed point values $(g_*, \lambda_*) = (0.403, 0.330)$ in (2.3.9) and for $G_0 = 1$, $\xi = 1$, $\Lambda_0 = -0.001$.

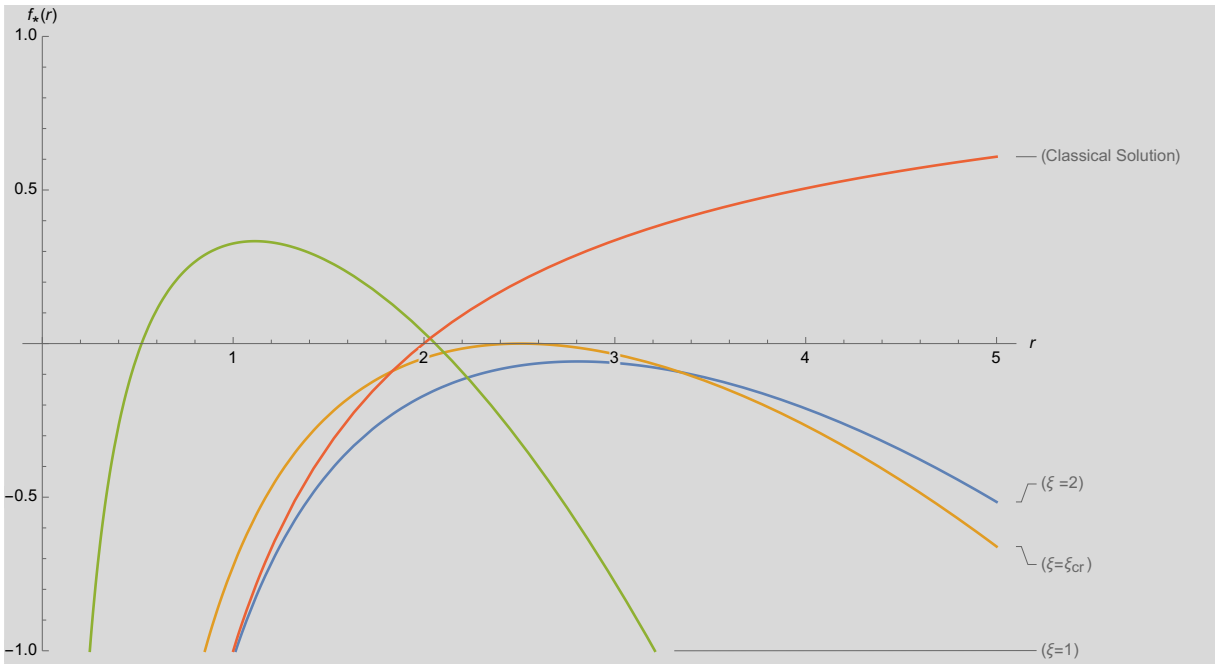

Figure 3.4: The RG improved lapse function of the classical Schwarzschild-AdS black holes for different values of ξ. The curves are obtained for UV fixed point values $(g_*, \lambda_*) = (0.403, 0.330)$ in (2.3.9) and for $G_0 = 1$, $M = 1$, $\Lambda_0 = -0.001$.

- The RG-improved solution has a similar structure to its classical counterpart. In the short distance regime, the Kretschmann invariant reads

$$\mathcal{K}^*_{Schw-(A)dS}(r) = R_{\mu\nu\rho\sigma}R^{\mu\nu\rho\sigma} = \frac{48G_0^2M^2}{r^6}\left(\frac{3}{4}\lambda_*\xi^2\right)^2 + \frac{8}{3}\left(\frac{4g_*}{3G_0\xi^2}\right)^2 \tag{3.2.32}$$

  For a vanishing UV fixed point value of λ_*, the RG-improved geometry is regular. However, for $\lambda_* \neq 0$, RG-improvement does not provide any resolution to the classical singularity as the Kretschmann scalar still diverges as r^{-6} (see figure 3.5). This is very different from the conclusion in the case of asymptotically flat Schwarzschild solution (cf. (3.2.15)). Thus, this suggest that the inclusion of cosmological constant spoils the regularity of the quantum improved geometry. The severe change under the inclusion of the cosmological constant could imply that the physical consequencies of the fixed point scaling of λ have not yet been fully understood. Moreover, such a significant change under the inclusion of λ points towards an insufficiency of the Einstein-Hilbert truncation. In order to achieve robust results, more extended truncation would be required.

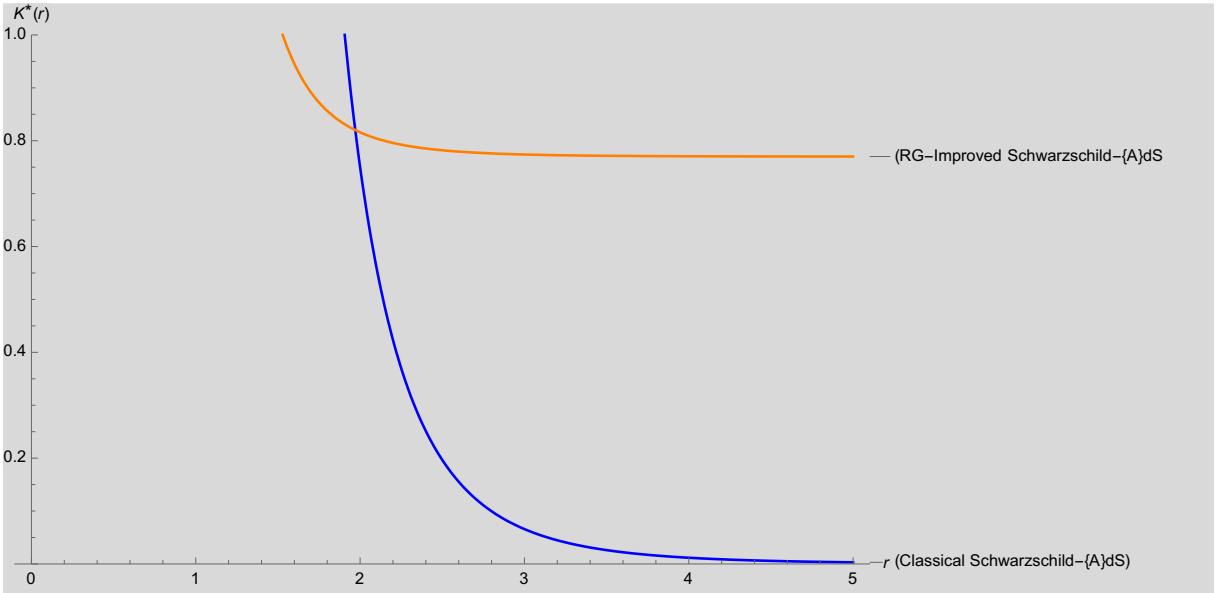

Figure 3.5: Kretschmann invariant of the classical and improved Schwarzschild-AdS black hole solutions. The curves are obtained for UV fixed point values $(g_*, \lambda_*) = (0.403, 0.330)$ in (2.3.9) and for $G_0 = 1$, $M = 1$, $\Lambda_0 = -0.001$, $\xi = 1$.

- Nevertheless, there is an important lesson we learn from this, and in particular, the exchange of the r^{-1} term for the r^2 term. One notes that in the absence of the cosmological constant where one start with just the classical Schwarzschild solution, i.e. $f(r) = 1 - 2G_0Mr^{-1}$, the RG-improvement exchanges the r^{-1} term into r^2, and the improved solution with lapse function

$$f_*(r) = 1 - \frac{1}{3}\left(\frac{4g_*}{3G_0\xi^2}\right)r^2 \,, \tag{3.2.33}$$

  is ultimately de sitter since the effective cosmological constant is strictly positive at the fixed point:

$$\Lambda^*_{\text{eff}} = \frac{4g_*}{3G_0\xi^2} > 0 \tag{3.2.34}$$

This is true since both the IR and UV values of the Newton's couplings G_0 and g_* are strictly positive.

This suggests that, *in $d = 4$, any classical asymptotically flat solution in the Schwarzschild family is effectively de Sitter at the asymptotically safe UV fixed point of its renormalization group flow.*

We also note that the effective Λ^*_{eff} is independent of the fixed point value of the dimensionless cosmological constant λ_*. Therefore, even when one finally include any cosmological constant Λ_0 into the classical solution, the effective cosmological constant Λ^*_{eff} remains free of λ_* and as long as G_0 and g_* remain positive, the spacetime at the UV fixed point continues to be Schwarzschild-de Sitter. This statement continues to be valid even when a gravity-matter system is considered, where the value of λ_* may be driven to be negative.

This suggests that, *in $d = 4$, any classical asymptotically Schwarzschild-(A)dS solution is effectively Schwarzschild-dS at the asymptotically safe UV fixed point of its renormalization group flow.*

On the other hand, supposing that one starts with a purely (A)dS spacetime with vanishing M, i.e. this is not a black hole solution but just a classical asymptotically (A)dS spacetime with lapse function

$$f(r) = 1 - \frac{1}{3}\Lambda_0 r^2. \tag{3.2.35}$$

This is a singularity-free spacetime solution of the Einstein field equation. Now, using a scale identification $k(r) = \frac{\xi}{r}$ which is associated to the proper distance on this spacetime, the RG-improvement procedure leads to a finite Riemann curvature tensor. However, the Ricci scalar diverges to order r^{-2} and the Kretschmann is

$$\mathcal{K}^*_{(A)dS}(r) = R_{\mu\nu\rho\sigma}R^{\mu\nu\rho\sigma} = \frac{4}{9}\frac{\lambda_*^2\xi^4}{r^4}, \tag{3.2.36}$$

which diverges to order r^{-4}. While the classical (A)dS spacetime solution (3.2.35) is singularity-free, singularity is generated from the solution at the UV fixed point of its renormalization group flow. This is in fact the origin of the singularity that persists at the UV fixed point of the RG flow Schwarzschild-(A)dS family.

This analysis hints at the conclusion that, *in $d = 4$, any classical asymptotically (A)dS spacetime of the type (3.2.35) is effectively singular at the asymptotically safe UV fixed point of its renormalization group flow.*

Conclusion and Outlook

In conclusion, while quantum gravity effect remove the physical singularity in the Schwarzschild geometry, the singularity is inevitable in the full Einstein-Hilbert truncation including a cosmological constant. Thus, if the resolution of pathologies featuring in classical gravity is set as a viability criterion for any quantum gravity theory, then one must appeal to black hole solutions beyond the Einstein-Hilbert truncation. Classical black hole solutions in a higher gravity action truncation are technically daunting to solve and their improved geometry is expected to be different from those we see at the level of the Einstein-Hilbert truncation.

In spite of the challenges at hand, there is still more to study at the level of Einstein-Hilbert truncation, namely, one can seek for a bound on the critical exponent for which the black hole singularity is resolved. Indeed, all our investigations so far are based on studies at the fixed point $\mathbf{g}^*$, however, the behaviour of the dimensionless coupling away from the fixed point regime at the linearized level,

$$\mathbf{g}_i = \mathbf{g}_i^* + \sum_\alpha c_\alpha \, \mathbf{v}_i^\alpha \left(\frac{k}{k_0}\right)^{-\theta_\alpha},$$

features the universal critical exponent θ_α, which could in turn be restricted by the requirement of singularity-free asymptotically safe black holes.

Chapter 4

Quantum Gravity Bound on the Critical Exponent

The field theoretic renormalization group has proven to be very illuminating for physics. Various scaling laws associated with phase transitions at criticality have been found. Indeed, the RG implementation has led to the extraction of qualitative information on the corresponding universality classes [108]-[110]. Critical phenomena of physical systems are characterized by fixed points, the later of which also underlie asymptotically safe quantum field theories in high energy physics.

Diverse RG based physical studies have shown the relationship between critical phenomena and QFT. By standard scaling arguments, it is possible to determine the behaviour of correlation functions and some local and nonlocal observables through their renormalization group behavior that is controlled by the universal critical exponents. In 2.1.2, we introduce the local behaviour of the RG flow in the neighbourhood of the fixed point $\mathbf{g}_i^*$. The scaling solution of the dimensionless coupling is

$$\mathbf{g}_i = \mathbf{g}_i^* + \sum_\alpha c_\alpha \, \mathbf{v}_i^\alpha \left(\frac{k}{k_0}\right)^{-\theta_\alpha} , \tag{4.0.1}$$

which features the critical exponent θ_α, for which classification of scaling eigenvectors $\mathbf{v}_i$ are based (see table 2.1). Furthermore, we showed that the universal critical exponents θ_i is related to the canonical mass dimension $d_{\bar{\mathbf{g}}_i}$ of the coupling, wherein we obtain the relation

$$\theta_i \simeq d_{\bar{\mathbf{g}}_i} - \left.\frac{\partial \eta_i(\mathbf{g}_i)}{\partial \mathbf{g}_i}\right|_{\mathbf{g}_i = \mathbf{g}_i^*} , \tag{4.0.2}$$

where $\left.\frac{\partial \eta_i(\mathbf{g}_i)}{\partial \mathbf{g}_i}\right|_{\mathbf{g}_i = \mathbf{g}_i^*}$ is called the anomalous dimension around the UV fixed point. The running of the anomalous dimension stops at the fixed point and the realized critical exponents guarantees universality. We further emphasize that the critical exponents associated to the non-trivial fixed point of asymptotic safety receive extra contribution from the anomalous dimension. Nevertheless, (4.0.2) suggests that the canonical mass dimension will continue to dominate, unless quantum effect becomes very large.

In $d = 4$, the value of the universal gravitational critical exponent have been extracted through several techniques ranging from the 1-loop perturbative $2 + \epsilon$ expansion[67] to exact renormalisation group approach[58] and from lattice gravity [111]. We already saw those from exact

renormalisation group approach in (2.3.9). Table 4.1 summarize the main results from other approaches.

We will explore the implications of demanding a regular black hole solution on the critical exponent. Indeed, we saw in the last chapter that, if the microscopic fixed point value of the dimensionless cosmological constant vanishes, the classical singularity is ultimately resolved. This provides an avenue to seek for such bound since it enters directly into the full curvature invariant in the fixed point regime. Before we embark on this, we shall outline the renormalization group scaling relation for gravity and provide the main results of studies of the critical exponents from some approaches to quantum gravity. This will allow for s robust analysis of our result.

4.1 RG Scaling Relations for Gravity

In the infrared regime, gravity is very weak, in the sense that the Newtonian gravitational potential is small. For example, throughout the solar system, the geometry of spacetime only deviate a little from flat Minskowski space. The effective field theory approach capture the behaviour of gravity in this regime. In the very strong gravity regime, one expect depatures from flat Minkowski space.

Aymptotic safety suggests that fundamental structure of quantum spacetime depart from the classical Minkowskian picture of the classical spacetime, and spacetime may be characterized by a fractal-like structure at criticality, with spectral properties of spacetime changing on various typical length scales [79]. The fractal-like properties are linked to a scale-invariant fixed point regime. The fixed point can be interpreted as implying that quantum gravity in $d = 4$ exhibits a phase transition in the Newton's coupling between two physically different phases at critical coupling G_c, so that spacetime is smooth in the infrared and becomes fractal-like at criticality and beyond.

The existence of the phase transition in G lead all the way to the ultraviolet fixed point of the renormalization group flow of G, where the dimensionless Newton's coupling takes a non-trivial fixed point value. For example, in the $2 + \epsilon$-expansion, the structure of the flow equation of the dimensionless Newton's coupling $g = k^{\epsilon}G$ is given as

$$\beta_g := \frac{d}{d\ln k} g = \epsilon g - \gamma g^2, \tag{4.1.1}$$

for which fixed points appear at

$$g^* = 0 \ \text{(Free)} \ \text{ and } \ g^* = \frac{\epsilon}{\gamma} \ \text{(Safe for } \gamma > 0).$$

Integrating (4.1.1) in the neighbourhood of the nontrivial fixed point, one obtains

$$\int_m^{\Lambda} d\ln k = \int^g \beta_g^{-1} dg,$$

where m is a constant of integration with dimension of mass, related to the scale below criticality and Λ is the cutoff scale beyond criticality. This results in a mass scaling

$$m = \Lambda \ \exp\left(\int^g \beta_{g'}^{-1} dg'\right) \underset{g\to g_c}{\sim} \Lambda \ |g_c - g|^{-1/\beta'_{g_c}}. \tag{4.1.2}$$

The physical mass scale m is expected to play role in determining the qualitative scaling corrections. In the fixed point regime, the derivative of the β-function defines the critical exponent θ, which is the eigenvalue of the stability matrix (see (2.1.12)). Therefore $\beta'_{g_c} = -\theta$. In this way, we would have

$$m \underset{g\to g_c}{\sim} \Lambda\ |g_c - g|^{1/\theta}. \tag{4.1.3}$$

One can then identify this scale with the inverse of the gravitational correlation length

$$\zeta = \frac{1}{m}, \tag{4.1.4}$$

or some scale associated to curvature. This allows us to define the nonperturbative correlation length

$$\zeta^{-1}(g) \equiv m(g) \underset{g\to g_c}{\sim} \Lambda\ |g_c - g|^{1/\theta}. \tag{4.1.5}$$

There is a similar analogy in lattice approach to quantum gravity, where the nonperturbative correlation length is defined as

$$\zeta(k) \underset{k\to k_c}{\sim} \mathcal{A}_\zeta\ |k_c - k|^{-\nu}, \tag{4.1.6}$$

where $k^{-1} \equiv 8\pi G$, $\mathcal{A}_\zeta$ is the correlation length amplitude and ν is the correlation length exponent characterizing the divergence of ζ in the critical regime [111]. What follows is then that, (4.1.5) and (4.1.6) relates the critical exponent θ from continuum asymptotic safety to the critical exponent ν in the lattice setting according to

$$\theta = \frac{1}{\nu}. \tag{4.1.7}$$

Accordingly, one can compute the local average curvature using

$$\frac{1}{V}\langle \int d^d x\ \sqrt{-g}\ R\rangle \equiv \mathcal{R}(k) \underset{k\to k_c}{\sim} -\mathcal{A}_\mathcal{R}\ |k_c - k|^{d\nu-1}, \tag{4.1.8}$$

where V is the d-dimensional volume and R is the scalar curvature. The integration is done over spacetime, with all quantities in units of the lattice spacing $a = \Lambda^{-1}$. The curvature correlation function is given as

$$\langle\sqrt{-g}R(x)\ \sqrt{-g}R(y)\ \delta(|x-y|-d)\rangle_c \sim \begin{cases} e^{-D/\zeta} & for \quad D \gg \zeta, \\ D^{-2(d-1/\nu)} & for \quad D \ll \zeta, \end{cases} \tag{4.1.9}$$

where

$$D(x,y|g) = \min_\zeta \int_{\tau(x)}^{\tau(y)} d\tau \sqrt{g_{\mu\nu}(\zeta)\frac{d\zeta^\mu}{d\tau}\frac{d\zeta^\nu}{d\tau}}, \tag{4.1.10}$$

is the distance between points x and y in the background geometry.

By relating the quantum curvature average in (4.1.10) to the physical correlation in (4.1.6), one obtains an equivalent result for local average curvature as

$$\mathcal{R}(\zeta) \underset{k\to k_c}{\sim} \zeta^{\frac{1}{\nu}-d}. \tag{4.1.11}$$

The following table 4.1 provides estimates of the leading universal gravitational critical exponent θ from various approaches in $d = 4$ and $d = 3$ spacetime dimensions. This includes some estimates from the $2 + \epsilon$ expansion up to 2-loop order, exact renormalization group approach and those from the euclidean lattice quantum gravity.

Gravitational critical exponents	
QG Approaches in $d = 4$	Critical Exponent $\theta = 1/\nu$
Perturbative $2 + \epsilon$ expansion at 1-loop	2 [112, 113]
Exact Renormalization Group	1.941 [58], 8/3 [60], 3.35 [117].
Geometric argument on Lattice	$d - 1 = 3$ [114, 115]
Euclidean Lattice Quantum Gravity	2.997 [116].

Table 4.1: Gravitational scaling exponent from different quantum gravity approach

Within the asymptotic safety paradigm, a fixed point exists in the $d > 4$ pure gravity system. However, the universal scaling exponent seems to be increasing with increase in spacetime dimension [118]. Table 4.2 shows the real part of the gravitational critical exponent associated with the non-trivial fixed point for the Einstein-Hilbert truncation in more than four dimensions, using the following momentum cutoffs:

$$\mathcal{R}_k(y) = k^2 r(y) \tag{4.1.12}$$

with dimensionless cutoff profile

$$\begin{cases} r_{\rm exp}(y) = \frac{1}{\exp cy^b - 1}, & \text{Exponential cutoff,} \\ r_{\rm mexp}(y) = \frac{b}{(b+1)^y - 1}, & \text{Modified Exponential cutoff I} \\ r_{\rm mod}(y) = \frac{1}{\exp\left[\left(c(y+(b-1)y^b)/b\right)\right]-1}, & \text{Modified Exponential cutoff II.} \\ r_{\rm opt}(y) = b(1/y - 1)\theta(1 - y), & \text{Litim optimized cutoff.} \end{cases} \tag{4.1.13}$$

The momentum cutoffs include the sharp cutoff for $b \to \infty$. Numerical values are independent of large b, while they depend on small b. Thus, there is a b_{bound} to avoid such a dependency of the numerical value on regulators.

Gravitational critical exponents in extra dimensions								
Regulator	Critical Exponent θ							
$r_{\rm exp}(y)$	1.53	2.83	4.60	6.68	9.03	11.6	14.5	17.6
$r_{\rm mexp}(y)$	1.51	2.80	4.58	6.71	9.14	11.9	14.9	18.2
$r_{\rm mod}(y)$	1.51	2.77	4.50	6.54	8.86	11.4	14.2	17.3
$r_{\rm opt}(y)$	1.48	2.69	4.33	6.27	8.46	10.9	13.5	16.4
n	0	1	2	3	4	5	6	7

Table 4.2: The leading ritical exponents in $d = 4 + n$ dimensions for various momentum cutoffs [118].

We shall now investigate whether the two leading critical exponents, associated to the two eigendirections of the fixed point, in the (g, λ)-plane, can be bounded from below or above by demanding regularity of the RG-improved black hole solution.

4.2 QG Bound on θ

We start by recalling that the critical exponents (2.1.19), that characterize the local behaviour of the RG flow, can in general be $\mathbb{C}$-values, so that a pair of the critical exponents assumes the form

$$\theta_\alpha = \mathbf{Re}\,(\theta_\alpha) \pm i\ \mathbf{Im}\,(\theta_\alpha)\,. \tag{4.2.1}$$

Thus, for a pure gravity action projected on the Einstein-Hilbert truncation (2.3.3), where θ_1 and θ_2 are associated with the scaling behaviour of the dimensionless Newton's coupling and the cosmological constant at the UV fixed point regime, one can essentially distinguish between two classes of the critical exponent. While **Class I** critical exponents are those for which $\theta_{1,2} \in \mathbb{R}$, **Class II** critical exponents have non-vanishing imaginary part and form a complex conjugate pair

$$\theta_{1,2} = \sigma_1\ \pm i\ \sigma_2, \qquad with \qquad \sigma_1, \sigma_2 \in \mathbb{R}. \tag{4.2.2}$$

The real part controls the amplitude of the dimensionless counterpart of Newton's coupling and the cosmological constant, while the imaginary part controls the the spiral nature of the RG flow in the fixed point regime. We shall now proceed in investigating them one after the other.

4.2.1 Class I: Real Critical Exponent

For the class $\theta_{1,2} \in \mathbb{R}$, the solution (4.0.1) to the linearized approximation (2.1.15) can be expressed as follows for the dimensionless Newton's coupling $g_k = k^2\, G_k$ and the dimensionless cosmological $\lambda_k = k^{-2}\, \Lambda_k$:

$$\begin{cases} g_k = g_* + c_1 v_1^1 \left(\frac{k}{k_0}\right)^{-\theta_1} + c_2 v_1^2 \left(\frac{k}{k_0}\right)^{-\theta_2}, \\ \lambda_k = \lambda_* + c_1 v_2^1 \left(\frac{k}{k_0}\right)^{-\theta_1} + c_2 v_2^2 \left(\frac{k}{k_0}\right)^{-\theta_2}. \end{cases} \tag{4.2.3}$$

The validity of this solution is at the linearized order beyond the fixed point regime, i.e. presumably below the Planck length $\ell_p = 1$ (in planck unit). At distances larger than the Planck length, $r > \ell_p$, these solutions no longer represent the solution flow from the fixed point regime, as higher orders in the expansion of the β-function around the fixed point start to play a role. As such, we shall keep trusting our result within a distance scale less than or equal to the Planck length, $r \leq \ell_p$.

Without loss of generality,

$$g_k = g_* + c_1 \left(\frac{k}{k_0}\right)^{-\theta_1} + c_2 \left(\frac{k}{k_0}\right)^{-\theta_2}, \tag{4.2.4}$$

and

$$\lambda_k = \lambda_* + d_1 \left(\frac{k}{k_0}\right)^{-\theta_1} + d_2 \left(\frac{k}{k_0}\right)^{-\theta_2}. \tag{4.2.5}$$

for some $c_{1,2}, d_{1,2} \in \mathbb{R}$. For brevity, we shall set $k_0 = 1$. This doesn't change the conclusion of our investigation. Let us now consider again the entire RG procedure of section 3.2.2. At the macroscopic regime, the cosmological constant may be very small but relevant, so that we may start with the Schwarzschild-AdS Black hole. The modification in the calcution now entails that the scaling behavior of (G_k, Λ_k) in the fixed point regime is given by

$$G_k = k^{-2}\left[g_* + c_1 k^{-\theta_1} + c_2 k^{-\theta_2}\right] \tag{4.2.6}$$

and

$$\Lambda_k = k^2\left[\lambda_* + d_1 k^{-\theta_1} + d_2 k^{-\theta_2}\right] \tag{4.2.7}$$

This identification will change the classical Schwarzschild-AdS black hole geometry into one associated with the effective lapse function

$$f_*(r,k(r)) = 1 - \frac{2M}{k^2 r}\left(g_* + c_1 k^{-\theta_1} + c_2 k^{-\theta_2}\right) - \frac{1}{3}k^2 r^2\left(\lambda_* + d_1 k^{-\theta_1} + d_2 k^{-\theta_2}\right) \tag{4.2.8}$$

Now, using the scale identification (3.2.28), the spacetime geometry in the fixed point regime is characterized by the lapse function

$$\begin{aligned} f_*(r) = 1 &- \frac{4r^2}{9G_0\xi^2}\left[g_* + c_1 2^{\theta_1/2}3^{-\theta 1}\left(\frac{\xi\sqrt{G_0 M}}{r^{3/2}}\right)^{-\theta_1} + c_2 2^{\theta_2/2}3^{-\theta_2}\left(\frac{\xi\sqrt{G_0 M}}{r^{3/2}}\right)^{-\theta_2}\right] \\ &- \frac{3G_0 M\xi^2}{2r}\left[\lambda_* + d_1 2^{\theta_1/2}3^{-\theta 1}\left(\frac{\xi\sqrt{G_0 M}}{r^{3/2}}\right)^{-\theta_1} + d_2 2^{\theta_2/2}3^{-\theta_2}\left(\frac{\xi\sqrt{G_0 M}}{r^{3/2}}\right)^{-\theta_2}\right] \end{aligned} \tag{4.2.9}$$

The behaviour of this improved lapse function is depicted in figure 4.1 and 4.2. The figure show the cases of vanishing and non-vanishing value of microscopic cosmological constant λ_*, and of various combinations of the critical exponents. We study the existence of horizon as well as the fate of the curvature singularity.

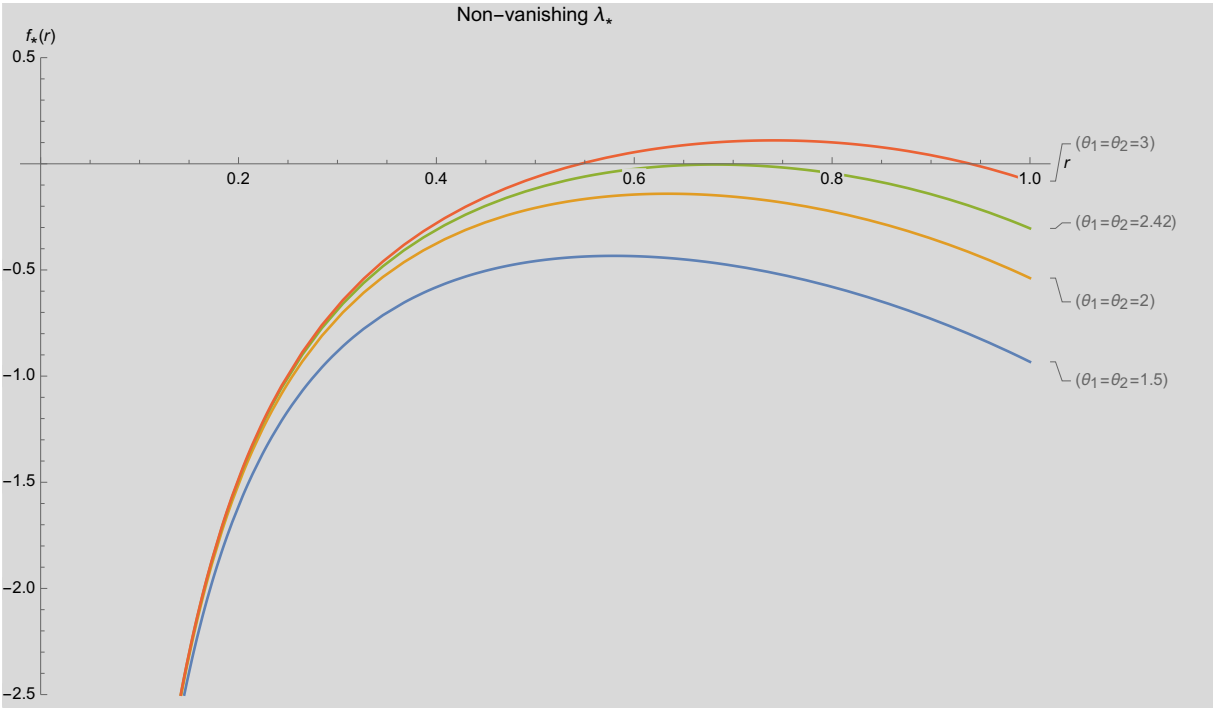

Figure 4.1: The RG improved lapse function of the classical Schwarzschild-AdS black holes for various combinations of the real critical exponent $\theta_{1,2}$. The curves are obtained for UV fixed point values $(g_*, \lambda_*) = (0.403, 0.330)$ in (2.3.9) and for $M = 1$, $G_0 = 1$, $\xi = 1$, $c_i = d_i = 1$.

- For $\lambda_* \neq 0$, we observe that it takes about $\theta_{1,2} = 2.42$ for event horizons to appear in the microscopic black hole, and this black hole deviates from the classical Schwarzschild-AdS solution. For $\theta_{1,2} > 2.42$, the black holes continues to have no more than two horizons.
- For the case $\lambda_* = 0$, this solution is covered by an event horizon for some combinations $\theta_{1,2} > 0.73$. The solution appears asymptotically flat as the critical exponents increase.

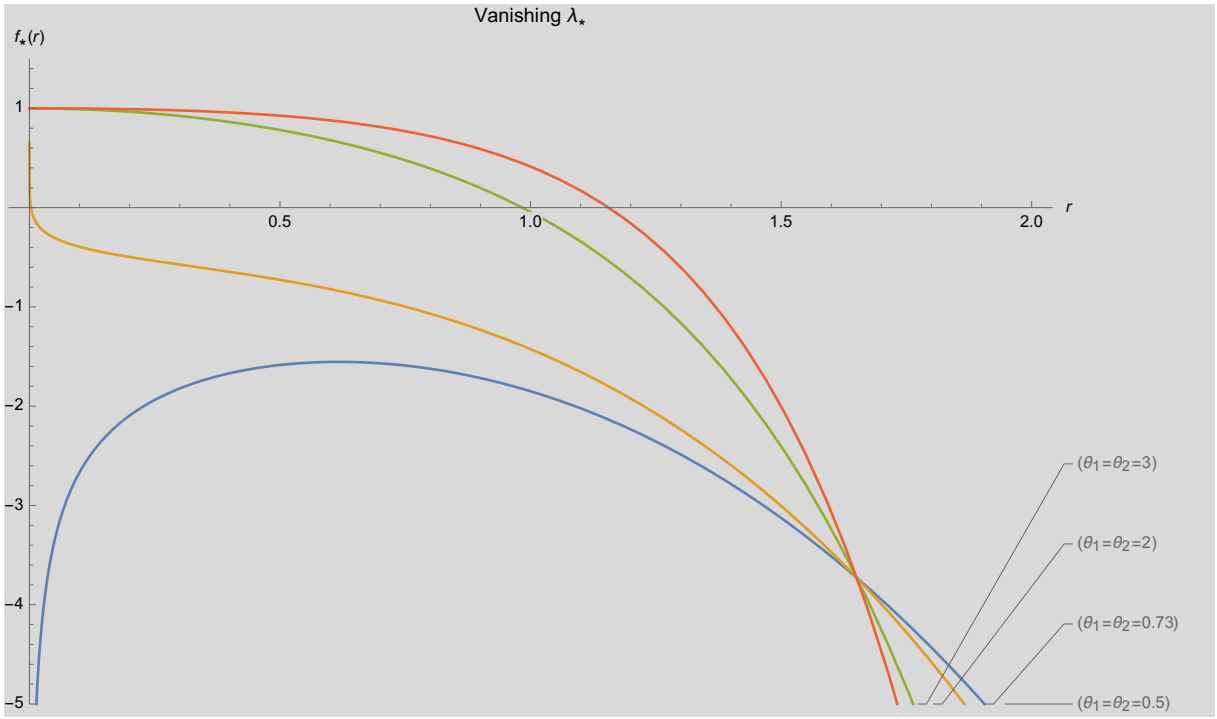

Figure 4.2: The RG improved lapse function of the classical Schwarzschild-AdS black holes for various combinations of the real critical exponents $\theta_{1,2}$. The curves are obtained for UV fixed point values $(g_*, \lambda_*) = (0.403, 0.00)$ in (2.3.9) and for $M = 1$, $G_0 = 1$, $\xi = 1$, $c_i = d_i = 1$.

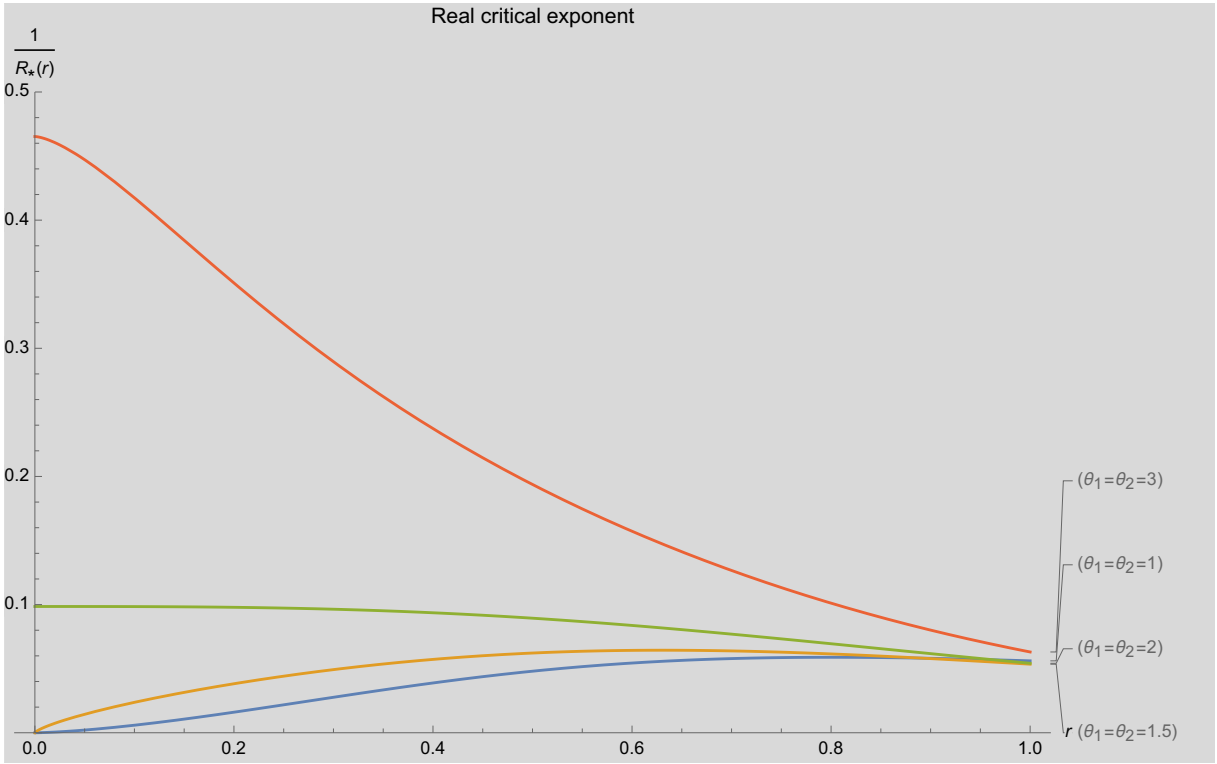

Figure 4.3: The inverse of the RG improved scalar curvature of the classical Schwarzschild-AdS black holes for various combinations of the real critical exponents $\theta_{1,2}$. The curves are obtained for UV fixed point values $g_* = 0.403$ in (2.3.9) and for $M = 1$, $G_0 = 1$, $\xi = 1$, $c_i = d_i = 1$.

- We compute the curvature scalar to investigate the combination of critical exponents required to have a well defined curvature at small distances. The scalar curvature is given by

$$R_*(r) = \frac{1}{8G_0\xi^2 r^3} 3^{-1-\theta_1-\theta_2} \left(\frac{\xi\sqrt{G_0 M}}{r^{3/2}}\right)^{-\theta_1-\theta_2} \Xi_*(r) \tag{4.2.10}$$

where

$$\begin{aligned}\Xi_*(r) = 3^{\theta_2}\left(\frac{\xi\sqrt{G_0 M}}{r^{3/2}}\right)^{\theta_2}&\left(c_1 2^{\frac{\theta_1}{2}+3}\left(3\theta_1^2+14\theta_1+16\right)r^3 + 27 d_1 G_0^2 2^{\theta_1/2}\theta_1(3\theta_1+2)M\xi^4\right)\\ &+ 128 g_* 3^{\theta_1+\theta_2} r^3\left(\frac{\xi\sqrt{G_0 M}}{r^{3/2}}\right)^{\theta_1+\theta_2} + d_2 G_0^2 3^{\theta_1+3} 2^{\theta_2/2}\theta_2(3\theta_2+2)M\xi^4\left(\frac{\xi\sqrt{G_0 M}}{r^{3/2}}\right)^{\theta_1}\\ &+ c_2 3^{\theta_1} 2^{\frac{\theta_2}{2}+3}\left(3\theta_2^2+14\theta_2+16\right)r^3\left(\frac{\xi\sqrt{G_0 M}}{r^{3/2}}\right)^{\theta_1}\end{aligned} \tag{4.2.11}$$

- First, we notice that this fixed point curvature is independent of the microscopic value of the cosmological constant. This is in consonant with our ealier observation that the effective cosmological constant is free of the microscopic cosmological constant. The inverse of the curvature scalar is plotted in figure 4.3. It turns out that the regularity of the scalar curvature is realized only for $\theta_{1,2} \geq 2$. Below this scaling exponents, the curvature diverges as $r \to 0$ since the inverse of the curvature is ultimately driven to zero in this case.

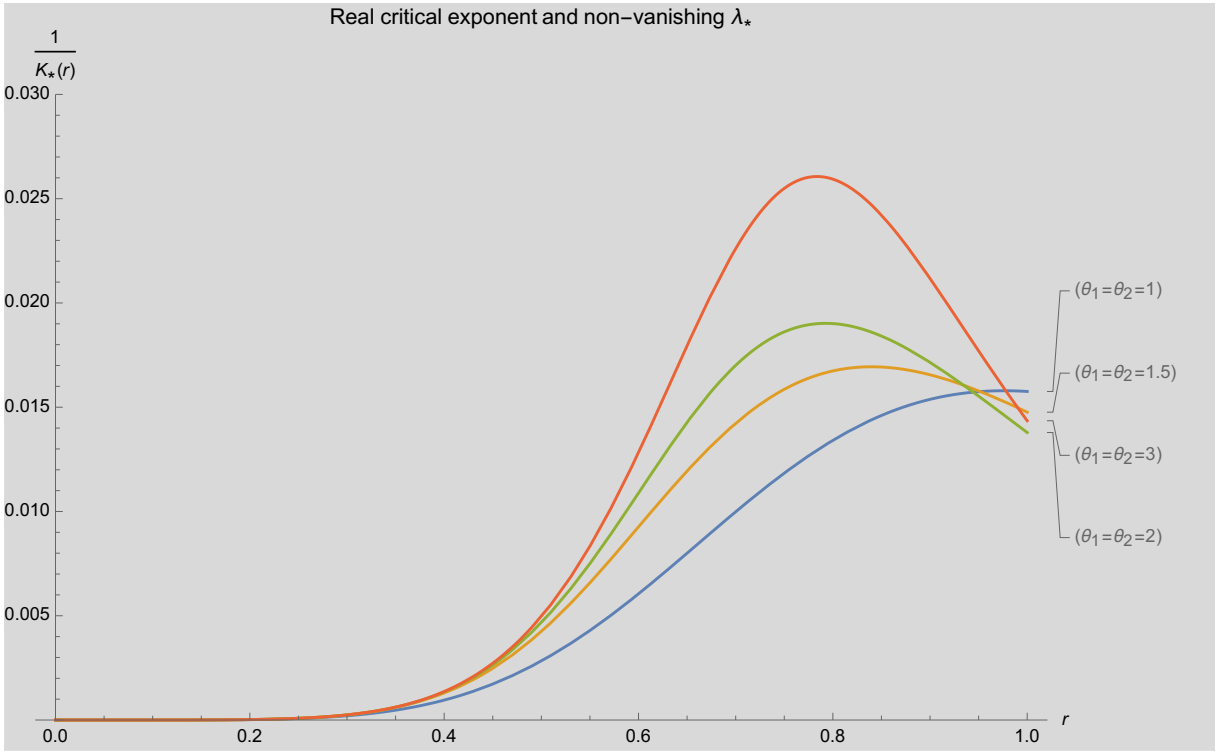

Figure 4.4: The inverse of the RG improved Kretschmann invariant of the classical Schwarzschild-AdS black holes for various combination of the real critical exponents $\theta_{1,2}$. The curves are obtained for UV fixed point values $(g_*, \lambda_*) = (0.403, 0.330)$ in (2.3.9) and for $M = 1$,$G_0 = 1$, $\xi = 1$, $c_i = d_i = 1$.

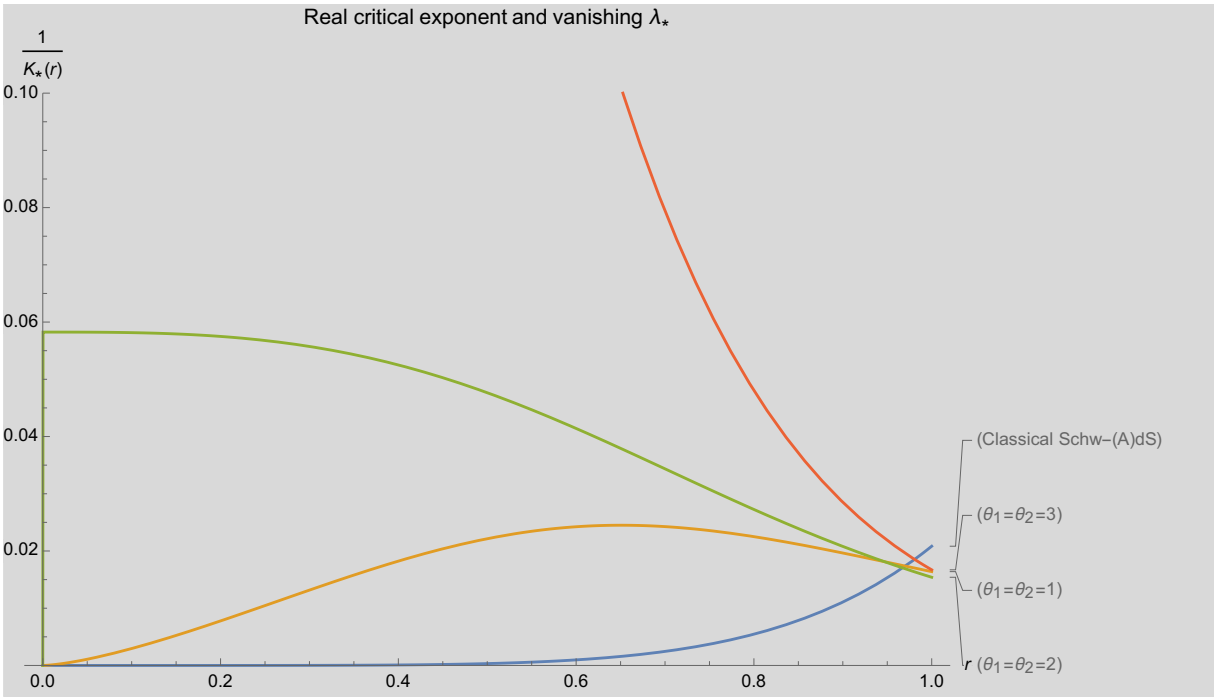

Figure 4.5: The inverse of the RG improved Kretschmann invariant of the classical Schwarzschild-AdS black holes for various combination of the real critical exponents $\theta_{1,2}$. The curves are obtained for UV fixed point values $(g_*, \lambda_*) = (0.403, 0.00)$ in (2.3.9) and for $M = 1$,$G_0 = 1$, $\xi = 1$, $c_i = d_i = 1$.

- The Kretschmann invariant $R_{\mu\nu\rho\sigma}R^{\mu\nu\rho\sigma}$, which measures gravitational field strength is important for our analysis. Its full expression is provided in Appendix II. However, what is important for the moment is their behaviour at small distances. This behaviour is depicted in figure 4.4 and 4.5, where we have show the cases of vanishing and non-vanishing value of microscopic cosmological constant λ_*, and for various combination of the critical exponent.

- First for $\lambda_* \neq 0$, the inverse of the improved Kretschmann invariant goes to zero for all scaling exponents $\theta_{1,2}$. This re-establishes the fact that a non-vanishing microscopic cosmological constant is tied to a curvature singularity at small distances.

- This structure changes for $\lambda_* = 0$, where the improved Kretschmann invariant is regular for all $\theta_{1,2} \geq 2$. The behaviour at $\theta_{1,2} = 2$ is worth mentioning as it seems in figure 4.5 that $1/K_*(r)$ might approach zero in the limit $r \to 0$. We thus analyse it very close to zero, and in fact, it has a limit greater than zero as long as $\theta_{1,2} \geq 2$. The limit is given by

$$\lim_{r\to 0,\theta_{1,2}=2} R^*_{\mu\nu\rho\sigma}R^{\mu\nu\rho\sigma}_* = \frac{8\left(3G_0\xi^2(d_1+d_2)+4g_*\right)^2}{27G_0^2\xi^4} \tag{4.2.12}$$

so that

$$\lim_{r\to 0,\ \theta_{1,2}=2} \frac{1}{K_*(r)} = 0.058 \tag{4.2.13}$$

4.2.2 Class II: Complex Critical Exponent

To study the case of the complex scaling exponents, the $\theta_{1,2}$ in (4.2.3) are modified to take the $\mathbb{C}$-values in (4.2.2):

$$\theta_{1,2} = \sigma_1 \pm i\,\sigma_2, \qquad with \qquad \sigma_1, \sigma_2 \in \mathbb{R}.$$

In this case, the eigenvectors $\mathbf{v}_i^\alpha$ are complex conjugate of each other and $c_{1,2}, d_{1,2} \in \mathbb{C}$. One redefines and normalizes these eigenvectors $\mathbf{v}_i^\alpha$ and parameters such that, after some algebra and up to some relabelling, we can bring (4.2.3) into the form

$$g_k = g_* + \left(p_1 \cos\left[\sigma_2 \ln\left(\frac{k}{k_0}\right)\right] + p_2 \sin\left[\sigma_2 \ln\left(\frac{k}{k_0}\right)\right]\right)\left(\frac{k}{k_0}\right)^{-\sigma_1}, \tag{4.2.14}$$

and

$$\lambda_k = \lambda_* + \left(q_1 \cos\left[\sigma_2 \ln\left(\frac{k}{k_0}\right)\right] + q_2 \sin\left[\sigma_2 \ln\left(\frac{k}{k_0}\right)\right]\right)\left(\frac{k}{k_0}\right)^{-\sigma_1}, \tag{4.2.15}$$

for some $p_{1,2}, q_{1,2} \in \mathbb{R}$. Again, we shall set $k_0 = 1$ for brevity. This will not change the conclusion of our investigation.

This scaling will change the classical Schwarzschild-AdS black hole geometry into one associated with the effective lapse function

$$\begin{aligned} f_*(r, k(r)) = 1 &- \frac{2M}{k^2 r}\left(g_* + k^{-\sigma_1}\left[p_1 \cos\left(\sigma_2 \ln k\right) + p_2 \sin\left(\sigma_2 \ln k\right)\right]\right) \\ &- \frac{1}{3}k^2 r^2\left(\lambda_* + k^{-\sigma_1}\left[q_1 \cos\left(\sigma_2 \ln k\right) + q_2 \sin\left(\sigma_2 \ln k\right)\right]\right) \end{aligned} \tag{4.2.16}$$

Now, using the scale identification (3.2.28), the spacetime geometry at the fixed point regime is characterized by the lapse function

$$f_*(r) = 1 - \frac{4r^2}{9G_0\xi^2}\chi_1(r) - \frac{3G_0 M\xi^2}{2r}\chi_2(r) \tag{4.2.17}$$

where

$$\chi_1(r) = g_* + 2^{\frac{\sigma_1}{2}} 3^{-\sigma_1}\left(\frac{\xi\sqrt{G_0 M}}{r^{3/2}}\right)^{-\sigma_1}\left[p_2 \sin\left(\sigma_2 \log\left(\frac{3\xi\sqrt{G_0 M}}{\sqrt{2}r^{3/2}}\right)\right) + p_1 \cos\left(\sigma_2 \log\left(\frac{3\xi\sqrt{G_0 M}}{\sqrt{2}r^{3/2}}\right)\right)\right] \tag{4.2.18}$$

and

$$\chi_2(r) = \lambda_* + 2^{\frac{\sigma_1}{2}} 3^{-\sigma_1}\left(\frac{\xi\sqrt{G_0 M}}{r^{3/2}}\right)^{-\sigma_1}\left[q_2 \sin\left(\sigma_2 \log\left(\frac{3\xi\sqrt{G_0 M}}{\sqrt{2}r^{3/2}}\right)\right) + q_1 \cos\left(\sigma_2 \log\left(\frac{3\xi\sqrt{G_0 M}}{\sqrt{2}r^{3/2}}\right)\right)\right] \tag{4.2.19}$$

In figure 4.6 and 4.7, we plotted the behaviour of this improved lapse function for vanishing and non-vanishing value of λ_*, and for some combination of the critical exponents.

- For $\lambda_* \neq 0$, we found that the imaginary part σ_2 of the critical exponent controls the existence of the event horizon. For $\sigma_2 \geq 1.3$, the microsocpic black hole continues to have an event horizon.
- For the case $\lambda_* = 0$, the behaviour of the solution shows that there are event horizons for many combinations of $\sigma_{1,2}$, although σ_2 still continues to dictate the position of the horizon. This is expected as it controls the sinusoidal nature of the improved lapse function.

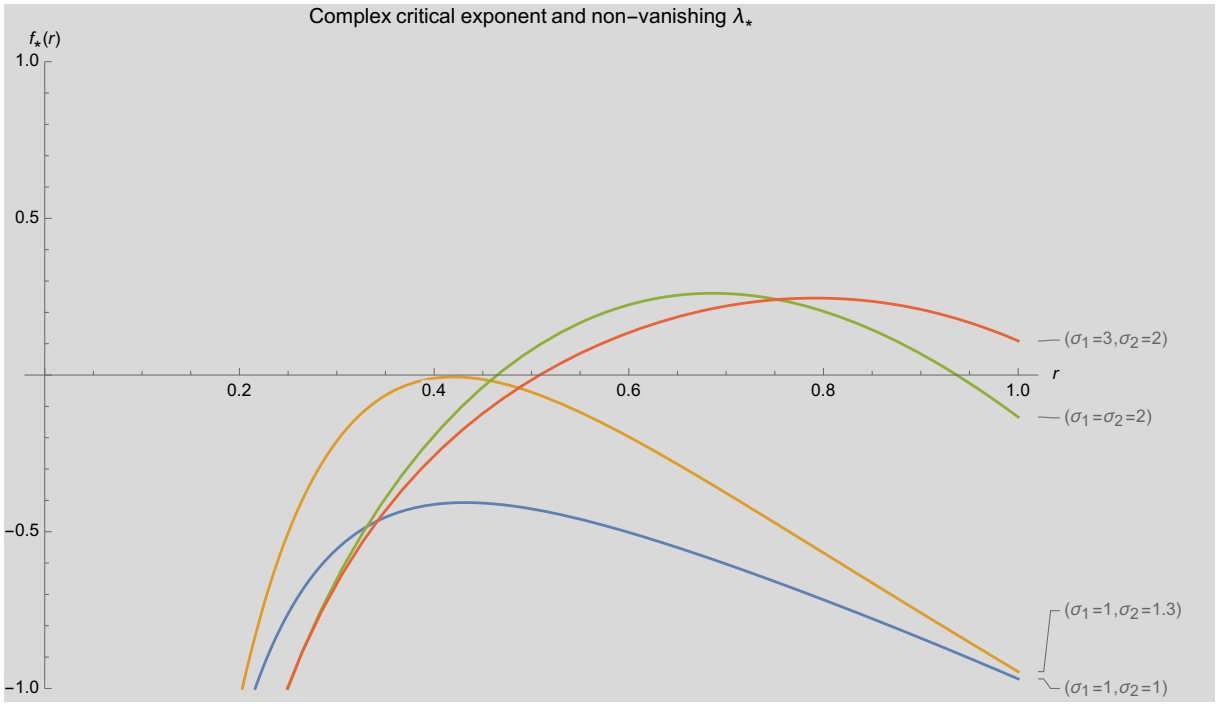

Figure 4.6: The RG improved lapse function of the classical Schwarzschild-AdS black holes for various combination of the complex critical exponents $\theta_{1,2}$. The curves are obtained for UV fixed point values $(g_*, \lambda_*) = (0.403, 0.330)$ in (2.3.9) and for $M = 1$, $G_0 = 1$, $\xi = 1$, $c_i = d_i = 1$.

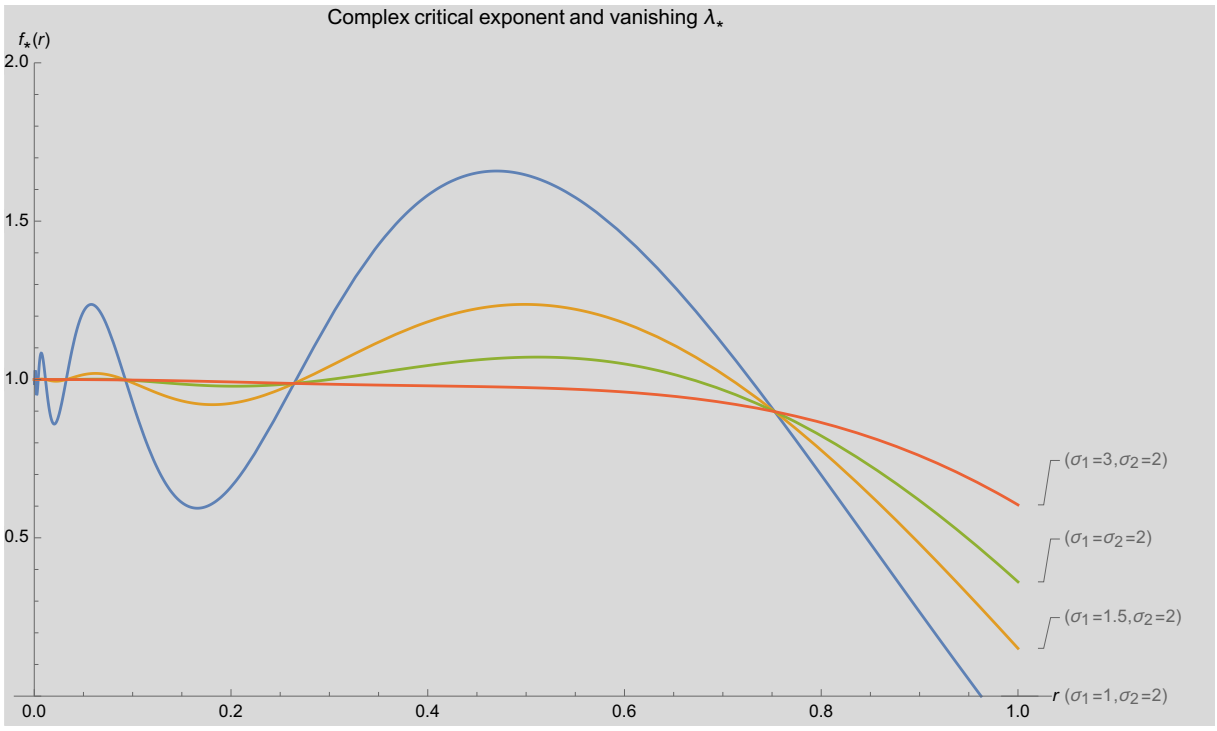

Figure 4.7: The RG improved lapse function of the classical Schwarzschild-AdS black holes for various combination of the complex critical exponents $\theta_{1,2}$. The curves are obtained for UV fixed point values $(g_*, \lambda_*) = (0.403, 0.00)$ in (2.3.9) and for $M = 1$, $G_0 = 1$, $\xi = 1$, $c_i = d_i = 1$.

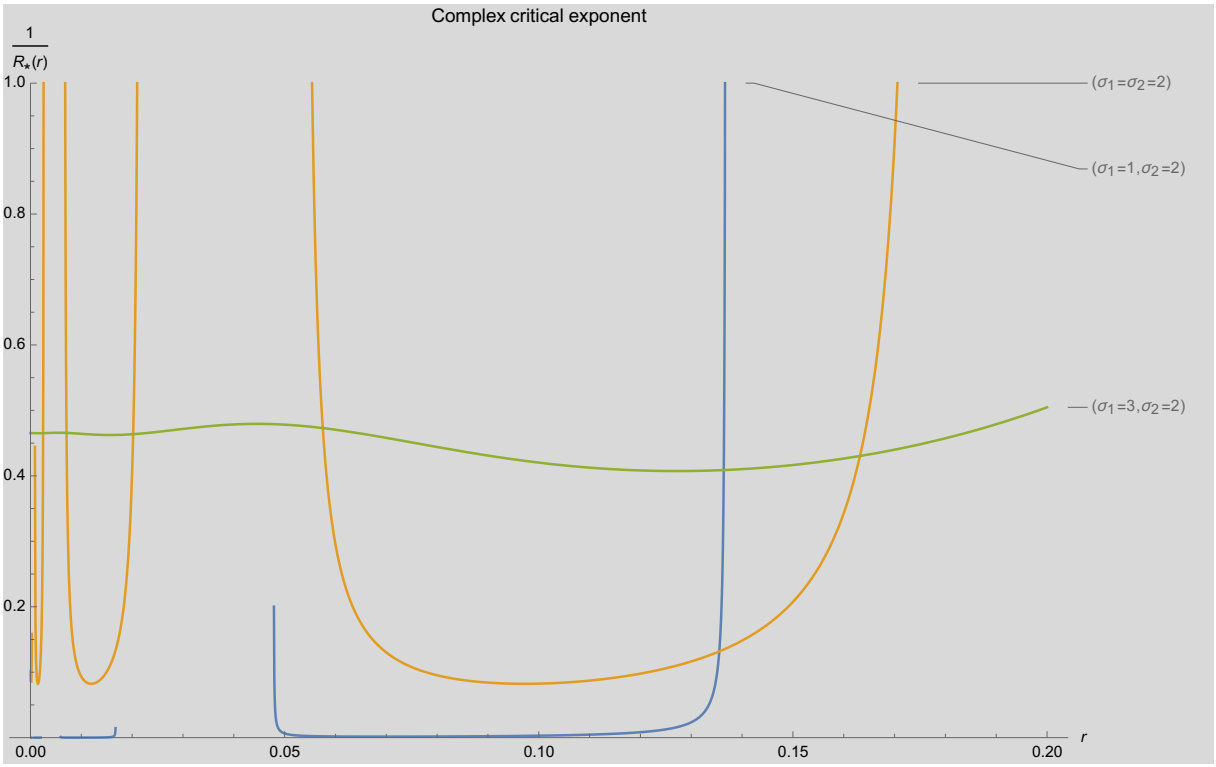

Figure 4.8: The inverse of the RG improved scalar curvature of the classical Schwarzschild-AdS black holes for various combination of the complex critical exponents $\theta_{1,2}$. The curves are obtained for UV fixed point values $g_* = 0.403$ in (2.3.9) and for $M = 1$,$G_0 = 1$, $\xi = 1$, $c_i = d_i = 1$.

- We investigate the scalar curvature at small distances. Its full expression is provided in the Appendix II.
- The scalar curvature continues to be independent of the microscopic value of the cosmological constant. The inverse of the curvature scalar is plotted in figure 4.8. Regularity of the scalar curvature is always realized for all combination of $\sigma_1 \geq 2$ and an arbitrary σ_2. For $\sigma_1 < 2$, curvature scalar diverges as $r \to 0$ for an arbitrary σ_2.

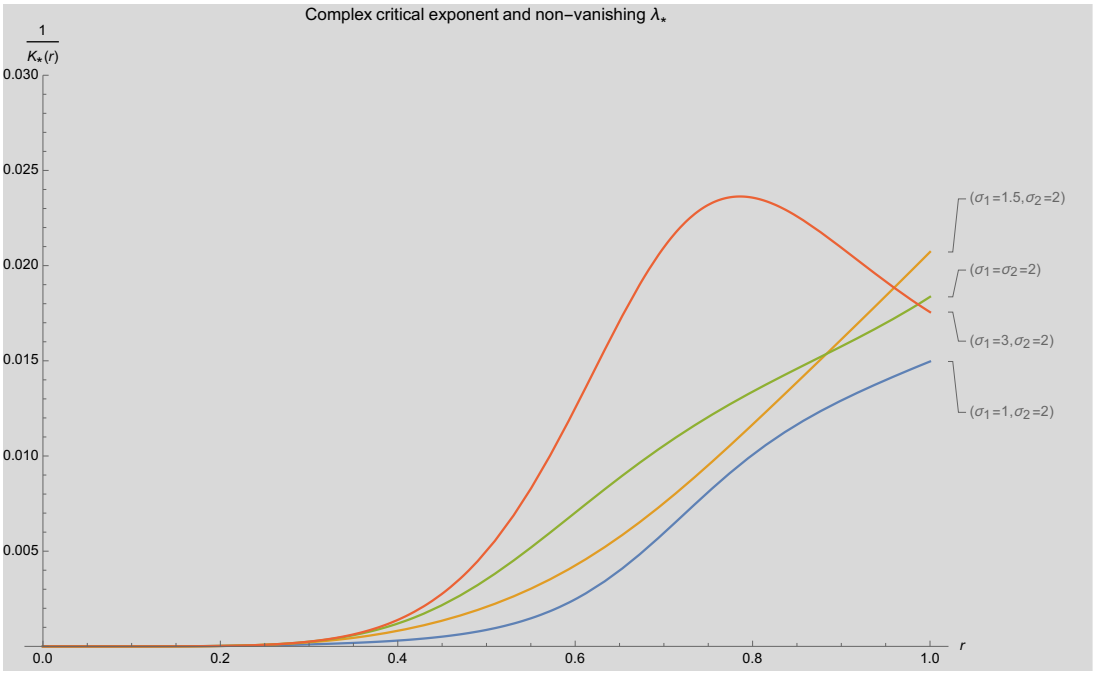

Figure 4.9: The inverse RG improved Kretschmann invariant of the classical Schwarzschild-AdS black holes for various combination of the complex critical exponent $\theta_{1,2}$. The curves are obtained for UV fixed point values $(g_*, \lambda_*) = (0.403, 0.330)$ in (2.3.9) and for $M = 1, G_0 = 1$, $\xi = 1$, $c_i = d_i = 1$.

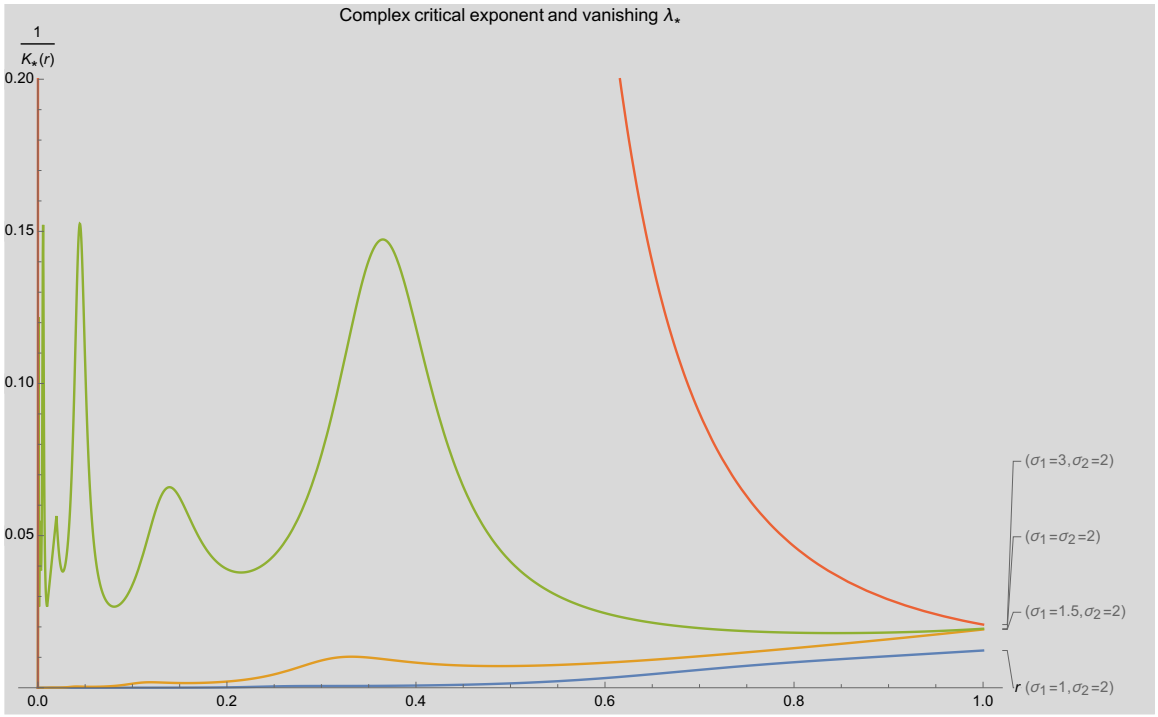

Figure 4.10: The inverse RG improved Kretschmann invariant of the classical Schwarzschild-AdS black holes for various combination of the complex critical exponent $\theta_{1,2}$. The curves are obtained for UV fixed point values $(g_*, \lambda_*) = (0.403, 0.00)$ in (2.3.9) and for $M = 1, G_0 = 1$, $\xi = 1$, $c_i = d_i = 1$.

- The full expression for the Kretschmann invariant $R^*_{\mu\nu\rho\sigma}R^{\mu\nu\rho\sigma}_*$ is provided in the Appendix II. Its small distances behaviour is shown in figure 4.9 and 4.10, where we have plotted for vanishing and non-vanishing value of the microscopic cosmological constant λ_*, and for various combination of the critical exponents.
- First for $\lambda_* \neq 0$, the inverse of the improved Kretschmann invariant goes down to zero for all scaling exponent $\sigma_{1,2}$. Again, the non-vanishing microscopic cosmological constant λ_* is at the root of the curvature singularity at small distances.
- This structure changes ultimately for $\lambda_* = 0$, for which the improved Kretschmann invariant is regular for all $\sigma_1 \geq 2$ and an arbitrary σ_2. Hence,

$$\lim_{r\to 0,\sigma_1\geq 2} R^*_{\mu\nu\rho\sigma}R^{\mu\nu\rho\sigma}_* = \text{finite}. \tag{4.2.20}$$

  so that

$$\lim_{r\to 0,\ \sigma_1\geq 2} \frac{1}{K_*(r)} = \text{finite}. \tag{4.2.21}$$

What is now obvious is that, for any critical exponent $\theta \in \mathbb{C}$ describing the scaling of the Newton's coupling at high energy regime, there exists a lower bound $\mathbf{Re}(\theta) = 2$, such that the classical curvature singularity of the Schwarzschild-AdS black holes is resolved for vanishing microscopic cosmological constant.

We note that this bound is in the vicinity of the estimates of the leading critical exponents coming from differnt studies of high energy gravity, some of which are enlisted in table 4.1 and 4.2. Accordingly, our study hints at a possibility of singularity resolution in black holes, as the qualitative estimates of the critical exponents point towards a possible realization of our bound.

4.3 Origin of the Singular-Free Improved Solution

We have observed that the vanishing value of the microscopic cosmological constant play a very crucial role in realizing a singularity-free improved black hole solution for $\mathbf{Re}(\theta) \geq 2$. Given the cumbersomeness of the full expression of the scalar curvature and the Kretschmann invariant, one could not easily track how the divergence that characterises the classical Schwarzschild-AdS black holes at $r = 0$ is fully suppressed. At this point, we shall provide a step-by-step analysis. For our analysis, it is sufficient to study the scalar curvature since it features all of the competing terms that play a role in the final structure of the RG-improved solution. We shall start with the analysis of the case of the real critical exponents and then generalize it to the complex critical exponents.

Starting again with the effective lapse function of the classical Schwarzschild-AdS black holes,

$$f_k(r) = 1 - \frac{2G_kM}{r} - \frac{1}{3}\Lambda_k r^2,$$

the RG-improvement consist in changing the k-dependence of the couplings into an r-dependence, so that the full improved lapse function is a pure fucntion r. We recall here that, up to some IR factors, our scale identification has a structure $k \sim \xi r^{-\gamma}$, where γ is motivated through appropriate scale identification. Consistency requirements on this identification imply that the RG-improved solution satisfies the scaling $R \sim k^2$ in the fixed point regime. For Schwarzschild-AdS, this is tantamount to $\gamma = 3/2$ (see (3.2.28)). In this case, the effective couplings are given

by

$$G_k \to G(r) = k^{-2}\left[g_* + c_1 k^{-\theta_1} + c_2 k^{-\theta_2}\right]\Big|_{k\sim\xi r^{-3/2}} \tag{4.3.1}$$

$$= \frac{r^3}{\xi^2}\left(g_* + c_1\left(\frac{\xi}{r^{3/2}}\right)^{-\theta_1} + c_2\left(\frac{\xi}{r^{3/2}}\right)^{-\theta_2}\right) \tag{4.3.2}$$

and

$$\Lambda_k \to \Lambda(r) = k^2\left[\lambda_* + d_1 k^{-\theta_1} + d_2 k^{-\theta_2}\right]\Big|_{k\sim\xi r^{-3/2}} \tag{4.3.3}$$

$$= \frac{\xi^2}{r^3}\left(\lambda_* + d_1\left(\frac{\xi}{r^{3/2}}\right)^{-\theta_1} + d_2\left(\frac{\xi}{r^{3/2}}\right)^{-\theta_2}\right) \tag{4.3.4}$$

In this sense, we have an effective lapse function

$$f_*(r) = 1 - \frac{2G(r)M}{r} - \frac{1}{3}\Lambda(r)r^2,$$

leading to an improved scalar curvature

$$R_*(r) = \Xi_1\left[G(r)\right] + \Xi_1\left[\Lambda(r)\right], \tag{4.3.5}$$

where

$$\Xi_1\left[G(r)\right] = \frac{2M}{r^2}\left(rG''(r) + 2G'(r)\right) \tag{4.3.6}$$

$$= \frac{3M}{2\xi^2}\left[16g_* + c_1\left(3\theta_1^2 + 14\theta_1 + 16\right)\left(\frac{\xi}{r^{3/2}}\right)^{-\theta_1} + c_2\left(3\theta_2^2 + 14\theta_2 + 16\right)\left(\frac{\xi}{r^{3/2}}\right)^{-\theta_2}\right], \tag{4.3.7}$$

and

$$\Xi_2\left[\Lambda(r)\right] = \frac{1}{3}\left[r\left(r\Lambda''(r) + 8\Lambda'(r)\right) + 12\Lambda(r)\right] \tag{4.3.8}$$

$$= \frac{\xi^2}{4r^3}\left[d_1\theta_1\left(3\theta_1 + 2\right)\left(\frac{\xi}{r^{3/2}}\right)^{-\theta_1} + d_2\theta_2\left(3\theta_2 + 2\right)\left(\frac{\xi}{r^{3/2}}\right)^{-\theta_2}\right]. \tag{4.3.9}$$

As expected, this structure is free of the microscopic cosmological constant and it features the scaling power of r as dictated by the universal gravitational critical exponent. We draw the following conclusions:

- The regularity of $\Xi_1\left[G(r)\right]$ is completely dictated by the appearance of the scaling terms $\left(\frac{\xi}{r^{3/2}}\right)^{-\theta_1}$ and $\left(\frac{\xi}{r^{3/2}}\right)^{-\theta_2}$. Obviously, these terms are regular for $\theta_{1,2} \geq 2$.
- On the other hand, the regularity of $\Xi_2\left[\Lambda(r)\right]$ is dictated by the appearance of the scaling terms $\frac{\xi^2}{4r^3}\left(\frac{\xi}{r^{3/2}}\right)^{-\theta_1}$ and $\frac{\xi^2}{4r^3}\left(\frac{\xi}{r^{3/2}}\right)^{-\theta_2}$. The $\frac{1}{r^3}$ factor emerges directly from the classical pole. One can see that any term that features any of the factor $r^{-3+3/2\theta_1}$ and $r^{-3+3/2\theta_2}$ are well behaved and remains finite for $\theta_{1,2} \geq 2$.

One can perform a similar analysis for the complex critical exponents. For brevity, set $\xi = 1$ in order to see the structure well enough. This does not change the conclusion of our analysis. In this case, the effective coupling becomes

$$G_k \to G(r) = k^{-2}\left[g_* + k^{-\sigma_1}\left[p_1 \cos\left(\sigma_2 \ln k\right) + p_2 \sin\left(\sigma_2 \ln k\right)\right]\right]\Big|_{k\sim r^{-3/2}} \tag{4.3.10}$$

$$\tag{4.3.11}$$

and

$$\Lambda_k \to \Lambda(r) = k^{2}\left[\lambda_* + k^{-\sigma_1}\left[q_1 \cos\left(\sigma_2 \ln k\right) + q_2 \sin\left(\sigma_2 \ln k\right)\right]\right]\Big|_{k\sim r^{-3/2}} \tag{4.3.12}$$

$$\tag{4.3.13}$$

This would lead to an improved scalar curvature

$$R_*(r) = \Xi_3\left[G(r)\right] + \Xi_4\left[\Lambda(r)\right] \tag{4.3.14}$$

where

$$\Xi_3\left[G(r)\right] = \frac{2M}{r^2}\left(rG''(r) + 2G'(r)\right) \tag{4.3.15}$$

$$= \#_0\ g_* + Mr^{\frac{3\sigma_1}{2}}\left[\#_1\ \sin\left(\frac{3\sigma_2}{2}\ln r\right) + \#_2\ \cos\left(\frac{3\sigma_2}{2}\ln r\right)\right] \tag{4.3.16}$$

and

$$\Xi_4\left[\Lambda(r)\right] = \frac{1}{3}\left[r\left(r\Lambda''(r) + 8\Lambda'(r)\right) + 12\Lambda(r)\right] \tag{4.3.17}$$

$$= r^{-3+\frac{3\sigma_1}{2}}\left[\#_3\ \sin\left(\frac{3\sigma_2}{2}\ln r\right) + \#_4\ \cos\left(\frac{3\sigma_2}{2}\ln r\right)\right] \tag{4.3.18}$$

Again, this structure is free of λ_* and it features the scaling power of r as dictated by the universal gravitational critical exponent. We draw the following conclusion:

- First we noticed that $\{\#_i\}_{i=0,1..,4}$ are some real functions of $p_{1,2}, q_{1,2}, \sigma_{1,2}$, and they remain finite for all finite values of $p_{1,2}, q_{1,2}, \sigma_{1,2}$. $\Xi_3\left[G(r)\right]$ and $\Xi_4\left[\Lambda(r)\right]$ now feature sine and cosine functions, which for all argument $\left(\frac{3\sigma_2}{2}\ln r\right)$, are bounded between 0 and 1. Thus, the regularity of the scalar curvature (4.3.14) is independent of σ_2.
- The regularity of $\Xi_3\left[G(r)\right]$ is completely dictated by the appearance of the scaling terms $r^{\frac{3\sigma_1}{2}}$, which is regular for all $\sigma_1 \geq 0$.
- On the other hand, the regularity of $\Xi_2\left[\Lambda(r)\right]$ is dictated by the appearance of the scaling terms $r^{-3+\frac{3\sigma_1}{2}}$, which continues to be well behaved for $\sigma_1 \geq 2$.
- Thus, the full scalar curvature (4.3.14) is regular only for $\sigma_1 \geq 2$. This therefore put a lower bound $\sigma_1 = 2$ on the real part of the critical exponents.
- In fact, in the case of the Kretschmann invariant $R^*_{\mu\nu\rho\sigma}R^{\mu\nu\rho\sigma}_*$, the divergence we found for non-vanishing value of the microscopic cosmological constant is due to the lack of suppressing term such as $\left(\frac{\xi}{r^{3/2}}\right)^{-\theta_1}$ and $\left(\frac{\xi}{r^{3/2}}\right)^{-\theta_2}$ in the $\frac{\lambda_*}{r^\beta}$-term, for some $\beta \in \mathbb{Z}^+$,

that controls the final form of divergences of the Kretschmann invariant. As such, even when all other terms have been fully suppressed, the $\frac{\lambda_*}{r^\beta}$-term eventually takes the leading role and thus, $R^*_{\mu\nu\rho\sigma}R^{\mu\nu\rho\sigma}_*$ would diverge to the order $\mathcal{O}(r^{-\max(\beta)})$ when the microscopic cosmological constant is non-vanishing, and thus, no values of $\theta_{1,2}$ could come to the rescue of regularity in the small distance regime.

- The origin of the singularity-free improved solution is now clear, that, once the microscopic cosmological constant is too small to vanish, the classical singularity of the Schwarzschild-AdS black holes is resolved by quantum gravitational effect which gaurantees a scaling associated with the universal gravitational exponent $\theta_{1,2} \geq 2$.

Chapter 5

Summary and Outlook

In this work, we studied the structural aspect of black holes in asymptotically safe gravity. In particular, we were keen on understanding the qualitative implications of asymptotic safety for the structure of the quantum improved black hole spacetime. Here, we briefly summarize our findings and discuss future outlook perspectives.

At the level of the Einstein-Hilbert approximation to the full dynamics, the asymptotic safety paradigm had been used to argue for a resolution of the black hole singularity. However, only for vanishing microscopic value of the dimensionless cosmological constant, λ_*. In this case, the quantum spacetime turns out to have a smooth de Sitter core and the improved solution appears Hayward-like, so that the RG-improved solution continues to avoid the cosmic censorship hypothesis even for mass $M < M_{\rm cr}$.

As a consequence of non-vanishing microscopic cosmological constant, the black hole spacetime singularity in the quantum improved spacetime reappears. We have also shown this in our study. The terms proportional to λ_* in the Kretschmann scalar do not contain enough suppresing power unlike the term featuring the dimensionless Newton's coupling g_*. As a consequence, these terms continue to be the leading term at small r as long as the microscopic value of the dimensionless cosmological constant is non-vanishing. This conclusion continues to hold even for all scale identifications associated with $d(r) \sim r^\gamma$, and there is therefore no remedy for this situation at the level of the Einstein-Hilbert truncation. Note that the effective cosmological constant of the improved black hole solution is independent of λ_* and strictly positive. This suggests that the observation of a finite cosmological constant at large scales need not be in contradiction with black hole singularity resolution, even in a simple approximation such as Einstein-Hilbert.

A vanishing microscopic fixed point value of the dimensionless cosmological constant offers an opportunity to seek for a bound on the universal gravitational critical exponents. In the fixed point regime, the critical exponents enter directly into the full curvature invariants, and as a consequence, demanding a regular improved black hole core puts a lower bound on the value of the critical exponents. We studied two classes of critical exponents. For the case of real critical exponents $\theta_{1,2}$, we found that the core of the RG-improved black holes continue to be regular only for $\theta_{1,2} \geq 2$. For the class of complex critical exponent $\theta_{1,2} = \sigma_1 \pm \sigma_2$, where $\theta_{1,2}$ form a complex conjugate pair, we found that the quantum improved spacetime geometry places a bound on the real part σ_1, so that the black hole singularity vanishes for all combination of $\sigma_1 \geq 2$ and an arbitrary value of σ_2. The arbitariness of σ_2 is understandable since it only controls the spiral nature of the RG-trajectories in the fixed point regime. It is very encouraging that the lower bound on the real critical exponents is in the vicinity of the estimates coming from different studies of gravity. Accordingly, our study hints at the possibility of singularity

resolution in black holes, as the explicit estimates of the critical exponents point towards a possible realization of our bound.

The realization of a regular core in the RG-improved Schwarzschild solution poses a question as to whether all asymptotically flat spacetime configurations are asymptotically safe in the sense that their classical singularity is resolved by RG-improvement. This question is left for future work. In the appendix, we instead broaden the application of the RG-improvement procedure to several other configurations beyond Einstein gravity. For this, we studied some non-trivial flat configurations of the pure R^2 gravity, as well as Hayward-like black holes. Hayward-like black holes features a regular de-Sitter core and they are asymptotically flat. Our investigation shows that these aymptotically flat configurations, characterized only by their mass M, continue to have regular de-Sitter core at their asymptotically safe UV fixed point, for any scale identification associated with $d(r) \sim r^\gamma$ with $\gamma \geq 3/2$. Therefore, we thus far found no counter-example to the proposal that an asymptotically safe regime generically results in singularity resolution. It is not yet obvious if such counter-example exists, however, what our study suggests is that families of asymptotically flat configurations, characterized by only mass, do features a leading order term like $\mathcal{O}(r^{-6+4\gamma})$, so that their configurations are always asymptotically safe for all $\gamma \geq 3/2$. This suggests the regularity of the improved flat geometry at the non-trivial fixed point of the renormalization group flows.

The study of the renormalization group improved configuration of the pure R^2 gravity may in fact be a good starting point of studying whether the eventual singularity of the improved Schwarzschild geometry, in the limit of non-vanishing value of the microscopic dimensionless cosmological constant, is a truncation artifact. Based on our studies, one may explore RG improvement beyond the Einstein-Hilbert truncation.

Going to the higher gravity truncation to seek for improved spacetime configurations is technically, a difficult task, as one will have to confront coupled differential equations of order greater than 2. At order 4, field equations are daunting to solve analytically, so that the renormalization group improvement would have to be done numerically. More recently, there has been some progress (cf. [126]-[128]) in confronting the first task and in particular, the spherically symmetric solutions have been explored to the second plus fourth-order pure gravity theory

$$S = \int d^4x\sqrt{-g}\left[\gamma(R - 2\Lambda) - \alpha C_{\mu\nu\rho\sigma}C^{\mu\nu\rho\sigma} + \beta R^2\right], \tag{5.0.1}$$

whose spectrum contains a massless graviton, a massive spin-2 ghost excitation of mass $(m_2)^2 = \frac{\gamma}{2\alpha}$ and a massive spin-0 mode with mass $(m_0)^2 = \frac{\gamma}{2\beta}$, where $\gamma = \frac{1}{16\pi G}$. The Frobenius method was employed to make a non-trivial asymptotic ansatz of the form

$$A(r) = a_s r^s + a_{s+1}r^{s+1} + a_{s+2}r^{s+2} + ..., \tag{5.0.2}$$

$$B(r) = b_t\left(r^t + b_{t+1}r^{t+1} + b_{t+2}r^{t+2} + ...\right), \tag{5.0.3}$$

with $a_s \neq 0 \neq b_t$, and an attempt was made to find a solution pair $(s,t)_{r_0}$ that exist for all α, β. The subscript r_0 indicates that the pair (s,t) is a near r_0 solution. Of interest are the near singularity solutions whose classical structure may constitute the starting point for further studies on RG-improved black holes. Three families of this kind were not ruled out by the Frobenius analysis, namely, the $(0,0)_0$, $(1,-1)_0$ and the $(2,2)_0$ family, whose Kretschmann invariant are respectively non-singular, diverges like r^{-6} and r^{-8}. These solutions contain some free parameters which are yet to be fixed. Take for instance the $(1,-1)_0$ family which, in the

limit of $\beta = 0$, corresponds to the two-function solution

$$A(r) = a_1 r - a_1^2 r^2 + a_1^3 r^3 + r^4 \left(\frac{5}{3} a_1 b_2 - a_1^4\right) + r^5 \left(a_1^5 - \frac{23}{6} a_1^2 b_2\right) + \mathcal{O}(r^6), \tag{5.0.4}$$

$$\frac{B(r)}{b_{-1}} = \frac{1}{r} + a_1 + b_2 r^2 + \frac{1}{6} a_1 b_2 r^3 - \frac{1}{5} r^4 a_1 b_2 + \mathcal{O}(r^5). \tag{5.0.5}$$

The solution is characterized by three free parameters. In the limit of $\beta \neq 0$, the classical solution is characterized by four free parameters. These parameters are expected to feature the coupling constants appearing in (5.0.1) as well as the mass of the system, so that a qualitative RG improvement could be done when these free parameters are known. Neverthelss, one could start gaining some insight into the RG-improved solution by starting from a dimensional argument to provide the scaling of these parameters at high energy. Namely, since $A(r)$ and $B(r)$ must be dimensionless, one should expect a scaling of the following form at high energy: $a_1 \sim a_1^* k$, $b_2 \sim b_2^* k^3$ and $b_{-1} \sim b_{-1}^* k^{-1}$. However, the tricky part of this starting point would be that, if the free parameters are functions of the mass of the system, the RG improvement is therefore tantamount to a running mass. If this is found physically reasonable, such RG improvement may start to hint at the structural aspects of quantum improved black holes in the quadratic gravity truncation. This is, in fact, worth studying.

In our study, using dimensional analysis as a guide, we proposed a scale identification associated with a diffeomorphic invariant distance of the type

$$d(r) = c_\gamma \; G(r)^{-\gamma+\delta+1} \; \Lambda(r)^{-\delta} \; r^\gamma,$$

which includes the effective Newton coupling $G(r)$ and the cosmological constant $\Lambda(r)$. For any scaling of this form, one can demand its self-consistency by requiring that the corresponding RG-improved spacetime geometry satisfies the scaling $R \sim k^2$ in the fixed point regime (cf. (3.1.7)). This is worth studying to understand what freedom is allowed for a physically motivated scale identification. Indeed, if such freedom exists, one can always check for how qualitative and well motivated a scale identification is, and it will in turn improve the robustness of the analysis.

Black holes are an intriguing test-field for quantum gravity as one cannot ignore the interplay between the central singularity and the microscopic dynamics of quantum spacetime. Insights from black hole physics could in turn hint at the quantum nature of spacetime. Thus, we can really start to truly understand how the macroscopic ideas of the universe and gravity arise from an underlying microscopic description of gravity. Whatever we learn is going to have a dramatic impact on the way we think about the fundamental nature of quantum spacetime.

Part I

On the Asymptotically Safe Flat Configurations

Flat Configurations and Asymptotic Safety

One of the lessons of the last chapters is that the classical singularity of the Schwarzschild geometry could be resolved by asymptotic safety. According to Birkhoff's theorem, any spherically symmetric solution of the Einstein field equations (EFE), without the cosmological constant, must be static and asymptotically flat, so that the only unique vacuum solution of the EFE is the Schwarzschild solution, satisfying the aymptotically flat requirement

$$R_{\mu\nu} = 0, \tag{.0.6}$$

and characterized by only it mass M.

One immediate question to ask is:

In $d = 4$, are all asymptotically flat configurations, characterized by only mass M, asymptotically safe?

In this chapter, we shall investigate this question by seeking for possible counter-example. Since all asymptotically flat configurations has the property that they approaches a Minkowski spacetime at infinity, one can seek for such non-trivial configurations that are different from the Schwarzschild family of solutions.

Some $f(R) = R+\mu R^n$ gravity models, for $n \in \mathbb{Z}$, are phenomenologically interesting, for example in cosmology [119]. The Starobinsky model [120]

$$S = \frac{1}{16\pi G}\int d^4x\sqrt{-g}\left(R + \mu R^2\right), \tag{.0.7}$$

which corresponds to the case $n = 2$, propagates a graviton and a massive spin-0 state. This model has given rise to a consistent cosmological inflationary model [121, 122] as it produces an accelerated epoch of time preceding the radiation and matter stage of the universe. That the existence of the quadratic term μR^2 lead to an asymptotically exact de Sitter solution is of particular interest. Spacetime configurations in pure R^2 gravity may have some interesting properties. The pure R^2 has been shown to be the only ghost-free theory in the quadratic curvature gravity theory [123].

Non-trivial flat configurations exist as global minima and maxima of pure R^2 gravity [124]. The static spherically symmetric configuration is characterized by just its mass. While the global analysis of this configuration and its stability to linearized gravitational perturbation have not been investigated (as far as we know), classical singularity is one of its main features. This suggests that the solution could be a black hole spacetime, or otherwise, a naked singularity. In any case, the appearance of such a spacetime singularity is an artifact of the classical description of gravity which must be overcome by a consistent quantum gravity theory.

Hayward type black holes [11] belong to the asymptotically flat family of solutions with a classical de-Sitter core, so that it is classically different in structure compared to the general spherically symmetric solution to (.0.6). It is not obvious if this regular core continues to remain when gravitational quantum effect are taken into consideration. Since this belongs to the class we would like to investigate, we shall include it in our analysis.

.1 The Non-trivial Flat Configuration of the Pure R^2

The pure R^2 gravity model is given by

$$S = \frac{1}{\kappa^2}\int d^4x\sqrt{-g}\ R^2. \tag{.1.1}$$

where $\kappa \in \mathbb{R}$ is a dimensionless coupling constant. Introducing a langrangian multiplier $\Phi = \frac{2}{\kappa}R$, this action can be written as Einstein gravity, non-minimally coupled with a scalar Φ :

$$S = \int d^4x\sqrt{-g}\ \left(\Phi R - \frac{\kappa}{4}\Phi^2\right). \tag{.1.2}$$

By performing a conformal transformation

$$g_{\mu\nu} = \frac{1}{2}M_{pl}^2\Phi^{-1}\bar{g}_{\mu\nu}, \tag{.1.3}$$

(.1.4) can be brought into the form

$$S = \int d^4x\sqrt{-g}\ \left(\frac{M_{pl}^2}{2}\bar{R} - \frac{3M_{pl}^2}{4}\frac{\partial_\mu\Phi\partial^\mu\Phi}{\Phi^2} - \frac{\kappa M_{pl}^4}{16}\right). \tag{.1.4}$$

Thus, one finds that the pure R^2 gravity theory is conformally equivalent to Einstein gravity, minimally coupled to a scalar Φ. Obviously, this conformal equivalence is possible only if the curvature scalar is non-vanishing, $R \neq 0$, otherwise, the conformal transformation is singular. In this case $R \neq 0$, the pure R^2 vacuum solution is conformally (A)dS, with $\Lambda = \frac{\kappa M_{pl}^4}{16}$ performing the role of the cosmological constant in the Einstein frame.

In the presence of matter $S = \int d^4x\sqrt{-g}\ \mathcal{L}_{\text{matter}}$, the field equation to (.1.1) is given as

$$J_{\mu\nu} \equiv RR_{\mu\nu} - \frac{1}{4}R^2g_{\mu\nu} - \nabla_\mu\nabla_\nu R + g_{\mu\nu}\nabla^2R = 4\kappa^2T_{\mu\nu}. \tag{.1.5}$$

One can show that $J_{\mu\nu}$ is covariantly constant, so that the energy-momentum tensor $T_{\mu\nu}$ is covariantly conserved.

We seek the solution to

$$J_{\mu\nu} = 0, \tag{.1.6}$$

whose trace lead to

$$\Box R = 0. \tag{.1.7}$$

We shall now employ a theorem on static solutions to fourth order gravity. This theorem provides the solution to (.1.7) that are asymptotically flat.

Theorem .1 (W. Nelson, 2010)**.** *If the spacetime is static* ($\mathcal{L}_t g_{\mu\nu}$)*, and* $\nabla_\mu R \to 0$ *sufficiently fast at infinity, then* $(\Box - m^2)R = 0$*, for* $0 \neq m \in \mathbb{R}$ *implies* $R = 0$*. If the spacetime is static and* $R \to 0$ *sufficiently fast at infinity, the equation* $\Box R = 0$ *implies* $R = 0$*.*

Proof. See [125]. ∎

One note that, since

$$S = \frac{1}{\kappa^2}\int d^4x\sqrt{-g}\ R^2 \geq 0, \tag{.1.8}$$

flat configurations, $R = 0$, satisfying (.1.7) are global maxima of (.1.8) for $\kappa^2 < 0$ and are global minima of (.1.8) for $\kappa^2 > 0$, both of which satisfies the bound in (.1.8). While there are trivial configurations like the Schwarzschild Ansatz, which continues to be among the solutions to pure R^2 gravity, there is non-trivial ansatz satisfying such bound and this has been constructed in [124].

A general static spherically symmetric spacetime ansatz is given as

$$ds^2 = -f(r)dt^2 + \frac{dr^2}{g(r)} + r^2 d\Omega_2^2, \tag{.1.9}$$

for some real functions $g(r)$ and $f(r)$. In the Schwarzschild case, this configuration is characterized by a single function, with

$$f(r) = g(r) = 1 - \frac{2GM}{r}. \tag{.1.10}$$

Inserting (.1.9) in the curvature scalar,

$$R = -\left(\frac{rg' + 4g}{2g}\right) f'(r) + \left(\frac{g'^2}{2g^2} - \frac{g''}{g} - \frac{2g'}{rg} - \frac{2}{r^2}\right) f(r) + \frac{2}{r^2}. \tag{.1.11}$$

Hence, we wish to solve a second order ordinary differential equation

$$f'(r) \ + \Delta_1(r)\ f(r) \ + \Delta_2(r) = 0, \tag{.1.12}$$

where

$$\Delta_1(r) = \frac{2r^2gg'' - r^2g'^2 + 4rgg' + 4g^2}{r^2gg' + 4rg^2}, \tag{.1.13}$$

and

$$\Delta_2(r) = -\frac{4g}{r^2g' + 4rg}. \tag{.1.14}$$

The structure of (.1.12) is such that, given a dimensionally correct ansatz for the lapse function $g(r)$ satisfying a required boundary condition, $f(r)$ can in fact be uniquely determined. This method of solution was used in [124] in solving for backgrounds that are global minima and maxima of the pure R^2 gravity.

Since we are seeking for asymptotically flat configurations, characterized by only mass M, we demand that spacetime be Minkowskian at infinity, so that

$$\lim_{r\to\infty} g(r) = 1, \qquad \text{and} \qquad \lim_{r\to\infty} f(r) = 1. \tag{.1.15}$$

Therefore, the non-trivial classical configurations are uniquely determined by the asymptotic conditions (.1.15) and the structure of the singularity. By structurthe e of singularity, we demand classical solutions whose geometry is regular everywhere except at $r = 0$. This requirement will in turn fix the integrating constant. of the solution to (.1.12). We shall now list some family of solutions satisfying R=0. To begin with, we shall first use this method to realize the extremal solution of the Reissner-Nordström metric. Afterward, we present the other non-trivial solutions.

.1.1 Extremal RN Black Holes

The extremal limit of the Reissner-Nordström charged black hole is completely characterized by its mass $M = Q$. This is an already known solution to the Einstein-Maxwell field equation. In this case, the general ansatz for the lapse function $g(r)$ is

$$g(r) = \left(1 - \frac{GM}{r}\right)^2. \tag{.1.16}$$

Solving for $f(r)$ in (.1.12), we obtain

$$f(r) = \frac{2r^2 - 2CGM + 4Cr + G^2M^2 - 2GMr}{2r^2}, \tag{.1.17}$$

so that the Kretschmann invariant is

$$R_{\mu\nu\rho\sigma}R^{\mu\nu\rho\sigma} = \frac{\Xi(r)}{r^8(r - GM)^2}, \tag{.1.18}$$

where

$$\begin{aligned}\Xi(r) = {} & 6r^4\left(4C^2 - 4CGM + 5G^2M^2\right) + 14G^4M^4(GM - 2C)^2 - 52G^3M^3r(GM - 2C)^2 \\ & + 2G^2M^2r^2(GM - 2C)(45GM - 58C) - 4GMr^3(GM - 2C)(19GM - 10C).\end{aligned} \tag{.1.19}$$

This geometry features a divergence to order $\mathcal{O}(r^{-8})$ at $r = 0$ and another irregularity at $r = GM$. By choosing $C = -GM/2$, the singularity at $r = GM$ vanishes, so that this choice correctly reproduces the lapse function

$$f(r) = \left(1 - \frac{GM}{r}\right)^2, \tag{.1.20}$$

of the extremal RN black holes.

This highlight that this method correctly provides some of the already known black holes that are characterized by only their mass. For the moment, we shall restrict to this feature of black holes.

Now, we shall obtain some other non-trivial flat solutions solution for which $f(r) \neq g(r)$.

.1.2 Non-trivial configurations

We begin in the usual manner by choosing an ansatz for $g(r)$[1].

Ansatz I:

Obviously, any ansatz of the form

$$g(r) = \left(1 - \frac{\alpha GM}{r}\right)^n, \tag{.1.21}$$

[1]We note that as we do not explicitly check, the form provided below might be a coordinate trasformation of the Schwarzschild solution.

for $n, \alpha \in \mathbb{R}$, is dimensionless and satisfies the asymptotic condition far away at infinity since

$$\lim_{r\to\infty}\left(1-\frac{\alpha GM}{r}\right)^n = 1.$$

Starting with an ansatz

$$g(r) = \left(1-\frac{GM}{2r}\right)^4, \tag{.1.22}$$

which corresponds to $n = 4$ and $\alpha = \frac{1}{2}$, and solving for $f(r)$ in (.1.12), we obtain

$$f(r) = \frac{9r\left(Ce^{-\frac{3GM}{2r}}+4r\right)+3G^2M^2-20GMr}{9(GM-2r)^2}, \tag{.1.23}$$

so that the corresponding Kretschmann scalar is

$$R_{\mu\nu\rho\sigma}R^{\mu\nu\rho\sigma} = \frac{e^{-\frac{3GM}{r}}}{162r^4(GM-2r)^6}\,\Xi(r), \tag{.1.24}$$

where

$$\begin{aligned}\Xi(r) = {} & 81C^2\left(27G^4M^4-144G^3M^3r+312G^2M^2r^2-64GMr^3+48r^4\right)\\ & -144CGMe^{\frac{3GM}{2r}}\left(27G^4M^4-252G^3M^3r+804G^2M^2r^2-880GMr^3-96r^4\right)\\ & +128G^2M^2e^{\frac{3GM}{r}}\left(27G^4M^4-306G^3M^3r+1332G^2M^2r^2-2648GMr^3+2040r^4\right).\end{aligned} \tag{.1.25}$$

Now, this geometry is irregular $r = 0$ and $r = GM/2$. The Kretschmann diverges up to order $\mathcal{O}(r^{-4})$ at $r = 0$. This singularity is classically weakened when compared to spacetime singularity the Schwarzschild and the RN black holes. By choosing $C = -\frac{4}{9}e^3GM$, the singularity $r = GM/2$ vanishes, so that

$$f(r) = \frac{3G^2M^2+4GMr\left(-e^{3-\frac{3GM}{2r}}-5\right)+36r^2}{9(GM-2r)^2}. \tag{.1.26}$$

The behaviour of the lapse functions and the Kretschmann invariant are respectively depicted in figure 1 and 2, showing an asymptically flat solution with an event horizon. The geometry is irregular at very small distances.

Ansatz II:

Another form of non-trivial ansatz are family of exponential functions satisfying the requirement (.1.15)[2]. One can therefore begin with an ansatz such as

$$g(r) = \exp\left(-\frac{\beta GM}{r}\right). \tag{.1.27}$$

This lapse function is dimensionally correct. In particular, $g(r)$ is dimensionless. This is what we want, so that the line element is of dimension length square. Solving for $f(r)$ in (.1.12), we obtain

$$f(r) = \frac{r^2}{(\beta GM+4r)^5}\left[Cr^2e^{\frac{\beta GM}{r}}+4\beta^3G^3M^3+72\beta^2G^2M^2r+456\beta GMr^2+1024r^3\right]. \tag{.1.28}$$

[2]Again, we don't explicitly check whether this is simply a coordinate transformation of Schwarzschild solution.

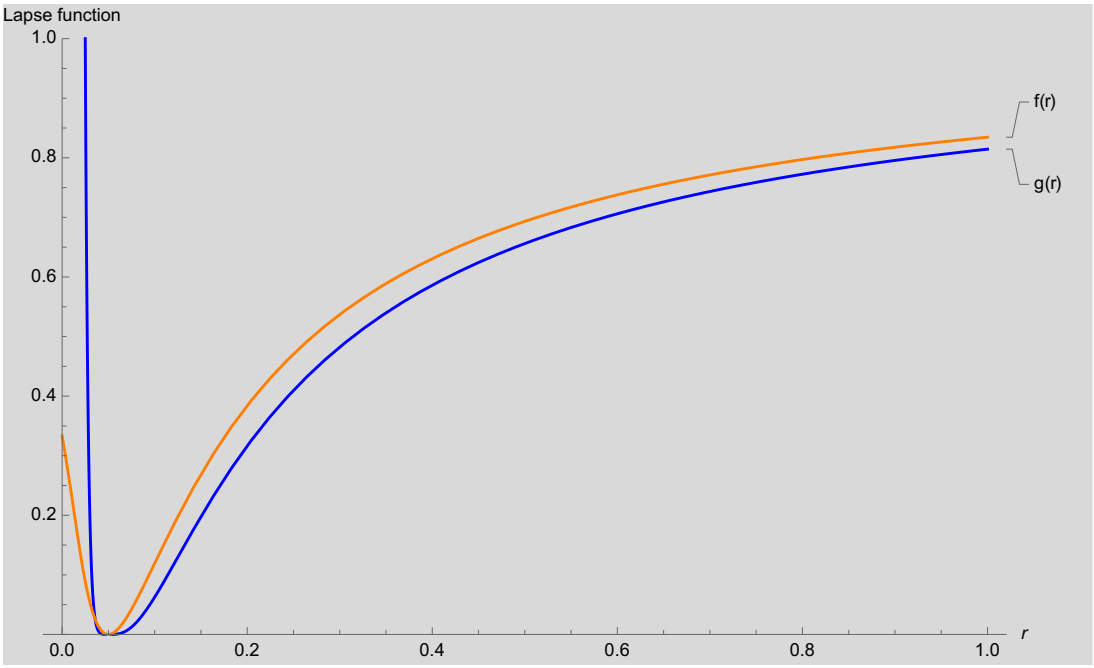

Figure 1: The profile function (.1.22) and (.1.26) of the non-trivial flat solution of the pure R^2. The curves are obtained for $M = 0.1$, $G_0 = 1$.

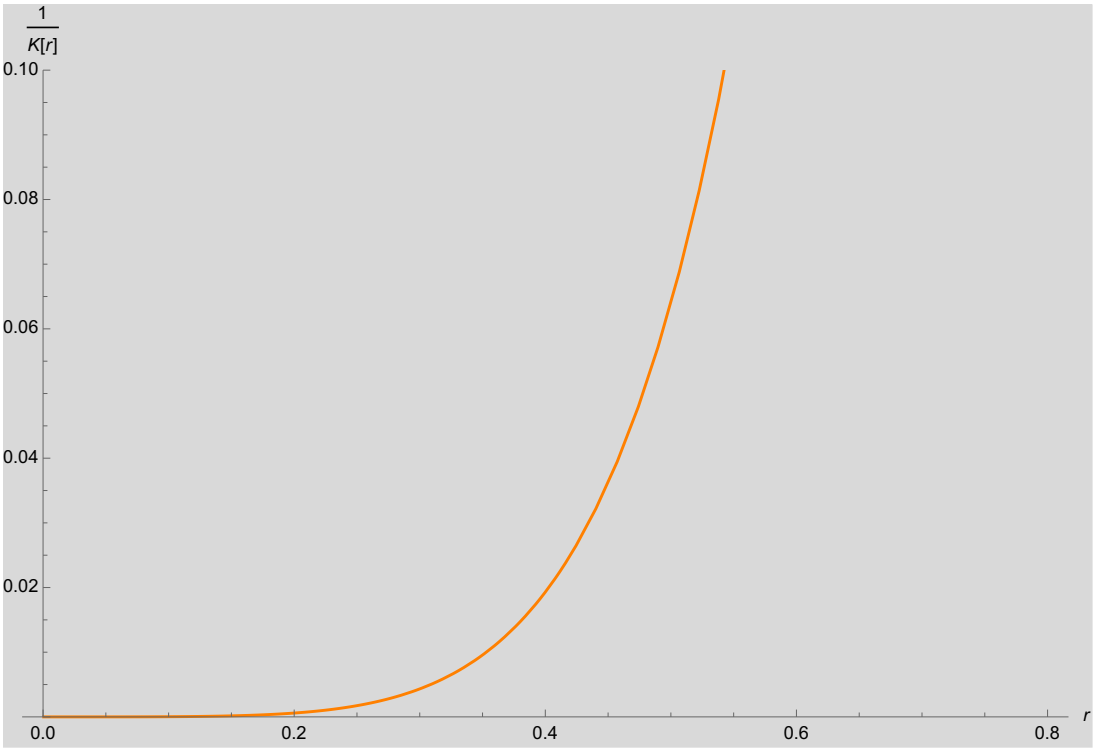

Figure 2: The Kretschmann invariant of the non-trivial flat solution (.1.22) and (.1.26). The curves are obtained for $\beta = 2$, $M = 0.1$, $G_0 = 1$

The corresponding Kretschmann scalar is

$$R_{\mu\nu\rho\sigma}R^{\mu\nu\rho\sigma} = \frac{4}{r^4(\beta GM+4r)^{12}}\,\Xi(r), \tag{.1.29}$$

where

$$\begin{aligned}\Xi(r) = {} & C^2r^6e^{\frac{2\beta GM}{r}}\left(\beta^4G^4M^4+4\beta^3G^3M^3r+38\beta^2G^2M^2r^2+8\beta GMr^3+24r^4\right)\\ & -8\beta CGMr^4e^{\frac{\beta GM}{r}}\left(\beta^6G^6M^6+20\beta^5G^5M^5r+142\beta^4G^4M^4r^2+316\beta^3G^3M^3r^3\right)\\ & -8\beta CGMr^4e^{\frac{\beta GM}{r}}\left(-724\beta^2G^2M^2r^4-2624\beta GMr^5+4944r^6\right)\\ & +2\beta^2G^2M^2\left(\beta^{10}G^{10}M^{10}+44\beta^9G^9M^9r+868\beta^8G^8M^8r^2+10112\beta^7G^7M^7r^3\right)\\ & +2\beta^2G^2M^2\left(77392\beta^6G^6M^6r^4+413120\beta^5G^5M^5r^5+1621408\beta^4G^4M^4r^6\right)\\ & +2\beta^2G^2M^2\left(4972544\beta^3G^3M^3r^7+12292288\beta^2G^2M^2r^8+22189824\beta GMr^9+20730624r^{10}\right)\end{aligned} \tag{.1.30}$$

This configuration is irregular $r=0$ and $r=-\beta GM/4$. The singularity at $r=-\beta GM/4$ is unphysical as long as $\beta\geq 0$, with $\beta=0$ realizing a Minkowski spacetime. The Kretschmann diverges up to order $\mathcal{O}(r^{-4})$ at $r=0$. By choosing $C=24e^4\beta GM$, the singularity $r=-\beta GM/4$ vanishes, so that

$$f(r) = \frac{4r^2\left(\beta^3G^3M^3+18\beta^2G^2M^2r+6\beta GMr^2\left(e^{\frac{\beta GM}{r}+4}+19\right)+256r^3\right)}{(\beta GM+4r)^5}. \tag{.1.31}$$

For $\beta=2$, the behaviour of the lapse functions and the Kretschmann invariant are respectively depicted in figure 3 and 4. For a very small mass, a naked singularity may arise.

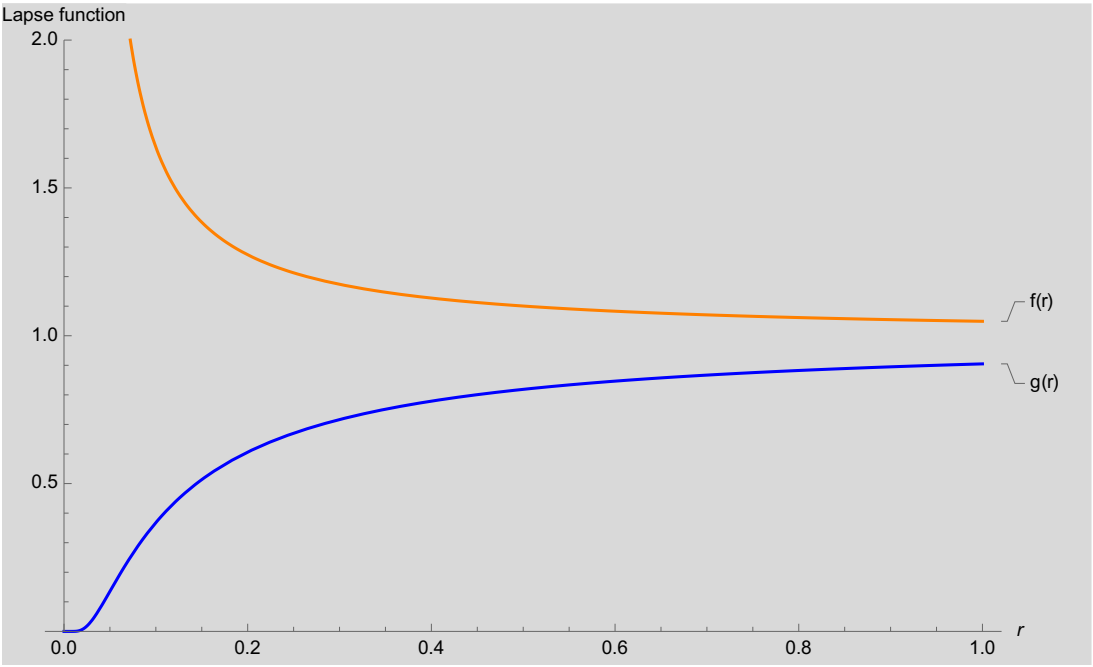

Figure 3: The profile function (.1.27) and (.1.31) of the non-trivial flat solution of the pure R^2. The curves are obtained for $M=0.05$, $G_0=1$

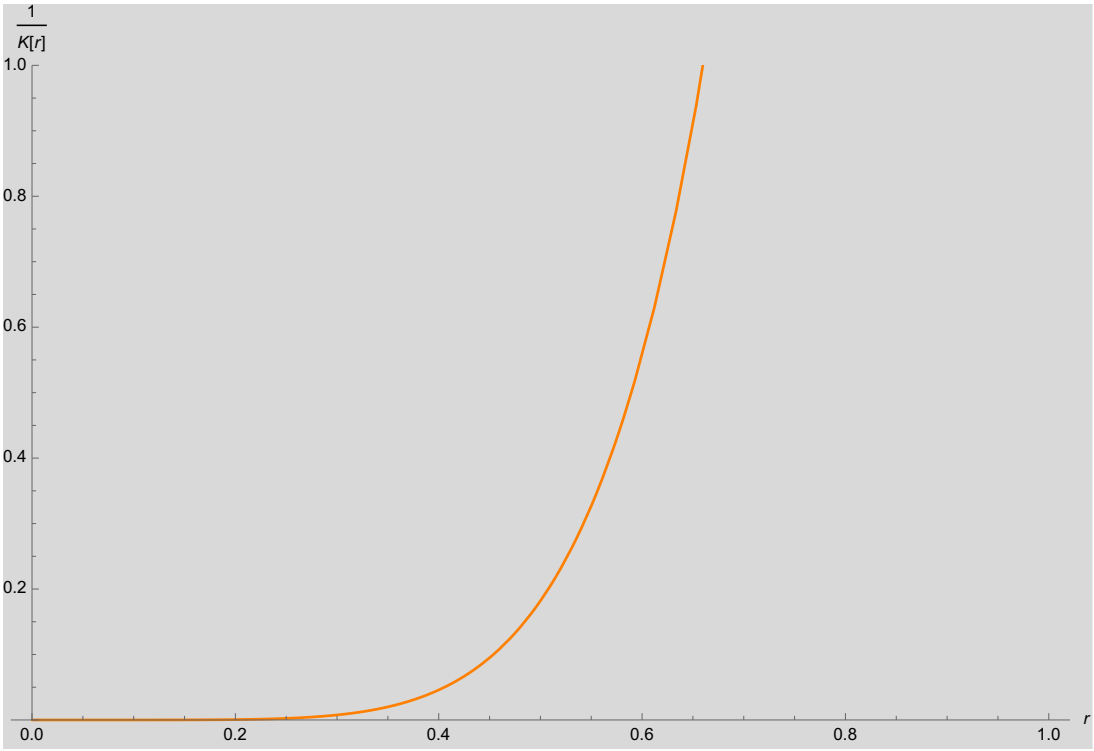

Figure 4: The Kretschmann invariant of the non-trivial flat solution (.1.27) and (.1.31). The curves are obtained for $M = 0.05$, $G_0 = 1$

Some other asymptotically flat configurations can be obtained in this way. The level of complexity depends on the choice of ansatz for $g(r)$. While the global and stability analysis of these configurations has not been investigated, what is however obvious is that a classical singularity is one of their main features. This suggests that the solutions could be black hole spacetime, or otherwise, a naked singularity. In any case, the appearance of a spacetime singularity is an artifact of the classical description of gravity which must be overcome by a consistent quantum gravity theory. This, we shall investigate.

.2 Structural Aspect of AS Flat Configurations

The structural aspect of asymptotically safe Schwarzschild geometry has been summarized in 3.2.1 and it is straightforward to show that asymptotic safety could resolve the classical singularity of the extremal RN black hole, so that we can focus on the non-trivial flat configurations and asymptotically flat regular black holes.

RG Improvement: Ansatz I

We begin with the classical configuration represented by the two-function solution (.1.22) and (.1.26) given as

$$f(r) = \frac{3G^2M^2 + 4GMr\left(-e^{3-\frac{3GM}{2r}} - 5\right) + 36r^2}{9(GM - 2r)^2} \quad \text{and} \quad g(r) = \left(1 - \frac{GM}{2r}\right)^4. \tag{.2.1}$$

RG improvement follows in the usual fashion. We promote the Newton's coupling to its scale-dependent analog, so that its behaviour at the non-trivial fixed point is $G_k = k^{-2} g_*$. For brevity, we shall use the scale identification motivated by dimensional analysis,

$$d(r) = \delta \, r^{\gamma}, \tag{.2.2}$$

so that the relevant scale identification capturing the gravitational quantum effect is

$$k(r) = \frac{\xi}{\delta} \, r^{-\gamma}. \tag{.2.3}$$

δ is an IR value to be fixed by experiment (see (3.1.13)). Usually, it depends on the macroscopic Newton's coupling G_0. Hence, the free parameter δ will not change the conclusion of our investigation. Later on, we shall make contact with the scale identification with the proper time.

Performing the RG improvement, the quantum improved spacetime geometry is associated with the lapse functions

$$f_*(r) = \frac{3\delta^4 g_*^2 M^2 r^{4\gamma} + 4\delta^2 \xi^2 g_* M r^{2\gamma+1} \left(-e^{3 - \frac{3\delta^2 g_* M r^{2\gamma-1}}{2\xi^2}} - 5 \right) + 36\xi^4 r^2}{9 \left(\delta^2 g_* M r^{2\gamma} - 2\xi^2 r \right)^2}, \tag{.2.4}$$

and

$$g_*(r) = \left(1 - \frac{\delta^2 g_* M r^{2\gamma-1}}{2\xi^2} \right)^4. \tag{.2.5}$$

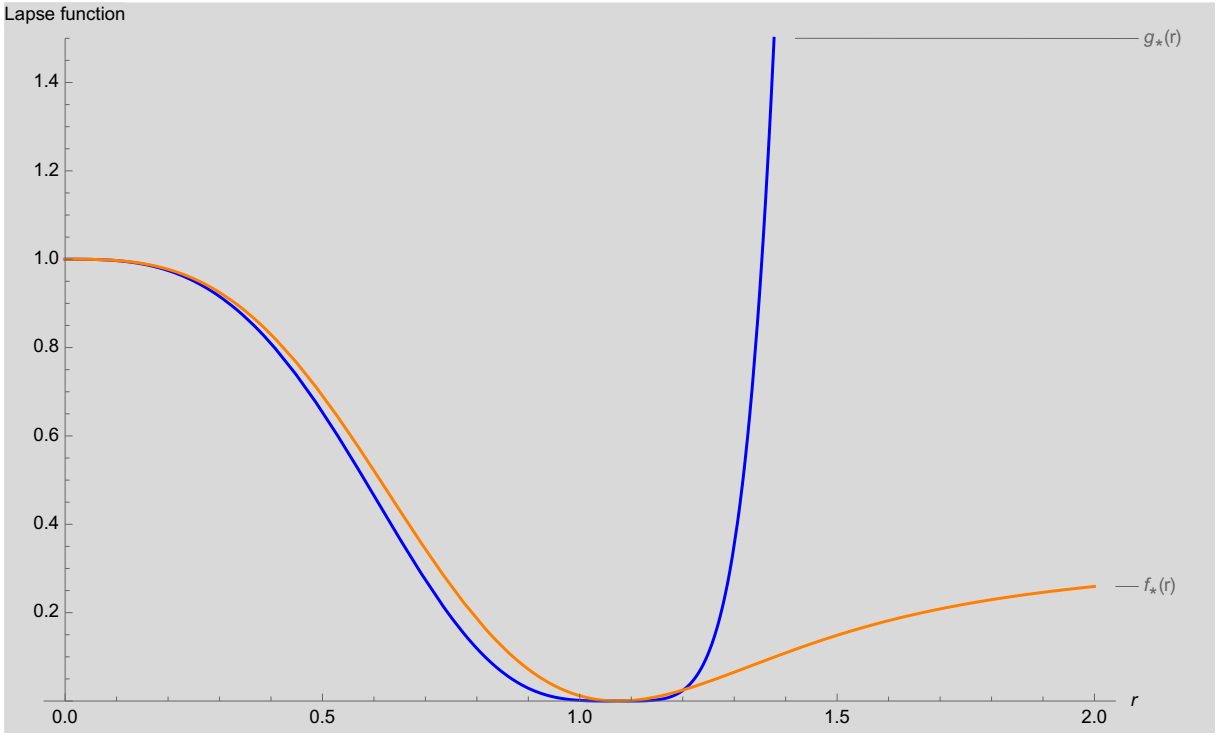

Figure 5: The profile function (.2.4) and (.2.5) of the non-trivial flat solution of the pure R^2. The curves are obtained for $M = 0.5$, $G_0 = 1$, $g_* = 0.403$, $\delta = 2$, $\gamma = 2$

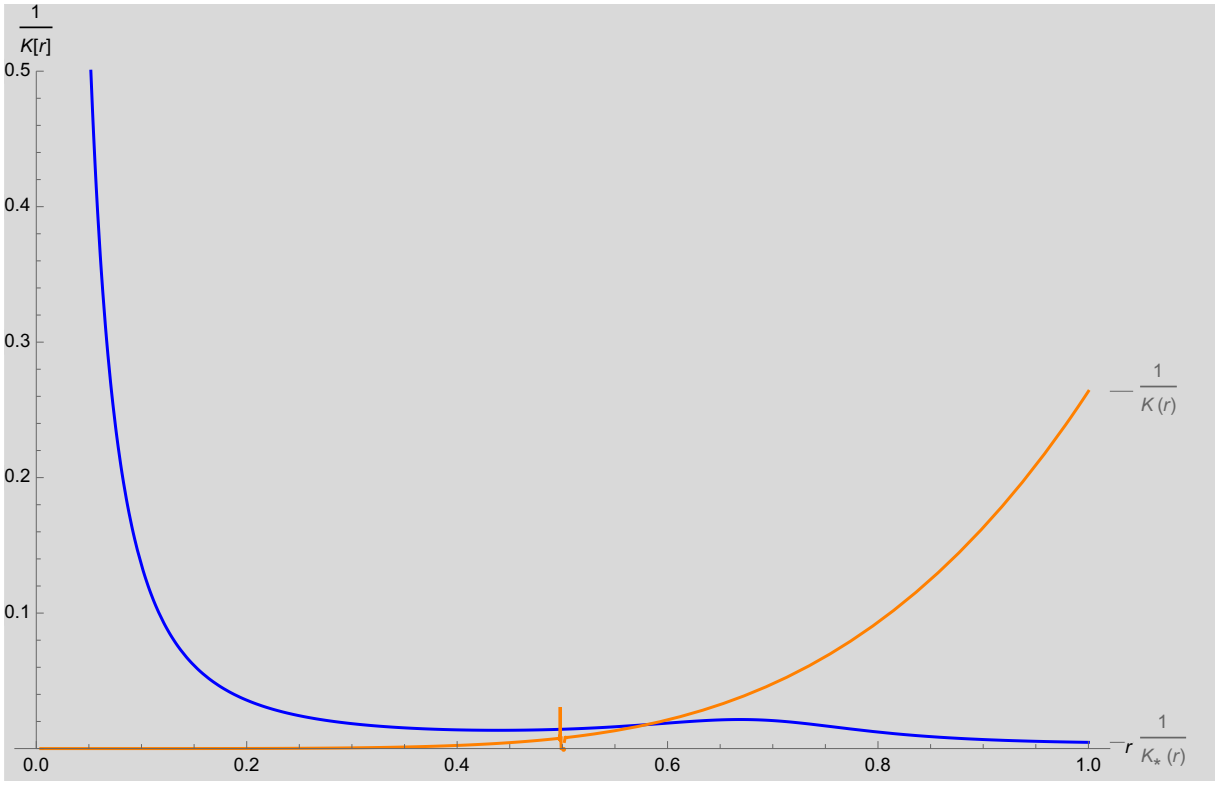

Figure 6: The Kretschmann invariant of the non-trivial flat solution (.2.4) and (.2.5). The curves are obtained for $M = 0.5$, $G_0 = 1$, $g_* = 0.403$, $\delta = 2$, $\gamma = 2$

- First we observe that the spacetime configuration features an event horizon and continues to be asymptotically flat. The radius of the event horizon may be greater than the Planck length for mass comparable with $M = 1$. The corresponding lapse functions are depicted in 5.
- The behaviour of the improved geometry at small distances is depicted in figure 6. It is shown that the improved solution is well behaved as $r \to 0$ only for $\gamma \geq 3/2$
- By identifying the RG scale with the proper time, the scale identification is associated with $\gamma = 3$ which is within $\gamma \geq 3/2$.
- We have not checked whether this ansatz is just a coordinate transformation of the Schwarzschild. If so, then it is reassuring that our conclusion, namely the absence of the singularity after RG improvement, persist under this changes.

RG Improvement: Ansatz II

The two-function solution, (.1.27) and (.1.31), of Ansatz II are given as

$$f(r) = \frac{4r^2\left(\beta^3 G^3 M^3 + 18\beta^2 G^2 M^2 r + 6\beta G M r^2\left(e^{\frac{\beta GM}{r}+4} + 19\right) + 256 r^3\right)}{(\beta GM + 4r)^5}, \tag{.2.6}$$

and

$$g(r) = \exp\left(-\frac{\beta GM}{r}\right). \tag{.2.7}$$

Performing the RG improvement, the quantum improved spacetime geometry is associated with the lapse functions

$$f_*(r) = \frac{4\xi^4 r^2}{\left(\beta\delta^2 g_* M r^{2\gamma} + 4\xi^2 r\right)^5}\mathcal{F}_*(r), \tag{.2.8}$$

with

$$\mathcal{F}_*(r) = \beta^3\delta^6 g_*^3 M^3 r^{6\gamma} + 18\beta^2\delta^4 g_*^2 M^2\xi^2 r^{4\gamma+1} + 6\beta\delta^2 g_* M\xi^4 r^{2\gamma+2}\left(e^{\frac{\beta\delta^2 g_* M r^{2\gamma-1}}{\xi^2}+4} + 19\right) + 256\xi^6 r^3,$$

and

$$g_*(r) = e^{-\frac{\beta\delta^2 g_* M r^{2\gamma-1}}{\xi^2}}. \tag{.2.9}$$

- For $\beta = 2$, the behaviour of the improved geometry at small distances is depicted in figure 8. It is shown that the improved solution is well behaved as $r \to 0$ only for $\gamma \geq 3/2$
- By identifying the RG scale with the proper time, the scale identification is associated with $\gamma = 2$ which is within $\gamma \geq 3/2$.
- We plot the lapse function of the improved solution. It seem that there might be no event horizon below the Planck scale, so that for some mass below the Planck mass, the improved configuration is an ordinary spacetime. The corresponding lapse functions are depicted in 7.

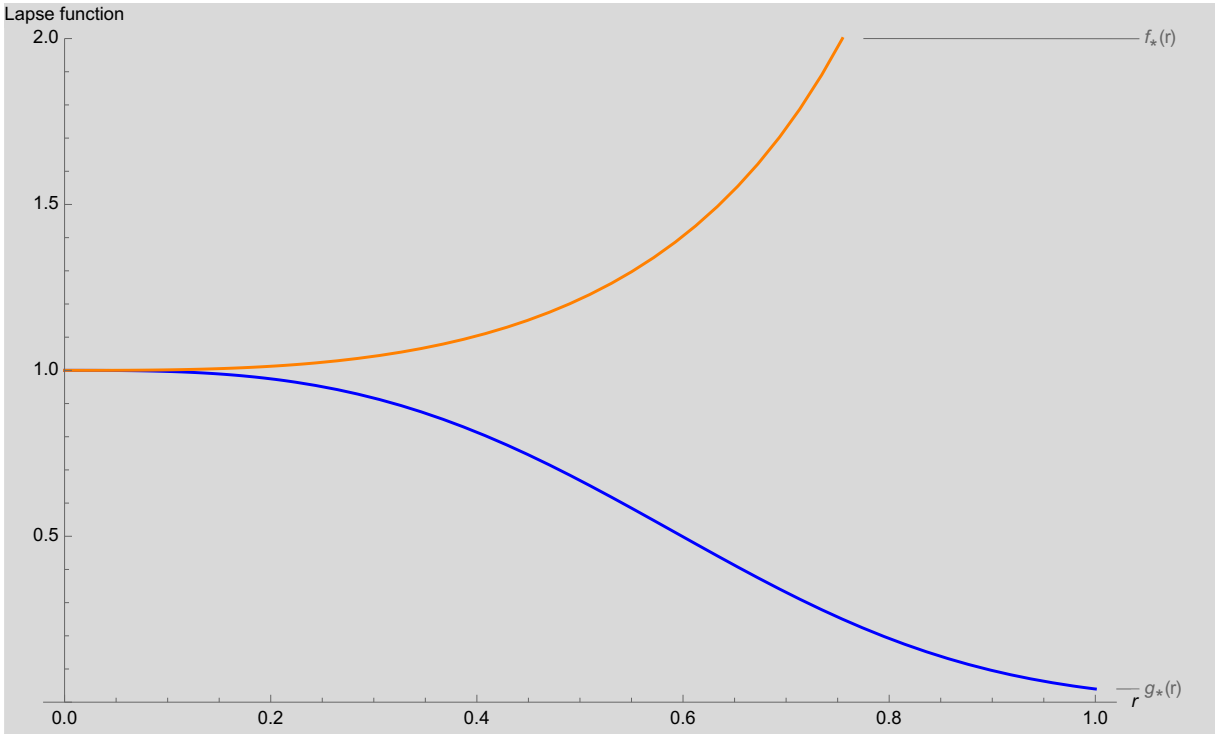

Figure 7: The profile function (.2.8) and (.2.9) of the non-trivial flat solution of pure R^2. The curves are obtained for $M = 0.8$, $G_0 = 1$, $g_* = 0.403$, $\delta = 2.5$, $\gamma = 2$, $\beta = 2$.

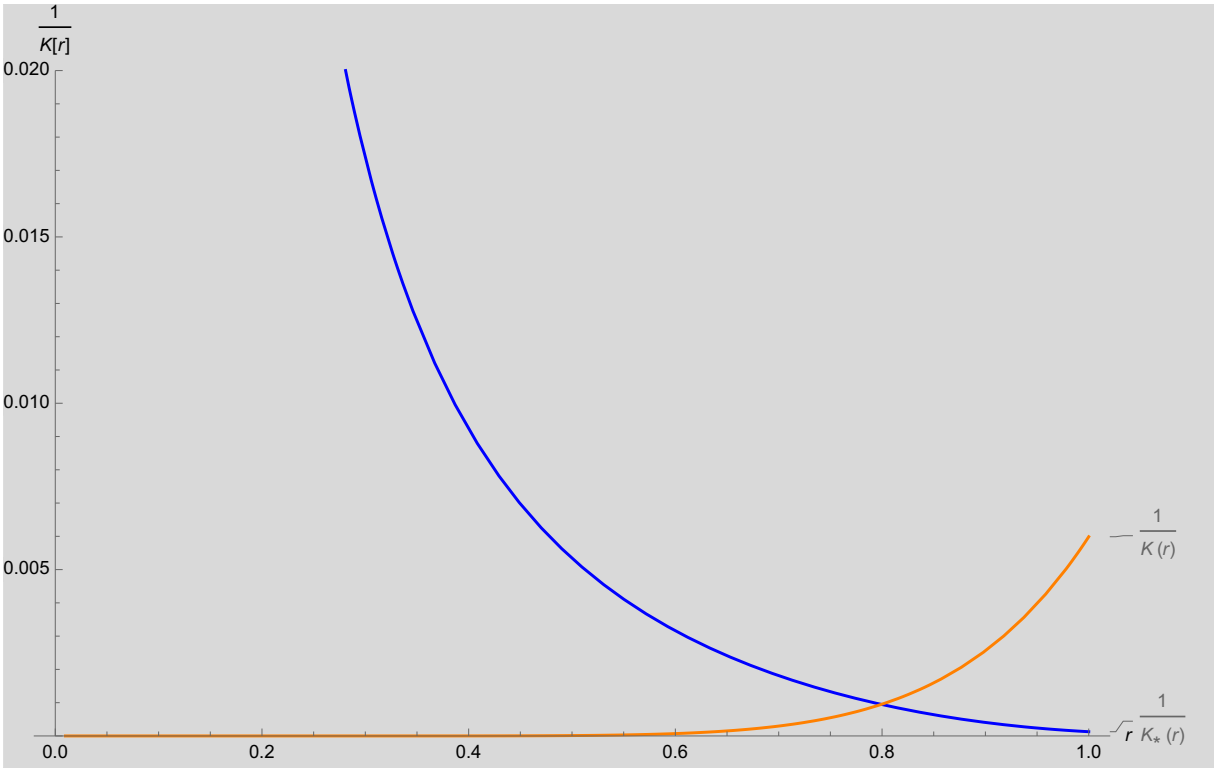

Figure 8: The Kretschmann invariant of the non-trivial flat solution (.2.8) and (.2.9). The curves are obtained for $M = 0.5$, $G_0 = 1$, $g_* = 0.403$, $\delta = 2$, $\gamma = 2$, $\beta = 2$.

.3 Hayward Type Black Holes

We found four possible models of Hayward-type black holes in the literature, but they are similar in contruction [11]-[16]. Without loss of generality, the classical geometry of a spherically symmetric black hole with de-Sitter core is described by the line element

$$ds^2 = -e^{-2\phi(r)}F(r)dt^2 + F(r)^{-1}dr^2 + r^2 d\Omega^2, \tag{.3.1}$$

where $\phi(r)$ is a real function, and

$$F(r) = 1 - \frac{2GM(r)}{r}, \tag{.3.2}$$

with $M(r)$ and $\phi(r)$ given in the table 1.

Hayward Type Black Holes		
MODELS	METRIC	
	$M(r)$	$\phi(r)$
Hayward [11]	$\frac{MGr^3}{r^3+2MG^2}$	0
Bardeen [12]	$\frac{2MGr^3}{\left[r^2+(2MG^2)^{2/3}\right]^{3/2}}$	0
Dymnikova [14]	$M\left[1-\exp\left(-r^3/2MG^2\right)\right]$	0
Hayward-Frolov-Zelnikov [15]	$\frac{MGr^3}{r^3+2MG^2}$	$< \infty$

Table 1: Gravitational scaling exponent from different quantum gravity approach

As it turns out, all of these solutions have regular geometry regular and are similar to to each other. Therefore, it suffices to consider just the Hayward black hole.

The RG improvement is straightfowrad. Performing the RG improvement, the quantum improved spacetime is associated with the lapse functions

$$f_*(r) = 1 - \frac{\beta\delta^2 g_* M \xi^2 r^{2\gamma+2}}{\alpha\delta^4 g_*^2 M r^{4\gamma} + \xi^4 r^3} \tag{.3.3}$$

- Hayward black hole continues to be regular for $\gamma \geq 3/2$. For $\gamma = 3/2$,

$$\lim_{r\to 0} R^*_{\mu\nu\rho\sigma} R_*^{\mu\nu\rho\sigma} = \frac{96\delta^4 g_*^2 M^2}{\xi^4}$$

- For a small mass M and the IR value δ comparable to 1 or more, there is no more event horizon as it would be for small mass of its classical analog. However, if the IR value is less than or comparable to 0.86, event horizon forms for small black hole mass.

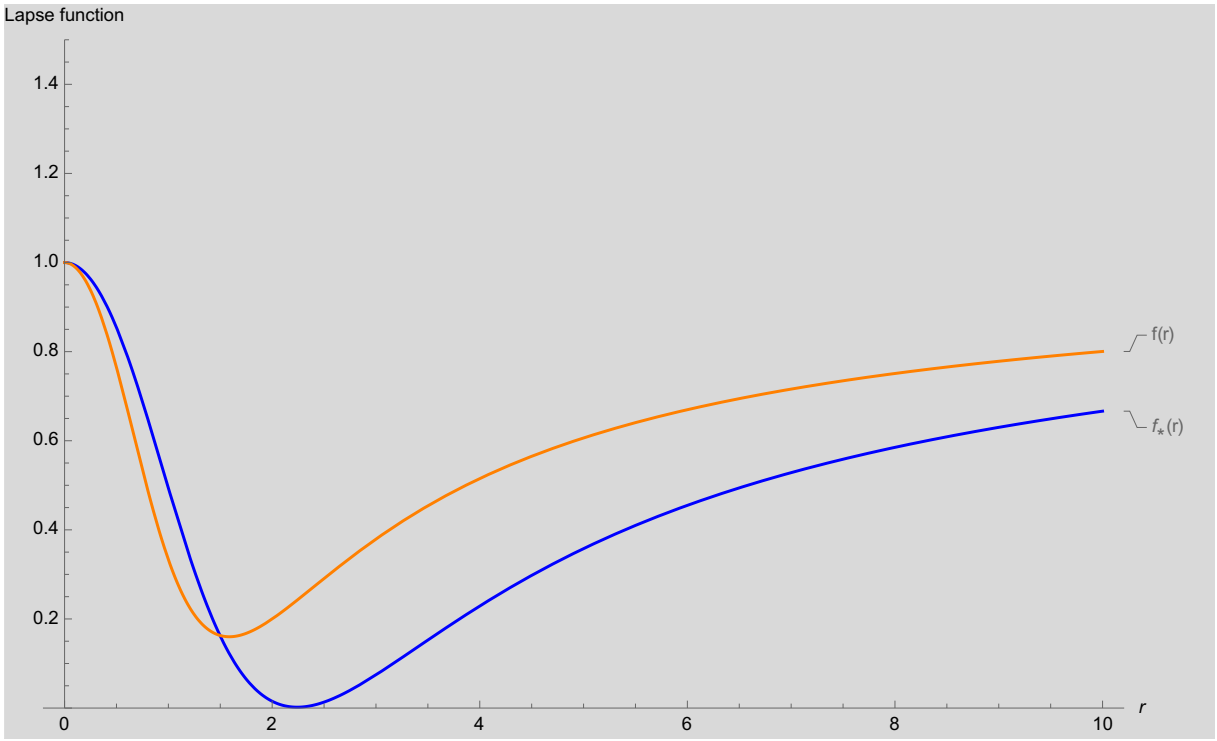

Figure 9: The Lapse function of the improved Hayward Black hole. The curves are obtained for $M = 1$, $G_0 = 1$, $g_* = 0.403$, $\delta = 0.86$, $\gamma = 3/2$.

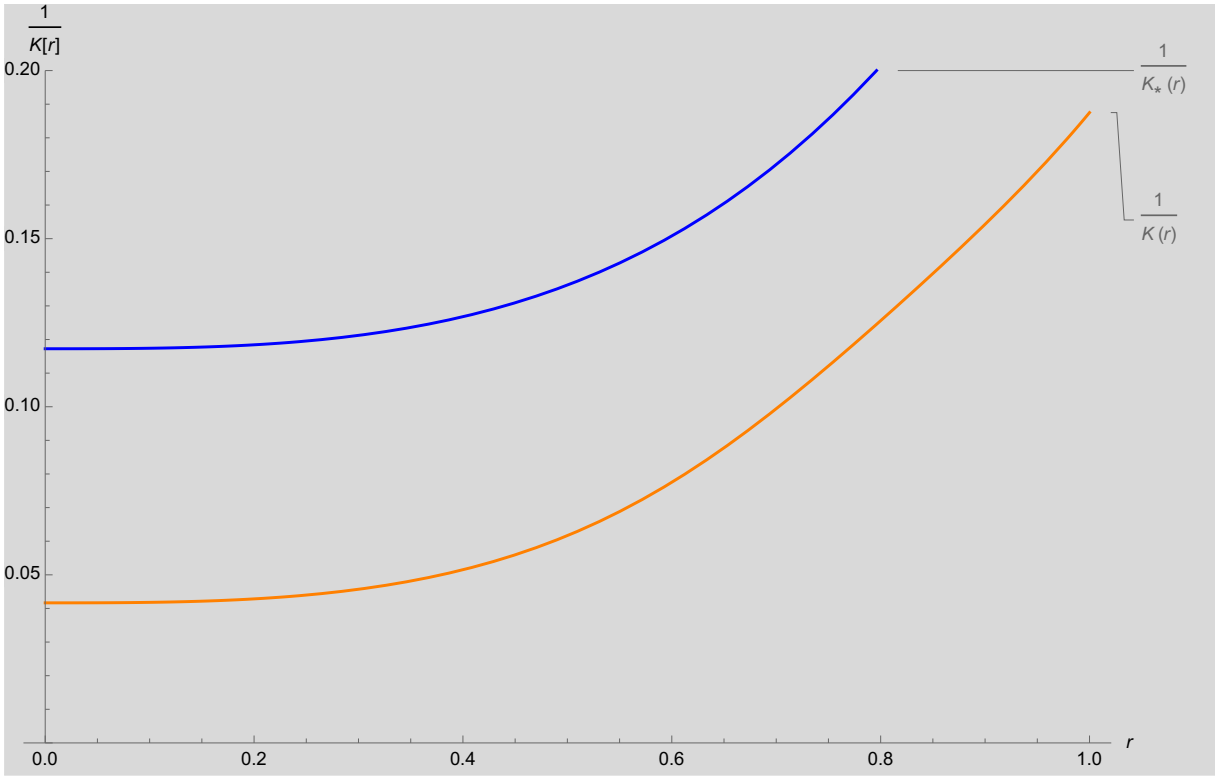

Figure 10: The Kretschmann invariant of the improved Hayward Black hole. The curves are obtained for $M = 1$, $G_0 = 1$, $g_* = 0.403$, $\delta = 0.86$, $\gamma = 3/2$.

On the structural aspect of classically flat configurations, the analysed geometries, so far, continue to be regular for scale identification associated with $\gamma \geq 3/2$, and thus, we have found no counter-example. While there are still some other flat geometries, characterized only by their mass, for which we have not analysed, it is obvious they are similar to the asymptotic structure considered in our analysis, and they may have similar structure when quantum gravitational effect is taken into consideration.

We can already understand why this is the case. For these families of solutions, RG improvement is tantamount to the appearance of a leading order term of the likes $\mathcal{O}\left(r^{-6+4\gamma}\right)$. This term is therefore fully suppressed only for $\gamma \geq 3/2$, so that the classical spacetime singularity is resolved.

Part II

Curvature Scalars and Invariants

On the QG Bound on θ

.1 The Real Critical Exponents

$$R^*_{\mu\nu\rho\sigma}R^{\mu\nu\rho\sigma}_* = \frac{\Xi_1}{324G_0^2\xi^4 r^6} \tag{.1.1}$$

where

$$\begin{aligned}\Xi = 9^{-\theta_1-\theta_2}&\left[A_1+A_2+3^{\theta_2}\left(A_3+A_4\right)\left(\frac{\xi\sqrt{MG_0}}{r^{3/2}}\right)^{\theta_2}\right]^2\left(\frac{\xi\sqrt{MG_0}}{r^{3/2}}\right)^{-2(\theta_1+\theta_2)}\\ &+\frac{1}{16}9^{-\theta_1-\theta_2}\left[B_1+B_2+3^{\theta_2}\left(B_3+B_4+B_5\right)\left(\frac{\xi\sqrt{MG_0}}{r^{3/2}}\right)^{\theta_2}\right]^2\left(\frac{\xi\sqrt{MG_0}}{r^{3/2}}\right)^{-2(\theta_1+\theta_2)}\\ &+1296r^2\xi^4G_0^2+4\left(C_1-18rG_0\xi^2+C_2\right)^2-144r\xi^2G_0\left(C_3+18rG_0\xi^2-C_4\right)\end{aligned} \tag{.1.2}$$

for

$$A_1 = 2^{\frac{\theta_2}{2}}3^{\theta_1+3}M\xi^4d_2G_0^2\left(3\theta_2-2\right)\left(\frac{\xi\sqrt{MG_0}}{r^{3/2}}\right)^{\theta_1}$$

$$A_2 = 2^{\frac{\theta_2}{2}+3}3^{\theta_1}r^3c_2\left(3\theta_2+4\right)\left(\frac{\xi\sqrt{MG_0}}{r^{3/2}}\right)^{\theta_1}$$

$$A_3 = 2\ 3^{\theta_1}\left(16r^3g_* - 27M\xi^4G_0^2\lambda_*\right)\left(\frac{\xi\sqrt{MG_0}}{r^{3/2}}\right)^{\theta_1}$$

$$A_4 = 27\ 2^{\frac{\theta_1}{2}}M\xi^4d_1G_0^2\left(3\theta_1-2\right) + 2^{\frac{\theta_1}{2}+3}r^3c_1\left(3\theta_1+4\right)$$

$$B_1 = 2^{\frac{\theta_2}{2}}3^{\theta_1+3}M\xi^4d_2G_0^2\left(9\theta_2^2-18\theta_2+8\right)\left(\frac{\xi\sqrt{MG_0}}{r^{3/2}}\right)^{\theta_1}$$

$$B_2 = 2^{\frac{\theta_2}{2}+3}3^{\theta_1}r^3c_2\left(9\theta_2^2+18\theta_2+8\right)\left(\frac{\xi\sqrt{MG_0}}{r^{3/2}}\right)^{\theta_1}$$

$$B_3 = 8\ 3^{\theta_1}\left(27MG_0^2\lambda_*\xi^4+8r^3g_*\right)\left(\frac{\xi\sqrt{MG_0}}{r^{3/2}}\right)^{\theta_1}$$

$$B_4 = 27\ 2^{\frac{\theta_1}{2}}M\xi^4d_1G_0^2\left(9\theta_1^2-18\theta_1+8\right)$$

$$B_5 = 2^{\frac{\theta_1}{2}+3} r^3 c_1 \left(9\theta_1^2 + 18\theta_1 + 8\right)$$

$$C_1 = 27MG_0^2 \left(2^{\frac{\theta_1}{2}} 3^{-\theta_1} d_1 \left(\frac{\xi\sqrt{MG_0}}{r^{3/2}}\right)^{-\theta_1} + 2^{\frac{\theta_2}{2}} 3^{-\theta_2} d_2 \left(\frac{\xi\sqrt{MG_0}}{r^{3/2}}\right)^{-\theta_2} + \lambda_*\right)\xi^4$$

$$C_2 = 8r^3 \left(2^{\frac{\theta_1}{2}} 3^{-\theta_1} c_1 \left(\frac{\xi\sqrt{MG_0}}{r^{3/2}}\right)^{-\theta_1} + 2^{\frac{\theta_2}{2}} 3^{-\theta_2} c_2 \left(\frac{\xi\sqrt{MG_0}}{r^{3/2}}\right)^{-\theta_2} + g_*\right)$$

$$C_3 = -27MG_0^2 \left(2^{\frac{\theta_1}{2}} 3^{-\theta_1} d_1 \left(\frac{\xi\sqrt{MG_0}}{r^{3/2}}\right)^{-\theta_1} + 2^{\frac{\theta_2}{2}} 3^{-\theta_2} d_2 \left(\frac{\xi\sqrt{MG_0}}{r^{3/2}}\right)^{-\theta_2} + \lambda_*\right)\xi^4$$

$$C_4 = 8r^3 \left(2^{\frac{\theta_1}{2}} 3^{-\theta_1} c_1 \left(\frac{\xi\sqrt{MG_0}}{r^{3/2}}\right)^{-\theta_1} + 2^{\frac{\theta_2}{2}} 3^{-\theta_2} c_2 \left(\frac{\xi\sqrt{MG_0}}{r^{3/2}}\right)^{-\theta_2} + g_*\right)$$

.2 Complex Critical Exponents

.2.1 Scalar Curvature

$$R_* = \frac{\Xi}{8G_0\xi^2 r^3} 3^{-\sigma_1 - 1} \left(\frac{\xi\sqrt{G_0 M}}{r^{3/2}}\right)^{-\sigma_1} \tag{.2.1}$$

where

$$\begin{aligned}
\Xi = {} & 128 g_* r^3 3^{\sigma_1} \left(\frac{\xi\sqrt{G_0 M}}{r^{3/2}}\right)^{\sigma_1} + 81G_0^2 M\xi^4 q_1 2^{\frac{\sigma_1}{2}} \sigma_1^2 X_1 + 81G_0^2 M\xi^4 q_2 2^{\frac{\sigma_1}{2}} \sigma_1^2 X_2 \\
& - 81G_0^2 M\xi^4 q_1 2^{\frac{\sigma_1}{2}} \sigma_2^2 X_1 - 81G_0^2 M\xi^4 q_2 2^{\frac{\sigma_1}{2}} \sigma_2^2 X_2 + 27G_0^2 M\xi^4 q_1 2^{\frac{\sigma_1}{2}+1} \sigma_1 X_1 \\
& + 27G_0^2 M\xi^4 q_2 2^{\frac{\sigma_1}{2}+1} \sigma_1 X_2 - 27G_0^2 M\xi^4 q_2 2^{\frac{\sigma_1}{2}+1} \sigma_2 X_1 + 27G_0^2 M\xi^4 q_1 2^{\frac{\sigma_1}{2}+1} \sigma_2 X_2 \\
& - 81G_0^2 M\xi^4 q_2 2^{\frac{\sigma_1}{2}+1} \sigma_1\sigma_2 X_1 + 81G_0^2 M\xi^4 q_1 2^{\frac{\sigma_1}{2}+1} \sigma_1\sigma_2 X_2 \\
& + p_2 r^3 2^{\frac{\sigma_1}{2}+3} \left(3\sigma_1^2 X_2 + 2\sigma_1 \left(7X_2 - 3\sigma_2 X_1\right) - 3\sigma_2^2 X_2 - 14\sigma_2 X_1 + 16X_2\right) \\
& + p_1 r^3 2^{\frac{\sigma_1}{2}+3} \left(3\sigma_1^2 X_1 + 2\sigma_1 \left(3\sigma_2 X_2 + 7X_1\right) - 3\sigma_2^2 X_1 + 14\sigma_2 X_2 + 16X_1\right)
\end{aligned} \tag{.2.2}$$

for

$$X_1 = \cos\left(\sigma_2 \log\left(\frac{3\xi\sqrt{G_0 M}}{\sqrt{2} r^{3/2}}\right)\right)$$

and

$$X_2 = \sin\left(\sigma_2 \log\left(\frac{3\xi\sqrt{G_0 M}}{\sqrt{2} r^{3/2}}\right)\right)$$

.2.2 Kretschmann Scalar

$$R^*_{\mu\nu\rho\sigma}R^{\mu\nu\rho\sigma}_* = \frac{\Xi}{324G_0^2\xi^4 r^6} \tag{.2.3}$$

where

$$\Xi = 1296G_0^2\xi^4r^2 + 9^{-\sigma_1}Y_1\mathcal{A}_1^2 + \frac{1}{16}9^{-\sigma_1}Y_1\mathcal{A}_2^2 + 144G_0\xi^2r\mathcal{A}_3 + 4\mathcal{A}_3^2 \tag{.2.4}$$

for

$$\begin{aligned}\mathcal{A}_1 = {} & 32g_*r^3 3^{\sigma_1}Y_2 - 27G_0^2M\xi^4q_1 2^{\frac{\sigma_1}{2}+1}X_1 - 27G_0^2M\xi^4q_2 2^{\frac{\sigma_1}{2}+1}X_2 + 81G_0^2M\xi^4q_1 2^{\frac{\sigma_1}{2}}\sigma_1X_1 \\ & + 81G_0^2M\xi^4q_2 2^{\frac{\sigma_1}{2}}\sigma_1X_2 - 81G_0^2M\xi^4q_2 2^{\frac{\sigma_1}{2}}\sigma_2X_1 + 81G_0^2M\xi^4q_1 2^{\frac{\sigma_1}{2}}\sigma_2X_2 \\ & - 2G_0^2\lambda_*M\xi^4 3^{\sigma_1+3}Y_2 + p_2r^3 2^{\frac{\sigma_1}{2}+3}\left(3\sigma_1X_2 - 3\sigma_2X_1 + 4X_2\right) \\ & + p_1r^3 2^{\frac{\sigma_1}{2}+3}\left(3\sigma_1X_1 + 3\sigma_2X_2 + 4X_1\right)\end{aligned} \tag{.2.5}$$

$$\begin{aligned}\mathcal{A}_2 = {} & 64g_*r^3 3^{\sigma_1}Y_2 + 243G_0^2M\xi^4q_1 2^{\frac{\sigma_1}{2}}\sigma_1^2X_1 + 243G_0^2M\xi^4q_2 2^{\frac{\sigma_1}{2}}\sigma_1^2X_2 - 243G_0^2M\xi^4q_1 2^{\frac{\sigma_1}{2}}\sigma_2^2X_1 \\ & - 243G_0^2M\xi^4q_2 2^{\frac{\sigma_1}{2}}\sigma_2^2X_2 + 27G_0^2M\xi^4q_1 2^{\frac{\sigma_1}{2}+3}X_1 + 27G_0^2M\xi^4q_2 2^{\frac{\sigma_1}{2}+3}X_2 \\ & - 243G_0^2M\xi^4q_1 2^{\frac{\sigma_1}{2}+1}\sigma_1X_1 - 243G_0^2M\xi^4q_2 2^{\frac{\sigma_1}{2}+1}\sigma_1X_2 + 243G_0^2M\xi^4q_2 2^{\frac{\sigma_1}{2}+1}\sigma_2X_1 \\ & - 243G_0^2M\xi^4q_1 2^{\frac{\sigma_1}{2}+1}\sigma_2X_2 - 243G_0^2M\xi^4q_2 2^{\frac{\sigma_1}{2}+1}\sigma_1\sigma_2X_1 + 243G_0^2M\xi^4q_1 2^{\frac{\sigma_1}{2}+1}\sigma_1\sigma_2X_2 \\ & + 8G_0^2\lambda_*M\xi^4 3^{\sigma_1+3}Y_2 + p_2r^3 2^{\frac{\sigma_1}{2}+3}\left(9\sigma_1^2X_2 + 18\sigma_1\left(X_2 - \sigma_2X_1\right) - 9\sigma_2^2X_2 - 18\sigma_2X_1 + 8X_2\right) \\ & + p_1r^3 2^{\frac{\sigma_1}{2}+3}\left(9\sigma_1^2X_1 + 18\sigma_1\left(\sigma_2X_2 + X_1\right) - 9\sigma_2^2X_1 + 18\sigma_2X_2 + 8X_1\right)\end{aligned} \tag{.2.6}$$

$$\begin{aligned}\mathcal{A}_3 = {} & -8r^3\left(g_* + 2^{\frac{\sigma_1}{2}}3^{-\sigma_1}Y_3\left(p_1X_1 + p_2X_2\right)\right) \\ & - 27G_0^2M\xi^4\left(\lambda_* + 2^{\frac{\sigma_1}{2}}3^{-\sigma_1}Y_3\left(q_1X_1 + q_2X_2\right)\right) + 18G_0\xi^2r\end{aligned} \tag{.2.7}$$

$$X_1 = \cos\left(\sigma_2\log\left(\frac{3\xi\sqrt{G_0M}}{\sqrt{2}r^{3/2}}\right)\right)$$

and

$$X_2 = \sin\left(\sigma_2\log\left(\frac{3\xi\sqrt{G_0M}}{\sqrt{2}r^{3/2}}\right)\right)$$

$$Y_1^{-1/2} = Y_2 = Y^{-1} = \left(\frac{\xi\sqrt{G_0M}}{r^{3/2}}\right)^{\sigma_1}$$

Bibliography

[1] Carlo Rovelli, *Notes for a brief history of quantum gravity*, arXiv:gr-qc/0006061; A. Ashtekar, M. Reuter, C. Rovelli, *From General Relativity to Quantum Gravity*, In "General Relativity and Gravitation: A Centennial Perspective", arXiv:1408.4336; Lee Smolin, *What are we missing in our search for quantum gravity?*, arXiv:1705.09208.

[2] Albert Einstein, *Die Feldgleichungen der Gravitation*, Sitzungsberichte der Königlich Preußischen Akademie der Wissenschaften zu Berlin (1915) 844–847; *Die Grundlage der allgemeinen Relativitätstheorie*, Annalen der Physik, 49 (1916) 769–822.

[3] Clifford M. Will, *The Confrontation between general relativity and experiment*,Living Rev. Rel. 9 (2006) 3; LIGO Scientific and Virgo Collaborations (B.P. Abbott et al.), *Tests of general relativity with GW150914*,Phys.Rev.Lett. 116 (22) (2016) 221101.

[4] M. E. Peskin, D. V. Schroeder, *An Introduction to quantum field theory*, Reading, USA: Addison-Wesley (1995) ISBN: 9780201503975.

[5] Tom W.B. Kibble, *The Standard Model of Particle Physics*, arXiv:1412.4094.

[6] S.W. Hawking, *Breakdown of Predictability in Gravitational Collapse*, Phys. Rev. D14 (1976) 2460–2473.

[7] S. W. Hawking, R. Penrose, *The singularities of gravitational collapse and cosmology*, Proc. Roy. Soc. Lond. A314 (1970) 529–548.

[8] Roger Penrose, *Gravitational Collapse and Space-Time Singularities*, Phys .Rev. Lett. 14 (1965) 57–59.

[9] R. Penrose, *Gravitational collapse: The role of general relativity*, Riv.Nuovo Cim. 1 (1969) 252–276.

[10] I. H. Dwivedi, P. S. Joshi, *On the occurrence of naked singularity in spherically symmetric gravitational collapse*, Commun. Math. Phys. 166 (1994) 117–128.

[11] Sean A. Hayward, *Formation and evaporation of regular black holes*, Phys. Rev. Lett. 96 (2006) 031103.

[12] J. M. Bardeen, *Non-singular general-relativistic gravitational collapse*, in Proceedings of International Conference GR5, Tbilisi, USSR, page 174, 1968.

[13] Arvind Borde, *Regular Black Holes and Topology Change*, Phys. Rev. D55 (1997) 7615–7617.

[14] Irina Dymnikova, *Vacuum nonsingular black hole*, Gen. Rel. Grav. 24 (1992) 235–242.

[15] Valeri P. Frolov, Andrei Zelnikov, *Quantum radiation from a sandwich black hole*, Phys.Rev. D95 (2017) no.4, 044042.

[16] Zhong-Ying Fan and Xiaobao Wang, *Construction of Regular Black Holes in General Relativity*, Phys.Rev. D94 (2016) no.12, 124027.

[17] Valeri P. Frolov, *Information loss problem and a 'black hole' model with a closed apparent horizon*, JHEP 1405 (2014) 049.

[18] R. Carballo-Rubio, *On the viability of regular black holes*, arXiv:1805.02675.

[19] Gerard 't Hooft, M.J.G. Veltman, *One loop divergencies in the theory of gravitation*, Ann. nst. H. Poincare Phys. Theor. A20 (1974) 69–94; S. Deser and P. van Nieuwenhuizen, *Nonrenormalizability of the Quantized Dirac-Einstein system*, Phys. Rev. D 10 (1974) 491 ; S. Deser, Hung-Sheng Tsao, and P. van Nieuwenhuizen *One-loop divergences of the Einstein-Yang-Mills system*, Phys. Rev. D10 (1974) 3337; Marc H. Goroff, Augusto Sagnotti, *The ultraviolet behavior of Einstein gravity* , Nucl. Phys. B266 (1986) 709–736;A. E. M. van de Ven, *Two loop quantum gravity*, Nucl.Phys. B378 (1992) 309–366.

[20] K.S. Stelle, *Renormalization of higher derivative quantum gravity*, Phys. Rev. D 16 (1977) 953.

[21] John F. Donoghue, *General relativity as an effective field theory: The leading quantum corrections*, Phys.Rev. D50 (1994) 3874–3888.

[22] Cliff P. Burgess, *Quantum gravity in everyday life: General relativity as an effective field theory*, Living Rev.Rel. 7 (2004) 5–56.

[23] John F. Donoghue, Mikhail M. Ivanov, Andrey Shkerin, *EPFL Lectures on General Relativity as a Quantum Field Theory*, arXiv:1702.00319, INR-TH-2017-001.

[24] N. E. J. Bjerrum-Bohr, John F. Donoghue, and Barry R. Holstein, *Quantum Gravitational Corrections to the Nonrelativistic Scattering Potential of Two Masses*, Phys. Rev. D 67: 084033; *Quantum corrections to the Schwarzschild and Kerr metrics*, Phys. Rev. D 68: 084005.

[25] Editor: Daniele Oriti, *Approaches to Quantum Gravity*, Cambridge University Press (2009) ISBN: 9780511575549.

[26] Steven Weinberg, *Ultraviolet divergences in quantum theories of gravitation*, In "S. W. Hawking; W. Israel, *General Relativity: an Einstein Centenary Survey* ", Cambridge University Press. (1979) 790–831. ISBN: 9780521137980.

[27] Ann Ewing, *"Black Holes" in Space*,Science News Letter, Vol. 85, January 18, 1964 issue; J.A. Wheeler and K. Ford, *Geons, Black Holes, and Quantum Foam: A Life in Physics*, New York: W.W. Norton and Co. (1998).

[28] C. T. Bolton, *Identification of Cygnus X-1 with HDE 226868*, Nature volume 235, (1972) 271–273.

[29] S. Gillesse et. al, *Monitoring stellar orbits around the Massive Black Hole in the Galactic Center*, Astrophys. J. 692 (2009) 1075–1109.

[30] B.P. Abbott et al. (LIGO Scientific Collaboration and Virgo Collaboration), *Observation of Gravitational Waves from a Binary Black Hole Merger*, Phys. Rev. Lett. 116 (2016) 061102; *GW151226: Observation of Gravitational Waves from a 22-Solar-Mass Binary Black Hole*, Phys. Rev. Lett. 116 (2016) 241103; *GW170104: Observation of a 50-Solar-Mass Binary Black Hole Coalescence at Redshift 0.2*, Phys. Rev. Lett. 118 (2017) 221101.

[31] John Michell, *On the Means of Discovering the Distance, Magnitude, &c. of the Fixed Stars, in Consequence of the Diminution of the Velocity of Their Light, in Case Such a Diminution Should be Found to Take Place in any of Them, and Such Other Data Should be Procured from Observations, as Would be Farther Necessary for That Purpose. By the Rev. John Michell, B.D.F.R.S. In a Letter to Henry Cavendish, Esq. F.R.S. and A.S*, Philosophical Transactions of the Royal Society of London. 74 (1784) 35–57; Von Peter Simon La Place, *Beweis des Satzes, daßdie anziehende Kraft bey einem Weltkörper so großseyn könne, daßdas Licht davon nicht ausströmen kann,*, AllgemeineGeographische Ephemeriden 4 (1799) 001–006; C. Montgomery, W. Orchiston and I. Whittingham, *Michell, Laplace and the origin of the black hole concept*, Journal of Astronomical History and Heritage, 12(2) (2009) 90–96.

[32] Kip S. Thorne, *Nonspherical Gravitational Collapse: A Short Review*, J R Klauder, Magic Without Magic, San Francisco (1972) 231-258.

[33] Karl Schwarzschild, *Über das Gravitationsfeld eines Massenpunktes nach der Einsteinschen Theorie*, Sitzungsberichte der Königlich Preußischen Akademie der Wissenschaften 7 (1916) 189-196.

[34] F. R. Tangherlini, *Schwarzschild field in n dimensions and the dimensionality of space problem*, Nuovo Cim (1963) 27: 636.

[35] Werner Israel, *Event Horizons in Static Vacuum Space-Times*, Phys. Rev. 164 (5) (1967)1776–1779.

[36] H. Reissner, *Über die Eigengravitation des elektrischen Feldes nach der Einsteinschen Theorie*, Annalen der Physik 50 (1916) 106–120; G. Nordström, *On the Energy of the Gravitational Field in Einsteins Theory*, Koninklijke Nederlandsche Akademie van Wetenschappen Proceedings 20 (2) (1918) 1238–1245.

[37] Roy P. Kerr, *Gravitational Field of a Spinning Mass as an Example of Algebraically Special Metrics*, Phys. Rev. Lett. 11 (1963) 237–238.

[38] E. T. Newman and A. I. Janis, *Note on the Kerr Spinning-Particle Metric*, Journal of Mathematical Physics. 6 (6) (1965) 915917.

[39] Robert Geroch, *What is a singularity in general relativity?*, Annals of Physics 48 (1968) 526 – 540.

[40] A. K. Raychaudhuri, *Relativistic Cosmology I*, Phys. Rev. 90 (1955) 11231126.

[41] R. Penrose, *Gravitational Collapse and Space-Time Singularities*, Physical Review Letters. 14 (3) (1965) 57– 59; S. W. Hawking, *Properties of expanding universes* , Doctoral thesis, 1966 .

[42] S. W. Hawking, R. Penrose, *The Nature of Space and Time*, Princeton University Press, 1996.

[43] Sumanta Chakraborty, Kinjalk Lochan, *Black Holes: Eliminating Information or Illuminating New Physics?*, Universe 2017, 3(3), 55.

[44] P.T. Chrúsciel, *On Uniqueness in the Large of Solutions of Einstein Equations ("Strong Cosmic Censorship")*, Contemporary Mathematics 132 (1992) 235–273; C.J.S Clarke, *A title of cosmic censorship*, Class. Quantum Grav. (1994) 252–276; S. W. Hawking, R. Penrose, *The Nature of Space and Time*, Princeton University Press, Princeton (1996) ISBN: 978-0691145709; T. P. Singh, *Gravitational collapse, black holes and naked singularities*,

J. Astrophys. Astron.20 (1999) 221–232; R. Penrose, *The Question of Cosmic Censorship*, J. Astrophys. Astron.20 (1999) 233–248; Andrzej Krolak, *Nature of Singularities in Gravitational Collapse*, Prog. Theor. Phys.Suppl. 136 (1999) 45–56; P. S. Joshi, D. Malafarina, *Recent developments in gravitational collapse and spacetime singularities*, Int. J. Mod. Phys. D, 20 (2011) 2641.

[45] R. Wald, *Gravitational Collapse and Cosmic Censorship*, Iyer, B.R. (ed.) et al.: Black holes, gravitational radiation and the universe (1997) 69–85.

[46] R. Wald, *Gedanken experiments to destroy a black hole*, Ann. Phys., Vol. 82 (1974) 548–556.

[47] Jacob D. Bekenstein, *Black Holes and Entropy*, Phys. Rev. D 7 (1973) 2333–2346; Larry Smarr, *Mass Formula for Kerr Black Holes*, Phys. Rev. Lett. 30 (1973) 71–73.

[48] J. M. Bardeen, B. Carter, S. W. Hawking, *The four laws of black hole mechanics*, Commun. Math. Phys. 31 (2) (1973) 161–170.

[49] S. W. Hawking, *Particle Creation by Black Holes*, Commun. Math. Phys. 43 (1975) 199–220.

[50] Michael E. Fisher, *Renormalization group theory: Its basis and formulation in statistical physics*, Rev. Mod. Phys. 70 (1998) 653–681.

[51] Max Niedermaier, Martin Reuter, *The Asymptotic Safety Scenario in Quantum Gravity*, Living Rev. Rel. 9 (2006) 5–173.

[52] Astrid Eichhorn, *Status of the asymptotic safety paradigm for quantum gravity and matter*, arXiv:1709.03696.

[53] Leo P. Kadanoff, *Scaling laws for Ising models near T_c*, Physics Physique Fizika 2 (1966) 263–272.

[54] K.G. Wilson, John B. Kogut, *The Renormalization group and the ϵ expansion*, Phys.Rept. 12 (1974) 75–200; Kenneth G. Wilson, *The renormalization group: Critical phenomena and the Kondo problem*, Rev. Mod. Phys. 47 (1975) 773–840.

[55] Mitchell J. Feigenbaum, *Universal behavior in nonlinear systems*, Physica D: Nonlinear Phenomena. 7 (13) (1983) 16–39;Leo P. Kadanoff, *Scaling and universality in statistical physics*, Physica A: Statistical Mechanics and its Applications. 163 (1) (1990) 1-14.

[56] D. J. Gross and F. Wilczek, *Ultraviolet Behavior of Nonabelian Gauge Theories*, Phys. Rev. Lett. 30 (1973) 1343–1346; H. David Politzer, *Reliable Perturbative Results for Strong Interactions?*, hys. Rev. Lett. 30 (1973) 1346–1349.

[57] Holger Gies, *Renormalizability of gauge theories in extra dimensions*, Phys. Rev. D 68 (2003) 085015.

[58] M. Reuter, *Nonperturbative evolution equation for quantum gravity*, Phys.Rev. D57 (1998) 971–985.

[59] Wataru Souma, *Non-Trivial Ultraviolet Fixed Point in Quantum Gravity*, Prog. Theor. Phys. 102 (1999) 181-195.

[60] Daniel F. Litim, *Fixed Points of Quantum Gravity*, Phys.Rev.Lett.92 (2004) 201301.

[61] A. Codello, R. Percacci, C. Rahmede, *Investigating the Ultraviolet Properties of Gravity with a Wilsonian Renormalization Group Equation*, Annals Phys. 324, (2009) 414–469.

[62] D. Benedetti, P. F. Machado, F. Saueressig, *Asymptotic safety in higher-derivative gravity*, Mod. Phys. Lett. A24 (2009) 2233–2241; *Taming perturbative divergences in asymptotically*

safe gravity, Nucl. Phys. B824 (2010) 168–191; N. Ohta, R. Percacci, *Higher Derivative Gravity and Asymptotic Safety in Diverse Dimensions*, Class.Quant.Grav. 31 (2014) 015024.

[63] Daniel F. Litim, *Optimized renormalization group flows*, Phys.Rev. D64 (2001) 105007.

[64] F. J. Wegner and A. Houghton, *Renormalization Group Equation for Critical Phenomena*, Phys. Rev. A 8 (1973) 401–412.

[65] Christof Wetterich, *Exact evolution equation for the effective potential*, Phys.Lett. B301 (1993) 90–94; Tim R. Morris, *The Exact Renormalisation Group and Approximate Solutions*, Int. J. Mod. Phys. A9 (1994) 2411–2450.

[66] R. Gastmans, R. Kallosh, C. Truffin, *Quantum Gravity Near Two Dimensions*, Nucl. Phys. B133 (1978) 417–434.

[67] M. Kawai, M. Ninomiya, *Renormalization Group and Quantum Gravity*, Nucl.Phys. B336 (1990) 115–145; M. Kawai, Y. Kitazawa, M. Ninomiya, *Ultraviolet Stable Fixed Point and Scaling Relations in* $2+\epsilon$ *Dimensional Quantum Gravity*, Nucl.Phys. B404 (1993) 684–716.

[68] Andreas Nink, *Field parametrization dependence in asymptotically safe quantum gravity*, Phys.Rev. D91 (2015) no.4, 044030; Andreas Nink, in the Wikipedia page of "Asymptotic safety in quantum gravity".

[69] Kevin Falls, *Physical renormalization schemes and asymptotic safety in quantum gravity*, Phys. Rev. D 96, 126016 (2017).

[70] M. Reuter, H. Weyer, *Quantum Gravity at Astrophysical Distances?*, JCAP 12 (2004) 001.

[71] Carlos Contreras et al, *Exact black hole solution for scale dependent gravitational couplings and the corresponding coupling flow*, Class.Quant.Grav. 30 (2013) 175009.

[72] U. Harst, M. Reuter, *QED coupled to QEG*, JHEP 1105 (2011) 119.

[73] R. P. Woodard, *The Theorem of Ostrogradsky*, arXiv:1506.02210 , Scholarpedia (2015) ; M. Crisostomi, R. Klein, D. Roest, *Higher Derivative Field Theories: Degeneracy Conditions and Classes*, JHEP 1706 (2017) 124 .

[74] D. Becker, C. Ripken, F. Saueressig, *On avoiding Ostrogradski instabilities within Asymptotic Safety*, JHEP 1712 (2017) 121.

[75] M. H. Goroff, A. Sagnotti, *Quantum Gravity At Two Loops*, Phys.Lett. 160B (1985) 81-86; *The Ultraviolet Behavior of Einstein Gravity*, Nucl.Phys. B 266 (1986) 709–736; A.E.M. van de Ven, *Two loop quantum gravity*, Nucl.Phys. B378 (1992) 309–366.

[76] H. Gies, B. Knorr, S. Lippoldt, F. Saueressig, *Gravitational Two-Loop Counterterm Is Asymptotically Safe*, Phys.Rev.Lett. 116 (2016) no.21, 211302.

[77] O. Lauscher, M. Reuter, *Fractal Spacetime Structure in Asymptotically Safe Gravity*, JHEP10 (2005) 050.

[78] M. Reuter and F. Saueressig, *Fractal space-times under the microscope: A Renormalization Group view on Monte Carlo data*, JHEP 1112 (2011) 012.

[79] G. Calcagni, A. Eichhorn, F. Saueressig, *Probing the quantum nature of spacetime by diffusion*, JHEP10 (2005) 050.

[80] A. Bonanno, M. Reuter, *Renormalization group improved black hole spacetimes*, Phys.Rev. D62 (2000) 043008.

[81] T. Burschil, B. Koch, *Renormalization group improved black hole space-time in large extra dimensions*, Jetp Lett. 92 (2010) 193-199.

[82] Yi-Fu Cai, Damien A. Easson, *Black holes in an asymptotically safe gravity theory with higher derivatives*, JCAP 09 (2010) 002.

[83] M. Reuter, E. Tuiran, *Quantum Gravity Effects in Rotating Black Holes*, arXiv:hep-th/0612037; *Quantum Gravity Effects in Rotating Black Holes*, Phys. Rev. D 83, 044041 (2011).

[84] K. Falls, D. F. Litim, A. Raghuraman, *Black holes and asymptotically safe gravity*, Int. J. Mod. Phys. A 27 (2012) 1250019.

[85] B. Koch, F. Saueressig , *Structural aspects of asymptotically safe black holes*, Class. Quantum Grav. 31 (2014) 015006.

[86] B. Koch, P. Rioseco, and C. Contreras, *Scale setting for self-consistent backgrounds*, Phys. Rev. D 91, no. 2 (2015) 025009 .

[87] A. Bonanno, B. Koch, A. Platania, *Cosmic Censorship in Quantum Einstein Gravity*, lass. Quantum Grav. 34 (2017) 095012.

[88] A. Bonanno, M. Reuter, *Spacetime structure of an evaporating black hole in quantum gravity*, Phys.Rev. D73 (2006) 083005.

[89] Kevin Falls, Daniel F. Litim, *Black hole thermodynamics under the microscope*, Phys. Rev. D 89 (2014) 084002.

[90] M. Reuter, F. Saueressig, *From Big Bang to Asymptotic de Sitter: Complete Cosmologies in a Quantum Gravity Framework*, JCAP 0509 (2005) 012.

[91] Steven Weinberg, *Asymptotically Safe Inflation*, Phys. Rev. D81 (2010) 083535.

[92] Yi-Fu Cai, Damien A. Easson, *Asymptotically safe gravity as a scalar-tensor theory and its cosmological implications* , Phys. Rev. D84 (2011) 103502.

[93] Zhong-Zhi Xianyu, Hong-Jian He, *Asymptotically Safe Higgs Inflation*, JCAP10 (2014) 083

[94] A. Bonanno, A. Platania, *Asymptotically safe inflation from quadratic gravity*, Phys. Lett. B750 (2015) 638–642.

[95] E. J. Copeland, C. Rahmede, I. D. Saltas, *Asymptotically Safe Starobinsky Inflation*, Phys. Rev. D91 (2015) 10, 103530

[96] A. Bonanno, F. Saueressig, *Asymptotically safe cosmology - a status report*, Comptes Rendus Physique 18 (2017) 254-264.

[97] C. Wetterich, *Graviton fluctuations erase the cosmological constant*, Phys. Lett. B 773 (2017) 6-19.

[98] M. Reuter, H. Weyer, *Renormalization group improved gravitational actions: a Brans-Dicke approach*, Phys.Rev. D69 (2004) 104022; *Quantum Gravity at Astrophysical Distances?*, Phys.Rev. D69 (2004) 104022.

[99] C. Contreras, B. Koch, P. Rioseco, *Exact black hole solution for scale dependent gravitational couplings and the corresponding coupling flow*, Class. Quantum Grav. 30 (2013) 175009.

[100] Benjamin Koch, Israel Ramirez, *Exact renormalization group with optimal scale and its application to cosmology*, Class. Quant. Grav. 28 (2011) 055008.

[101] Alfio Bonanno, *An effective action for asymptotically safe gravity*, Phys. Rev. D85 (2012) 081503 .

[102] Mark Hindmarsh, Ippocratis D. Saltas, $f(R)$ *Gravity from the renormalisation group*, Phys.Rev. D86 (2012) 064029 .

[103] Juergen A. Dietz, Tim R. Morris, *Asymptotic safety in the* $f(R)$ *approximation*, JHEP 1301 (2013) 108 .

[104] Edmund J. Copeland, Christoph Rahmede, Ippocratis D. Saltas, *Asymptotically Safe Starobinsky Inflation*, Phys.Rev. D91 (2015) no.10, 103530 .

[105] Davi C. Rodrigues, Patricio S. Letelier, Ilya L. Shapiro, *Galaxy rotation curves from General Relativity with Renormalization Group corrections*, JCAP 1004 (2010) 020 .

[106] Silvije Domazet, Hrvoje Stefancic, *Renormalization group scale-setting in astrophysical systems*, Phys.Lett. B703 (2011) 1-6.

[107] Hideo Kodama, Akihiro Ishibashi, *A master equation for gravitational perturbations of maximally symmetric black holes in higher dimensions*, Prog. Theor. Phys. 110 (2003) 701-722.

[108] John Cardy, *Scaling and Renormalization in Statistical Physics*, Cambridge University Press (1996) ISBN:9780521499590.

[109] Jean Zinn-Justin, *Quantum Field Theory and Critical Phenomena*, Oxford University Press (2002) ISBN-13: 9780198509233.

[110] Edouard Brezin, *Introduction to Statistical Field Theory*, Cambridge University Press (2010) ISBN: 9780511761546.

[111] Herbert W. Hamber, *On the Gravitational Scaling Dimensions*, Phys.Rev. D61 (2000) 124008.

[112] H. Kawai, Y. Kitazawa, M. Ninomiya, *Scaling Exponents in Quantum Gravity near Two Dimensions*, Nucl.Phys. B393 (1993) 280–300.

[113] H. Kawai, Y. Kitazawa, M. Ninomiya, *Ultraviolet Stable Fixed Point and Scaling Relations in* $2+\epsilon$ *Dimensional Quantum Gravity*, Nucl.Phys. B404 (1993) 684–716.

[114] Herbert W. Hamber, Ruth M. Williams, *Non-Perturbative Gravity and the Spin of the Lattice Graviton*, Phys. Rev. D70 (2004) 124007.

[115] Herbert W. Hamber, Ruth M. Williams, *Quantum Gravity in Large Dimensions*, Phys. Rev. D73 (2006) 044031.

[116] Herbert W. Hamber, *Scaling Exponents for Lattice Quantum Gravity in Four Dimensions*, Phys.Rev. D92 (2015) 6, 064017.

[117] Kevin Falls, *Asymptotic safety and the cosmological constant*, JHEP 1601 (2016) 069.

[118] Peter Fischer, Daniel F. Litim, *Fixed points of quantum gravity in extra dimensions*, Phys.Lett. B638 (2006) 497-502.

[119] Luca Amendola and Shinji Tsujikawa, *Dark Energy: Theory and Observations*, Cambridge University Press (2010) ISBN: 9780521516006.

[120] Alexei A. Starobinsky, *A new type of isotropic cosmological models without singularity*, Phys. Lett. 91B (1980) 99-102.

[121] Alan H. Guth, *The Inflationary Universe: A Possible Solution to the Horizon and Flatness Problems*, Phys. Rev. D 23 (1981) 347 .

[122] A. D. Linde, *A New Inflationary Universe Scenario: A Possible Solution of the Horizon, Flatness, Homogeneity, Isotropy and Primordial Monopole Problems*, Phys. Lett. B 108 (1982) 389.

[123] Luis Alvarez-Gaume et. al., *Aspects of Quadratic Gravity*, Fortsch. Phys. 64 (2016) no.2-3, 176-189.

[124] Alex Kehagias, Costas Kounnas, Dieter Lust, Antonio Riotto, *Black hole solutions in R^2 gravity*, JHEP 1505 (2015) 143.

[125] William Nelson, *Static Solutions for 4th order gravity*, Phys.Rev. D82 (2010) 104026.

[126] Alun Perkins, *Static spherically symmetric solutions in higher derivative gravity*, PhD Thesis, Imperial College London .

[127] H. Lu, A. Perkins, C.N. Pope, K.S. Stelle, *Black Holes in Higher-Derivative Gravity*, Phys.Rev.Lett. 114 (2015) no.17, 171601.

[128] H. Lu, A. Perkins, C.N. Pope, K.S. Stelle, *Spherically Symmetric Solutions in Higher-Derivative Gravity*, Phys.Rev. D92 (2015) no.12, 124019 .

Acknowledgement

"If I have seen further,
it is by standing on the shoulders of Giants."

Isaac Newton *in Letter to Robert Hooke, 1675.*

I am wholeheartedly grateful to Astrid Eichhorn for her roles at many stages of my study in Heidelberg. I have learned so much from her enthusiasm for physics and the diversity that distinguish her quantum gravity research group. I am very humbled by every act of kindness she stretched towards me at some of the critical moments of my study, memories of which I will carry for a very long time.

I would like to thank Alessia Platania for her guidiance and supporting role in improving me so much technically. I further appreciate many invaluable discussions with Alessia and Kevin Falls, which have greatly improved my knowledge of quantum gravity.

I acknowledge part supports from Ruperto Carola Campaign and Studierendenrat - Heidelberg.

I am grateful for friendly relationship and humanly support from the following: Eser Altun, Aian Khanakhmedov, Zhanhong Wei, Johannes Paulokat, Ines Woide.

I appreciate many shared time with the member of Astrid's Quantum gravity group of the 2017/2018 academic session, including Aaron, Antonio, Alessia, Artiom, Fleur, Giovanni, Johannes, Marc, Peter. All of the group activities have been helpful for me in learning new things ranging from Physics to the varied culture and traditions. I would like to further appreciate other great office mates, including Dennis, Coralie, Kim.

FAMILY: A unit of people that love and support each other through good times and bad: Atinshola Ajike, Folashade Adeifeoba, Safiu Muraina, Mujidat Adeifeoba, Oluseye Oyedeji, Anthony Oyedeji, Tolulope Oyedeji and my lovely Chinasa Omeazu. Thank you all for your immense support, patience and understanding, none of which I take for granted in my voyage of life.

'___